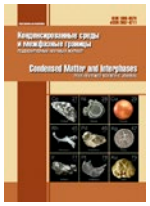

ISSN 1606-867X (Print)
ISSN 2687-0711 (Online)
Condensed Matter and Interphases
Kondensirovannye Sredy i Mezhfaznye Granitsy
https://journals.vsu.ru/kcmf/

Review

Review article
https://doi.org/10.17308/kcmf.2024.26/12367

Complex copper-based chalcogenides: a review of phase equilibria and thermodynamic properties

M. B. Babanly[1,2]✉, L. F. Mashadiyeva[1], S. Z. Imamaliyeva[1], D. M. Babanly[1,3], D. B. Tagiyev[1], Yu. A. Yusibov[4]

[1]*Institute of Catalysis and Inorganic Chemistry, 113 H. Javid av., Baku AZ-1143, Azerbaijan*

[2]*Baku State University, 23 Z. Khalilov st., Baku AZ-1148, Azerbaijan*

[3]*French-Azerbaijani University 183 Nizami st., Baku AZ-1010, Azerbaijan*

[4]*Ganja State University, 187 H. Aliyev av., Ganja AZ-2000, Azerbaijan*

Abstract

Complex copper-based chalcogenides are among the most important functional materials in modern engineering and technology due to their diverse physical and physicochemical properties, environmental safety and availability. The development of new similar materials and the improvement of the applied characteristics of known compounds is largely associated with the use of approaches based on the physicochemical analysis and, in particular, the "composition-structure-property" relationship.

This review summarizes the available data on phase equilibria in ternary systems Cu-Tl(B^{IV}, B^{V})-X (B^{IV}-Si, Ge, Sn; B^{V}-As, Sb, Bi; X-S, Se, Te) and the thermodynamic properties of their intermediate phases. Similar data are also considered for more complex systems forming solid solutions of various types of substitution based on known ternary copper chalcogenides. A significant part of the presented sets of mutually consistent data on phase equilibria and thermodynamic properties of the considered systems was obtained by our group over the past 10-15 years. Although these data cover only a small part of the systems described above, they provide great possibilities for manipulation of composition and structure, including entropic engineering strategies. The authors consider it extremely important to further develop fundamental research on phase equilibria and thermodynamic properties of complex copper chalcogenides and use their results widely in selecting alloy compositions for physical measurements.

Keywords: Environmentally friendly materials, Complex copper chalcogenides, Phase diagram, Solid solutions, Thermodynamic properties

Funding: The study was supported by the Azerbaijan Science Foundation - Grant No. AEF-MCG-2022-1(42)-12/10/4-M-10.

For citation: Babanly M. B., Mashadiyeva L. F., Imamaliyeva S. Z., Babanly D. M., Tagiyev D. B., Yusibov Yu. A. Complex copper-based chalcogenides: a review of phase equilibria and thermodynamic properties. *Condensed Matter and Interphases*. 2024;26(4): 579–619. https://doi.org/10.17308/kcmf.2024.26/12367

Для цитирования: Бабанлы М. Б., Машадиева Л. Ф., Имамалиева С. З., Бабанлы Д. М., Тагиев Д. Б., Юсибов Ю. А. Сложные халькогениды на основе меди: обзор по фазовым равновесиям и термодинамическим свойствам. *Конденсированные среды и межфазные границы*. 2024;26(4), 579–619. https://doi.org/10.17308/kcmf.2024.26/12367

✉ Mahammad B. Babanly, e-mail: babanlymb@gmail.com

1. Introduction

Metal chalcogenides are currently used or considered promising for use in various areas of modern high technologies as semiconductor, thermoelectric, photoelectric, optical, magnetic and other materials due to their diverse physical and physicochemical properties [1–9]. The discovery of a new quantum state of matter, a topological insulator, at the beginning of our century [10], provided new impetus to research of physics, chemistry and materials science of chalcogenides. It turned out that many-layered chalcogenides have the properties of a topological insulator [11–17], and some of them combine the properties of a topological insulator and a magnet [18–21] and are extremely promising for a variety of applications, including spintronics, quantum memory and information processing devices, security systems, and medicine [13, 14].

In recent decades, copper-based chalcogenides have also attracted attention from researchers as environmentally friendly, safe, and affordable functional materials [5–9, 22–30]. Many of these compounds, along with unique electronic properties, have high ionic conductivity and can be used as solid-state electrodes, selective membranes, sensors, etc. Synthetic analogues of natural copper chalcogenide minerals should be especially noted among the intensively studied similar materials [31–37]. These compounds are very attractive as mixed ion-electron conductors, thermoelectrics, photovoltaics, photocatalysts, and optical materials.

In addition, according to several recent studies, some copper-based chalcogenides are promising for use in medicine [22, 38–40]. It should also be noted that many copper chalcogenides exist in nature as minerals and are of great interest to the geochemistry of the Earth [41, 42].

Analysis of data from many studies [22, 34–37] on complex copper chalcogenides demonstrated that their functional properties can be significantly improved by manipulating the structure and composition, including the concept of entropy engineering. The latter implies thermodynamic stabilization of phases with favorable applied characteristics by increasing the complexity of the composition and structural disorder [35].

The solution to the most important problems of materials science, especially in the so-called alloy systems, which include chalcogenides, is mainly associated with the use of physicochemical analysis [43, 44]. At the initial stage of development of new materials, the application of this method involves obtaining reliable data on phase equilibria in the corresponding systems, which allows not only the identification of new compounds or phases of variable composition but also the establishment of their nature of formation, thermal stability, primary crystallization and homogeneity regions, the presence of phase transitions, etc. [14, 37, 45–47]. The combination of these data forms the basis for the development of methods for the synthesis and growth of crystals with specified composition and properties.

The use of physicochemical analysis is also very effective for the design of known materials and the optimization of their properties. It is based on the well-known relationship "composition-structure-property". For the optimization of the functional indicators of certain compounds of stoichiometric composition, it is important to establish the nature of the physicochemical interaction in complex systems that include such compounds - structural or formula analogues, since the formation of various types of solid solutions (cationic, anionic and both types simultaneously) of substitution can be expected [14, 37, 48]. This allows the control of properties by varying structure and composition.

Optimization of the indicated technological parameters and many other processes requires their deeper thermodynamic analysis and the implementation of appropriate thermodynamic calculations. The efficiency of such calculations is directly related to the reliability and accuracy of data on the thermodynamic properties of substances involved in the considered processes [47, 49].

Hence, the wide application of physicochemical analysis for solving problems of materials science of chalcogenides, in particular, conducting comprehensive studies of phase equilibria and thermodynamic properties of the corresponding systems is important. Some aspects of such complex studies were considered by us in several studies [47, 50, 51]. Due to the widespread application of this approach in the study of

complex copper-based chalcogenide systems discussed in this review, we will only note that the basis of the approach is the use of the EMF method in a complex of experimental methods for studying phase equilibria. The EMF method, being one of the most accurate equilibrium methods of chemical thermodynamics, allows combining studies of phase equilibria and thermodynamic properties. We have used this approach since the beginning of the 1980s for the investigation of ternary thallium-containing chalcogenide systems [51–55], and in subsequent years also for other systems [50, 56–59].

The purpose of this review was to demonstrate the importance of the physicochemical analysis method and, in particular, the development of studies on phase equilibria and thermodynamic properties of multicomponent copper-based chalcogenide systems for the elaboration of scientific foundations for obtaining new complex phases with controlled composition, structure and properties.

The three sections of the review present the results of a study of phase equilibria in ternary and quaternary systems composed of copper chalcogenides and p^1–p^3-elements. At the beginning of each section, a general description is provided, crystallographic data of the most characteristic compounds of the corresponding class are shown, and a brief overview of their functional properties is presented. After, data on phase equilibria in the considered ternary and quaternary systems and fundamental thermodynamic characteristics of intermediate phases are presented and discussed.

2. Copper-thallium chalcogenides and phases based on them

The most characteristic copper chalcogenides with p^1-elements are compounds of the chalcopyrite type with the general formula $CuB^{III}X_2$ (B^{III}-Al, Ga, In, Tl; X-S, Se, Te) [1, 22]. At the same time, thallium and copper form a series of chalcogenides (see subsection 2.1), in which thallium is present in a more characteristic oxidation state (1+): CuTlX, Cu_3TlX_2, Cu_9TlX_5 and others. The $CuTlS_2$ and CuTlS crystal structures are shown in Fig. 2.1 and crystallographic data of copper-thallium chalcogenides are presented in Table 2.1.

The crystal structure of the CuTlS was established in [60] by powder and single-crystal X-ray diffraction methods. It has been shown that it crystallizes in the tetragonal syngony in the PbFCl structural type. The layers of Cu_2S_2, formed by CuS_4 tetrahedra with common edges, placed between double foils of Tl atoms. The Cu atoms are located inside the layers at the centers of tetrahedra, and Tl atoms are located in square two-dimensional networks and determine the *a* parameter. Each Tl atom is located in a pyramid cup and is bonded to four sulfur atoms at the base.

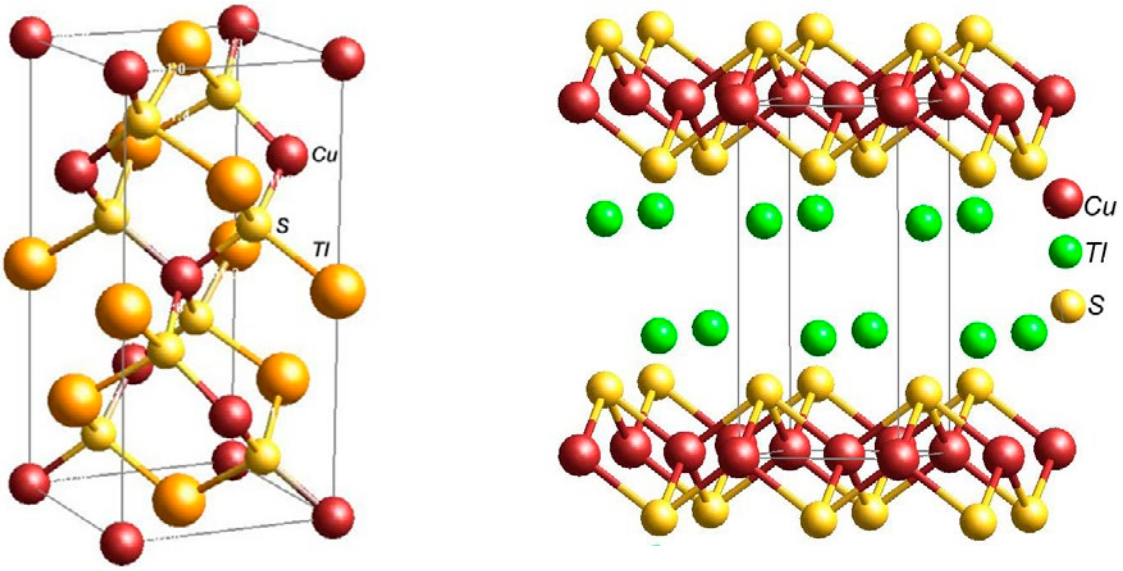

Fig. 2.1. Crystal structures of $CuTlS_2$ and CuTlS

Table 2.1. Crystallographic parameters of the copper-thallium chalcogenides

Compound	Crystal system, sp. gr. and lattice parameters, nm	Ref.
$CuTlS_2$	Tetragonal, $I\bar{4}2d$, a = 0.5576, c = 1.1256	[94]
CuTlS	Tetragonal, $P4/nmm$, a = 0.3922(2), c = 0.8123(6)	[60]
	Tetragonal, $P4/mmm$, a = 0.3912, c = 0.8164	[94]
Cu_3TlS_2	Monoclinic, $C2/m$, a = 1.463, b = 0.3863, c = 0.8298, β = 111.72°	[89]
Cu_7TlS_4	Tetragonal, $I4/m$, a = 1.01792(18), c = 0.38567(9)	[90]
$CuTlSe_2$	Tetragonal, $I\bar{4}2d$, a = 0.583, c = 1.162	[100]
CuTlSe	Tetragonal, $P4/nmm$, a = 0.4087(6), c = 0.8195(19)	[100]
Cu_3TlSe_2	Monoclinic, $C2/m$, a = 1.52128, b = 0.40115, c = 0.83944, β = 111.7°	[88]
Cu_2TlSe_2	Tetragonal, $I4/mmm$, a = 0.380, c = 1.377	[100]
Cu_7TlSe_4	Tetragonal, $I4/m$, a = 1.04453(18), c = 0.39735(8)	[90]
$CuTl_4Te_3$	Tetragonal, $I4/mcm$, a = 0.8929(1), c = 1.2603(1)	[106]
Cu_2TlTe_2	Tetragonal, $I4/mmm$, a = 0.4001, c = 1.4208	[100]
Cu_3TlTe_2	Tetragonal, $P4_2/nnm$, a = 0.8427(4), c = 1.4492(6)	[105]

Copper chalcogenides with elements of the gallium subgroup, as well as solid solutions and doped phases based on them, are excellent materials [22] for photovoltaic [62–70], optoelectronic [71–73], and thermoelectric [70, 75–80] devices, as well as luminescent materials [81–83].

The use of these materials as solar energy absorbers is because the width of their band gap correlates well with the maximum photon power density in the sunlight spectrum and at the same time demonstrates long-term stability and resistance to radiation [22, 84]. Several studies proposed changing the bulk or surface composition by sulphidization [65, 67, 68], regulation the ratios of constituent atoms, adding alloying components [61, 63, 66], and other strategies [22] to increase their efficiency. It should be noted that sulphidization of the Cu(Ga, In)Se_2 layers led to the record efficiency (23.35%) of the solar cell [85]. Thin-film solar cells based on Cu(Ga, In)Se_2 are also considered promising for generating electricity at space stations [86].

Copper chalcogenides with p^1-elements with a wide range of band gap energies and unique optical properties are very promising for use in optoelectronic and light-emitting devices [22, 72, 73]. The authors of [81] reported the development of quantum dot LEDs exhibiting red color with a narrow emission peak by controlling the copper content in Cu(GaIn)S_2 phases.

Copper-thallium selenides and tellurides are of interest as thermoelectric materials with abnormally low thermal conductivity [22, 75, 76, 80, 87].

The main reasons for the relatively low efficiency of photovoltaic and thermoelectric systems based on copper-gallium chalcogenides (indium, thallium) and the proposed optimization methods for obtaining their nanocrystals with specified characteristics are discussed in reviews [22, 66].

2.1. Phase equilibria in the Cu-Tl-X systems

The results of studies on phase equilibria in the indicated systems carried out before the beginning of the 90s of the last century are summarized in [91]. The results of the most important works of the indicated period, as well as the research performed in subsequent years by our group, are presented and discussed below.

The Cu-Tl-S system. The quasi-binary section of the Cu_2S-Tl_2S system was studied almost simultaneously by two groups of authors [92, 93]. According to [92] (Fig. 2.2), three ternary compounds are formed in the system: Cu_9TlS_5, Cu_3TlS_2, and CuTlS. The first two melt with decomposition by peritectic reactions at 706 and 693 K, respectively, and the last one melts congruently at 689 K. The phase diagram constructed in [93] reflects two congruently melting compounds CuTlS and $Cu_8Tl_2S_5$. Later, in the study [94], crystallographic data for the $CuTlS_2$ and CuTlS compounds are presented (Table 2.1). The phase diagram presented in [92]

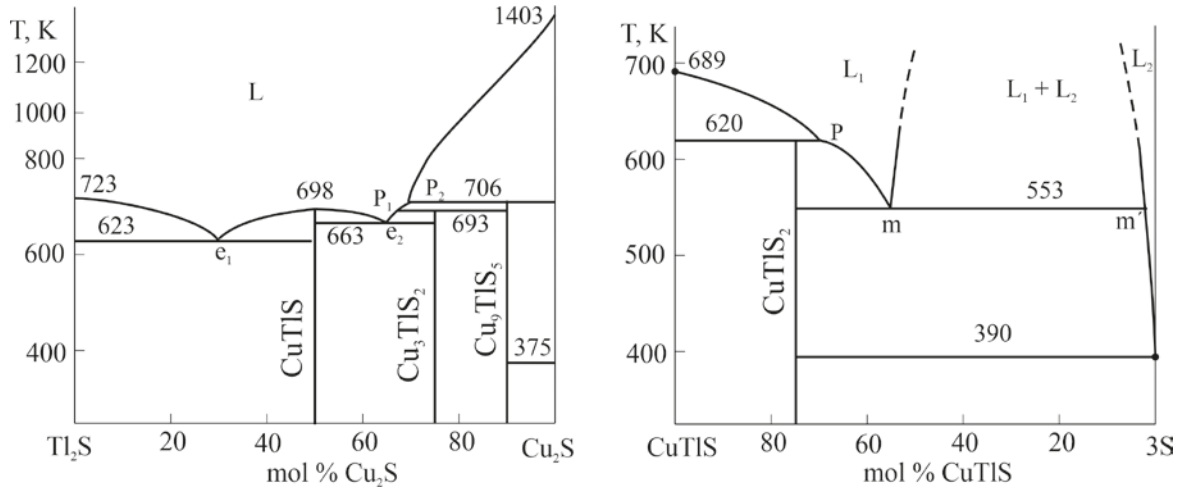

Fig. 2.2. Phase diagrams of the quasi-binary systems Cu_2S-Tl_2S and CuTlS-S

was confirmed by the authors of [95]. The CuTlS-S and CuTlS-Tl sections are also quasi-binary. The first is characterized by the formation of the compound $CuTlS_2$ with incongruent melting at 620 K [96] (Fig. 2.2), and the second is designated by the presence of a wide immiscibility region and degenerate eutectic [97].

The study [98] presents a complete *T-x-y* diagram of the Cu-Tl-S system, including a diagram of solid-phase equilibria at 300 K and a projection of the liquidus surface (Fig. 2.3). As can be seen, the system is characterized by the presence of four ternary compounds of practically constant composition. The liquidus surface consists of 10 primary crystallization fields, including four ternary compounds. A characteristic feature of the system is the presence of three wide immiscibility regions of two liquid phases and a region of immiscibility of three liquid phases.

The Cu-Tl-Se system. Quasi-binary section Cu_2Se-Tl_2Se (Fig. 2.4) of this system is characterized by the formation of ternary compounds CuTlSe, $Cu_7Tl_3Se_5$, Cu_3TlSe_2, $Cu_8Tl_2Se_5$ and Cu_9TlSe_5 [99]. According to [91], the CuTlSe-TlSe, CuTlSe-Tl, and CuTlSe-Se sections are also quasi-binary. The first one forms a phase diagram of a simple eutectic type, the second one forms a phase diagram of a monotectic type, and the third one is characterized by the formation of a ternary compound $CuTlSe_2$ that melts incongruently at 550 K (Fig. 2.4)

The literature contains information on the synthesis and crystal structure of about ten copper selenides with thallium [91, 100]. However, a complete picture of phase equilibria in the Cu-Tl-Se system has not been obtained yet. A fragment of the solid-phase equilibrium diagram, constructed by us based on the data of studies [91, 102] is shown in Fig.2.5 and a projection of the liquidus surface of the Cu-Cu_2Se-Tl_2Se-Tl subsystem is shown in Fig. 2.6. This projection, the corresponding sulfide projection, is characterized by the presence of wide double and triple immiscibility regions and is congruently triangulated into three elementary triangles.

The Cu-Tl-Te system. Phase equilibria in this system have been studied for the Cu_2Te-Tl_2Te_3 section [103, 104]. This section is not quasi-binary due to the incongruent melting of Tl_2Te_3, but is stable below the solidus and is characterized by the formation of the ternary compounds $CuTlTe_2$ and Cu_3TlTe_3 with incongruent melting at 573 and 673 K, respectively. According to [95, 101], the Cu_2Te-Tl_2Te section, unlike similar sulfide and selenide systems, is non-quasi-binary and unstable in the subsolidus. It is characterized by the formation of the ternary compounds Cu_9TlTe_5 and Cu_3TlTe_2 with incongruent melting.

There is also information about copper-thallium tellurides with Cu_2TlTe_2 and $CuTl_4Te_3$ compositions [91, 100, 105, 106] (Table 2.1).

In studies [104, 107] a fragment of the diagram of solid-phase equilibria of Cu-Tl-Te at 300 K was presented (Fig. 2.5), which reflects all of the above-mentioned ternary compounds.

2.2. Thermodynamic properties of copper-thallium chalcogenides

The thermodynamic properties of copper-thallium chalcogenides were investigated in

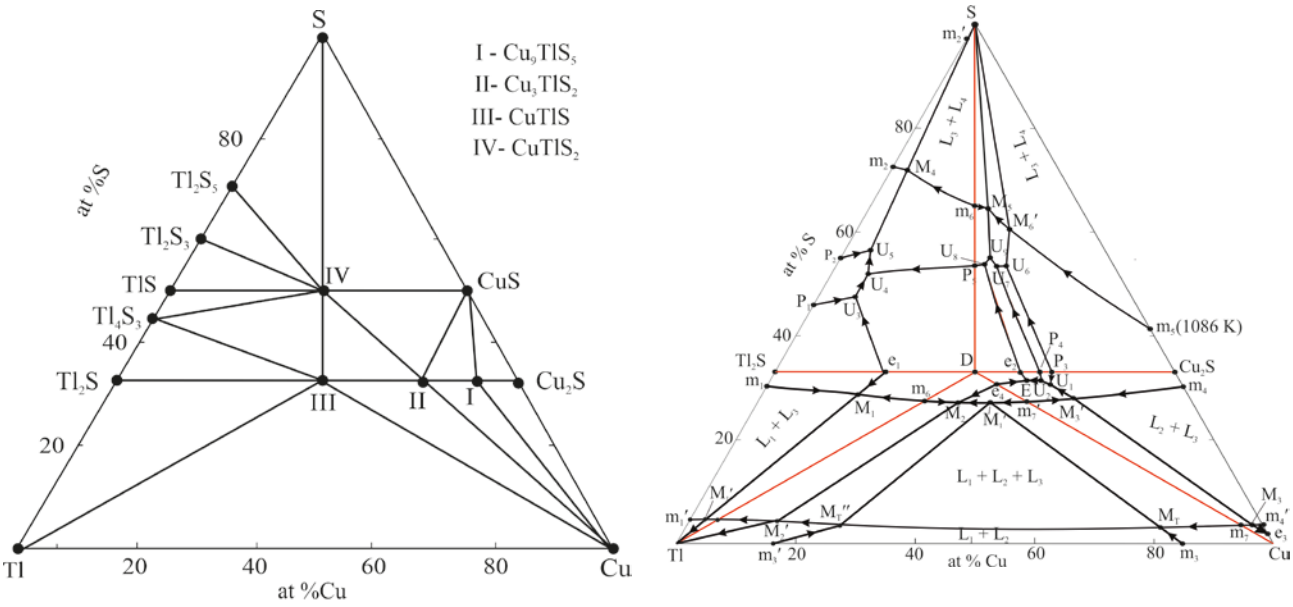

Fig. 2.3. Solid-phase equilibrium diagram at 300 K and liquidus surface projection of the Cu-Tl-S system. Red lines are quasi-binary sections

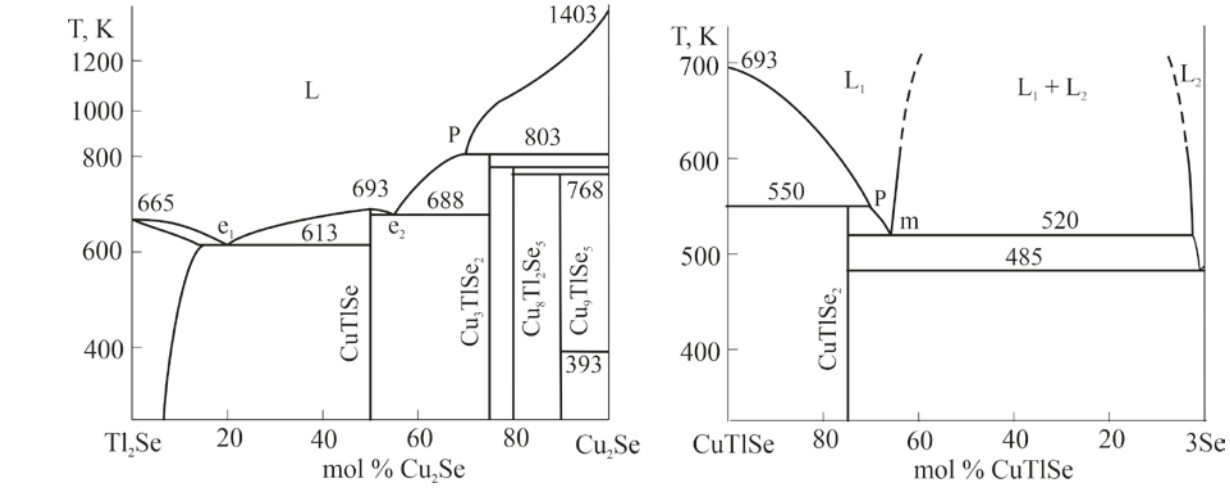

Fig. 2.4. Phase diagrams of the quasi-binary systems Cu_2Se-Tl_2Se and CuTlSe-Se

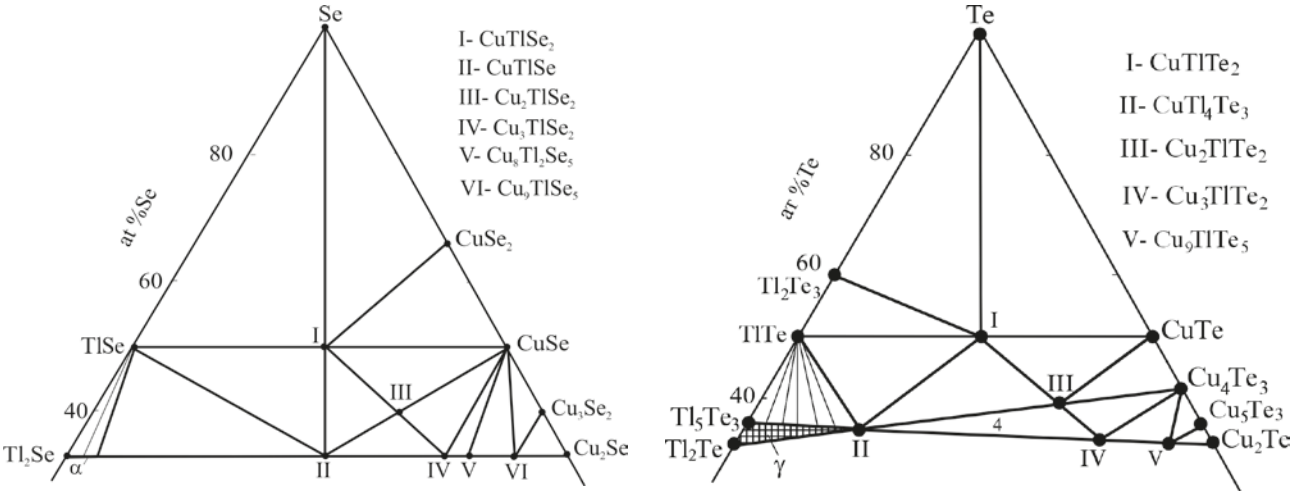

Fig. 2.5. Solid-phase equilibria diagrams of the Cu-Tl-Se and Cu-Tl-Te systems at 300 K

several studies [91, 98, 101, 104, 107-109] using the electromotive force (EMF) method. In these studies, the EMFs of two types of concentration circuits were measured:

(–) Tl (s.) | liquid + Tl^+ | (Tl in alloy) (s.) (+) (2.1)
electrolyte

(–) Cu (s.) | $Cu_4RbCl_3I_2$ (s.) | (Cu in alloy) (s.) (+)(2.2)

in a wide range of temperatures, starting from room temperature. The methods for compiling chains of (2.1) and (2.2) types, conducting experiments and processing their results are described in detail in [51, 109, 110]. It should be noted that various modifications of the EMF method with liquid [61-59, 109-115] and solid electrolytes [50, 51, 113, 116-120] are successfully used to study the thermodynamic properties and phase equilibria of various inorganic systems.

The results of thermodynamic studies of copper-thallium chalcogenides by measuring the EMF of type (2.1) concentration cells are shown in [98, 107, 109]. Later, in [101, 104, 108], a thermodynamic study of the indicated systems was carried out by measuring the EMF of type (2.2) concentration cells relative to a copper electrode. It should be noted that the thermodynamic data obtained in the above two series of studies are independent: they used the results of measurements of the EMF of concentration cells of various types, and based on these data, partial thermodynamic functions of different components (thallium or copper) which characterize completely different potential-forming reactions of the studied systems were calculated.

The obtained two series of data of standard integral thermodynamic functions of copper-thallium chalcogenides are shown in Table 2.2.

As can be seen from Table 2.2 the values of the standard thermodynamic functions for the formation of ternary compounds, obtained by two modifications of the EMF method, are generally in satisfactory agreement with each other. This confirms both the reversibility of types (2.1) and

Table 2.2. Standard integral thermodynamic functions of the copper-thallium chalcogenides

Compound	$-\Delta_f G^0$ (298 K)	$-\Delta_f H^0$ (298 K)	S^0_{298} J·K^{-1}·mol^{-1}	Ref.
	kJ·mol^{-1}			
$CuTlS_2$	91.5±0.5 94.3±0.7	98.6±4.0 93.6±1.4	172.7±2.8	[51, 98] [108]
CuTlS	84.1±1.5 90.3±0.7	82.1±4.9 88.3±2.1	132.4±6.2	[51, 98] [108]
Cu_3TlS_2	152.7±1.8 163.8±2.6	145.8±12.3 159.2±9.8	251.8±5.8	[51, 98] [108]
Cu_9TlS_5	354.6±4.5 373.8±3.9	339.7±30.8 371.8±21.4	529.0±19.0	[51, 98] [108]
$CuTlSe_2$	96.3±0.2 96.5±0.6	97.9±1.0 97.2±1.3	176.1±5.1	[101] [51]
CuTlSe	84.5±0.2 84.2±1.3	81.4±0.9 80.5±3.9	149.9±2.8	[101] [51]
Cu_2TlSe_2	119.1±0.3	118.6±1.5	216.2±6.8	[101]
Cu_3TlSe_2	150.8±3.7	150.7±9.8		[51]
Cu_9TlSe_5	333.6±10.1	350.5±28.6		[51]
$CuTlTe_2$	75.1±0.4	72.6±1.3	208±4	[104]
Cu_2TlTe_2	99.2±0.5 94.8±0.9	94.3±2.1 92±7	249±6 237±3	[104] [107]
Cu_3TlTe_2	122.0±0.6 117.1±1.2	115.2±2.7 117±5	288±8 263±4	[104] [107]
Cu_9TlTe_5	264.3±2.6 244.0±2.4	253.8±9.8 2431±14	637±15 621±7	[104] [107]
$CuTl_4Te_3$	201.4±1.4	203.8±2.6	433±9	[104]

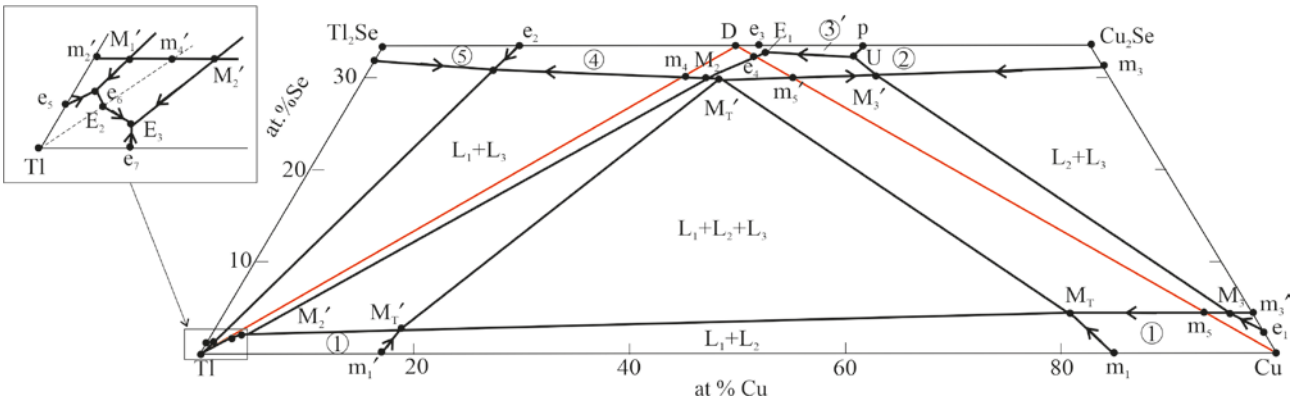

Fig. 2.6. Liquidus surface projection of the Cu-Cu_2Se-Tl_2Se-Tl subsystem. Red lines are quasi-binary sections

(2.2) concentration cells and the reliability of the thermodynamic data used in the calculations for binary copper and thallium chalcogenides.

2.3. Complex systems based on CuTlX compounds

The results of the study of phase equilibria in quasi-binary systems composed of the CuTlX compounds and their silver-containing analogues, as well as in mutual AgTlS+CuTlSe↔AgTlSe+CuTlS and quasi-ternary systems CuTlS-CuTlSe-AgTlTe were presented in [121-124]. It has been shown that the CuTlS-CuTlSe system was characterized by the formation of a continuous series of solid solutions [121], while systems of the CuTlX-AgTlX type [122–124] were characterized by limited mutual solubility of the components and eutectic equilibrium (Fig. 2.7).

The new phase of variable composition with a wide homogeneity region was identified in the CuTlS-AgTlS system [122]. According to the data [123, 124], wide homogeneity regions of

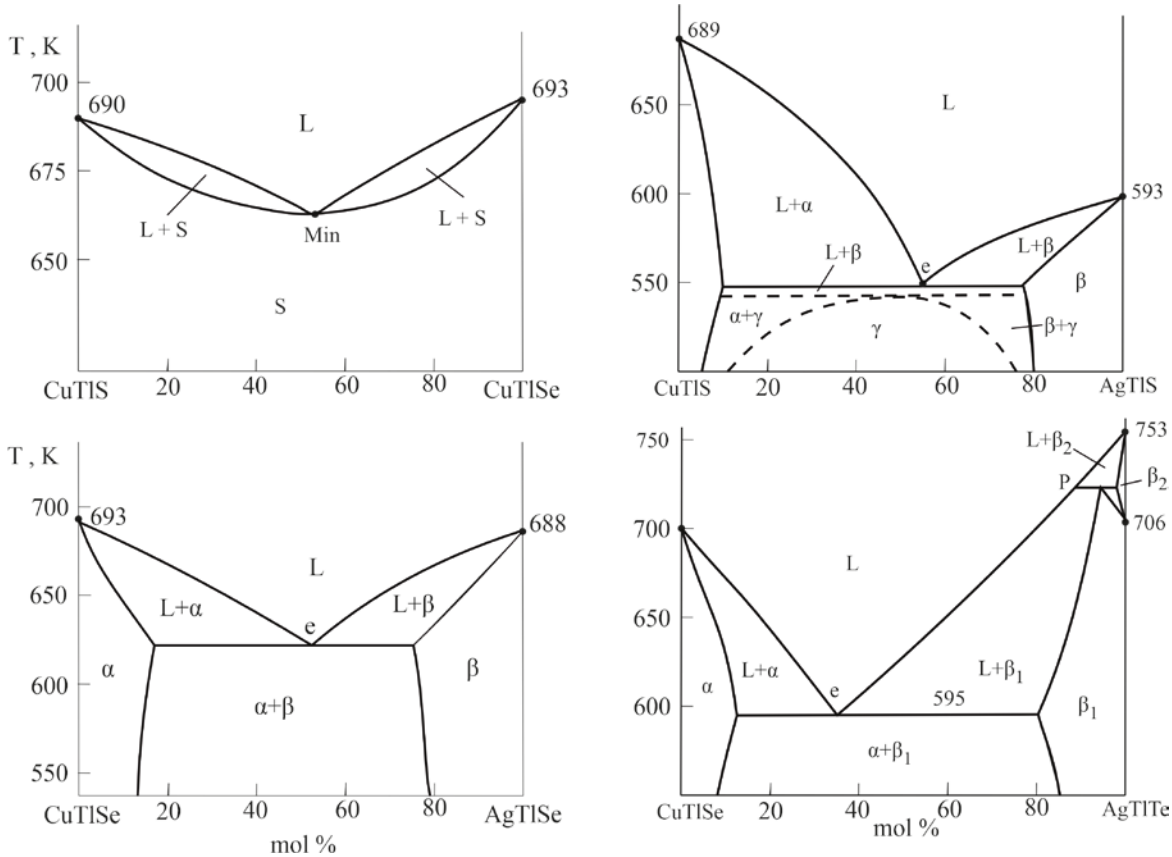

Fig. 2.7. *T-x* diagrams of some quasi-binary systems based on CuTlX compounds

solid solutions with simultaneous Cu ↔ Ag and chalcogen substitutions were revealed in the above-mentioned mutual and quasi-ternary systems.

3. Copper chalcogenides with Si, Ge, Sn

Triple compounds of Cu-B^{IV}-X (B^{IV} - Si, Ge, Sn; X – S, Se, Te) systems tend to crystallize in a large number of phases and structural forms, resulting in different functional properties and application possibilities [22]. In silicon- and germanium-containing systems (sections 3.1 and 3.2), the compounds of $Cu_2B^{IV}X_3$ and $Cu_8B^{IV}X_6$ types are the most characteristic and studied. The first group of compounds can be considered as synthetic analogues of the mineral mohite (Cu_2SnS_3), and the compounds of the second group are synthetic analogues of the mineral argyrodite (Ag_8GeS_6). The Cu-Sn-S system (section 3.3) is characterized by the formation of several ternary compounds with various compositions and structures. The crystal structures of some copper-tin sulfides are shown in Fig. 3.1, and crystallographic data of copper chalcogenides with p^2-elements are presented in Table 3.1.

The compounds of $Cu_2B^{IV}X_3$ type have various structural forms, such as cubic sphalerite-like (sp. gr. $F\bar{4}3m$), monoclinic sphalerite superstructure; orthorhombic structure (sp. gr. $Im2$) and a hexagonal structure of the wurtzite type (sp. gr. $P63/mc$) (Fig. 3.1). In the orthorhombic phase, the cations are ordered in a way that all cation positions in each plane are occupied by the same element and follow an ordered sequence of two planes with Cu cations and one plane with Ge cations. In contrast, in the cubic structure of zinc-blende, the Cu and Ge cations are randomly distributed over the cationic sites with filling factors of 2/3 and 1/3 for Cu and Ge, respectively [22, 115].

All compounds of the argyrodite family have a tetrahedral close-packed structure containing weakly bound cations A^+ [35, 36]. Cations B^{4+} tetrahedrally coordinated by 4 anions and form polyanions $[BX_4]^{8-x}$. These polyanions, along with the X^{2-} anions, form a rigid framework with vacancies for A^+ cations (Fig. 3.2). A characteristic feature of compounds of the argyrodite family is the presence of polymorphic phase transitions at

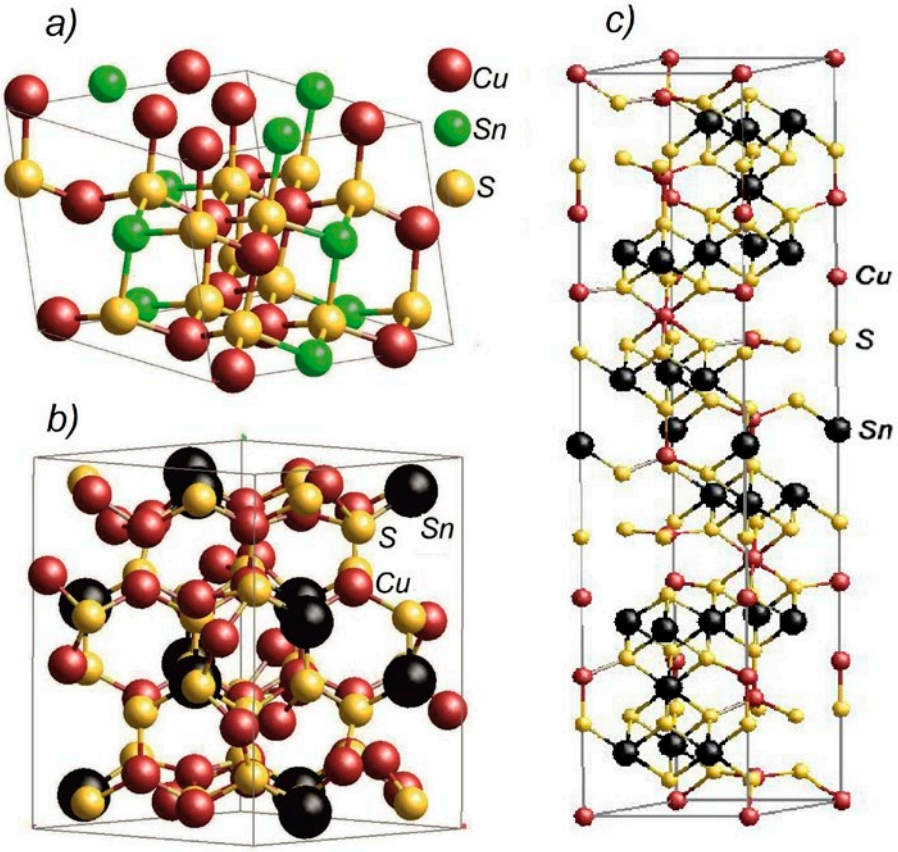

Fig. 3.1. Crystal structures of copper-tin sulfides: monoclinic Cu_2SnS_3 (a), orthorhombic Cu_4SnS_4 (b) and hexagonal $Cu_4Sn_7S_{16}$ (c)

relatively low temperatures (≤ 530 K) [37]. Low-temperature modifications have various ordered low-symmetry structures, which are described in detail in the literature [35–37]. They contain cations A^+ arranged in a specific order in certain positions. As a result of the distortion of the rigid anionic framework of the crystal lattice, a transition of low-temperature modifications into high-temperature disordered modifications occurs. Despite the relative diversity of the crystal structures of the low-temperature phases, all high-temperature argyrodites have a highly symmetrical cubic structure with sp. gr. *F*-43*m* (Table 3.1). Disordered high-temperature cubic

Table 3.1. Crystallographic parameters of ternary compounds of the Cu-B^{IV}-X systems

Compound	Crystal system, sp. gr. and lattice parameters, nm	Ref.
Cu_2SiS_3	Monoclinic, *C*1*c*1, *a* = 0.6332, *b* = 1.123, *c* = 0.6273, β = 107.49°	[159]
HT-Cu_8SiS_6	Cubic, *F*-43*m*, *a* = 0.976	[37]
RT-Cu_8SiS_6	Orthorhombic, $Pmn2_1$, *a* = 0.70445 (3), *b* = 0.69661(3), *c* = 0.98699 (5)	[37]
Cu_2SiSe_3	Monoclinic, *C*1*c*1, *a* = 0.6669(1), *b* = 1.1797(1), *c* = 0.6633(1), β = 107.67°	[159]
HT-Cu_8SiSe_6	Cubic, *F*-43*m*, *a* = 0.1017	[37]
Cu_2SiTe_3	Cubic, *F*-43*m*, *a* = 0.593	[160]
Cu_2GeS_3	Monoclinic, *C*1*c*1, *a* = 0.6449, *b* = 1.1319, *c* = 0.6428, β = 108.37	[125]
Cu_8GeS_6 HT	Cubic, *F*-43*m*, *a* = 0.99567	[37]
RT-Cu_8GeS_6	Orthorhombic, $Pmn2_1$, *a* = 0.70445, *b* = 0.69661, *c* = 0.98699	[37]
HT-Cu_2GeSe_3	Orthorhombic, *Imm*2, *a* = 1.1878, *b* = 0.3941, *c* = 0.5485	[168]
RT-Cu_2GeSe_3	Monoclinic, *Cm*, *a* = 0/6772, *b* = 0/3956, *c* = 0/3958, β = 125/83°	[164]
HT-Cu_8GeSe_6	Cubic, *F*-43*m*, *a* = 1.1020	[168]
IT-Cu_8GeSe_6	Hexagonal, $P6_3mc$, *a* = 0.7280, *c* = 1.167	[165]
RT-Cu_8GeSe_6	Hexagonal, $P6_3mcm$, *a* = 1.26438, *c* = 1.17570	[168]
Cu_2SnS_3	Monoclinic, *Cc*, *a* = 0.6653, *b* = 1.1537, *c* = 0.6665 β = 109.39°	[179]
Cu_4SnS_4	Orthorhombic, *Pnma*, *a* = 1.3558, *b* = 0.7681, *c* = 0.6412	[178]
$Cu_4Sn_7S_{16}$	Hexagonal, R-3*m*, *a* = 0.7372, *c* = 3.601	[180]
$Cu_4Sn_{15}S_{32}$	Cubic, *F*-43*m*, *a* = 1.0393	[182]
HT-Cu_2SnSe_3	Cubic, K(F), *a* = 0.56878	[183]
RT-Cu_2SnSe_3	Monoclinic, *Cc*, *a* = 0.65936, *b* = 1.21593, *c* = 0.66084, β = 108.56°	[183]
Cu_2SnTe_3	Cubic, *F*-43*m*, *a* = 0.60490	[189]

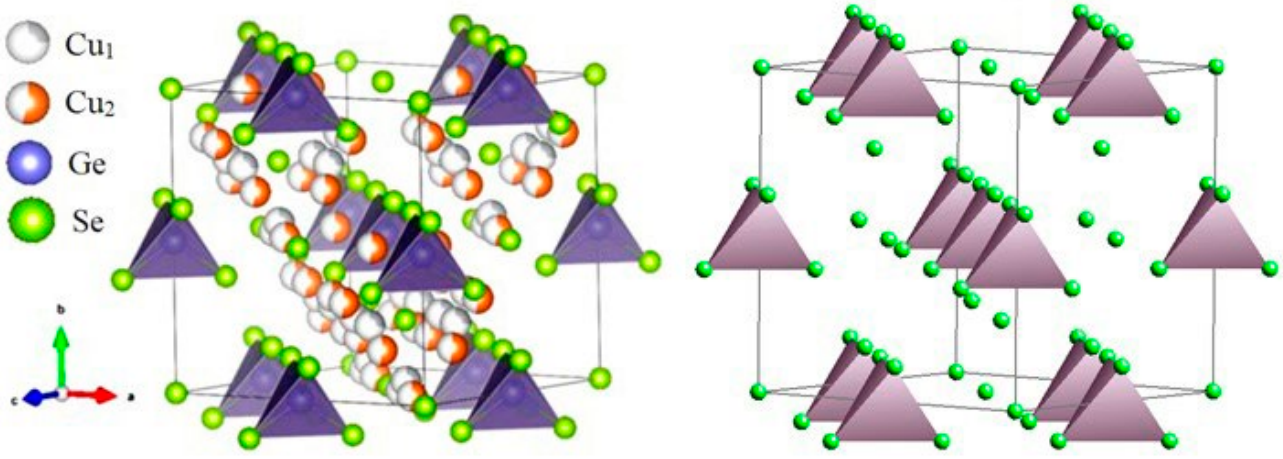

a b

Fig. 3.2. Crystal lattice of HT-Cu_8GeSe_6 (a) and anionic framework without Cu^+ ions (b)

phases are the aristotype of this structural family, and various low-temperature partially or completely ordered phases are the hettotype [37].

The schematic crystal structure of HT-Cu_8GeSe_6 and its anionic sublattice are shown in Fig. 3.2. In a unit cell containing 4 formula units, there are 32 Cu^+ cations statistically distributed in 2 crystallographic positions with a multiplicity of 24 (Cu1) and 48 (Cu2). The number of Cu^+ cations is more than twice lower than these cationic positions, therefore in HT-Cu_8GeSe_6 and other isostructural high-temperature phases, they are disordered and mobile as in a liquid.

Compounds of the mohite family, especially Cu_2SnSe_3, Cu_2GeSe_3, and alloys based on them have attracted considerable research interest as environmentally friendly and affordable thermoelectric materials [126–136]. It was shown that Cu_2SnSe_3 doped with various elements [126–134], as well as composites based on it [130–132], demonstrate good thermoelectric properties. The improvement of thermoelectric properties of Cu_2GeSe_3 doped with various elements [133–135], as well as solid solutions based on it [136], was achieved.

Studies have shown that compounds of the $Cu_2B^{IV}X_3$ type are also very promising for use as photovoltaic and optoelectronic materials [22, 34, 137–144]. The photoelectric and optical properties of the Cu_2SnS_3 and alloys based on it have been studied in more detail [139–142]. Reviews [22, 137] cover numerous studies on the synthesis, structural transformation, morphological engineering and band gap energy rearrangement of Cu–Sn–S (Se) nanoparticle systems and discuss the prospects for the development of solar cells based on them. They also highlight other photovoltaic applications such as photoelectrocatalytic hydrogen production and degradation of Cu–Sn–S (Se) nanoparticle dyes, etc.

According to the authors of another review [138], the ternary compound Cu_2SnS_3, consisting of non-toxic and readily available elements, is the most preferred photovoltaic material for solar cell applications due to its optimal structural and optical properties.

Copper-containing argyrodites are also of great interest as efficient ionic conductors, thermoelectric, photoelectric, and nonlinear optical materials [35–37]. These compounds, which are typical superionic semiconductors with two independent structural units (rigid anionic framework and weakly bound Cu^+ cations), can serve as very good base compounds for the development of high-performance thermoelectric materials by separate tuning of the electrical and thermal properties [35]. It should be noted that only a small part of the research on thermoelectric argyrodites is devoted to the study of stoichiometric compounds [35, 145, 146]. Most of the studies are focused on obtaining nano- and single crystals, thin films, polycrystals with a high density of complex phases and composite materials based on them [35, 147–149]. For the improvement of thermoelectric properties, researchers often complicate the composition by substituting analogous atoms, adding doping impurities, or creating a deficit of individual elements in the stoichiometric composition [37].

In [150] the production of thin-film layers of Cu_8SiS_6 and Cu_8SiSe_6 for optoelectronic applications was reported. The authors [151] noted that the replacement of Ag with Cu in isostructural compounds of the argyrodite family causes a clear increase in the generation of secondary harmonics. This result opens up the possibility of synthesizing high-quality infrared nonlinear optical materials based on them.

3.1. Phase equilibria in Cu-Si-X systems

The Cu-Si-S system was studied based on the quasi-binary section Cu_2S-SiS_2 [152–154]. The *T-x* diagram of this section in the composition range 0-50 mol. % SiS_2 was constructed in [152]. The formation of Cu_8SiS_6 congruently melting at 1468 K was demonstrated. In the study [153] this section was investigated in the entire composition range and two ternary compounds Cu_8SiS_6 and Cu_2SiS_3 were identified. It was found that the first melts congruently at 1473 K, and the second melts with decomposition according to the peritectic reaction at 1173 K. The latest version of the phase diagram of this system was presented by the authors [154]. According to their data, Cu_8SiS_6 and Cu_2SiS_3 compounds melt congruently at 1459 and 925 K. The *T-x* diagram constructed by us based on the data of [153, 154], taking into account the melting temperatures and polymorphic transitions of compounds specified in [155] is presented in Fig. 3.3.

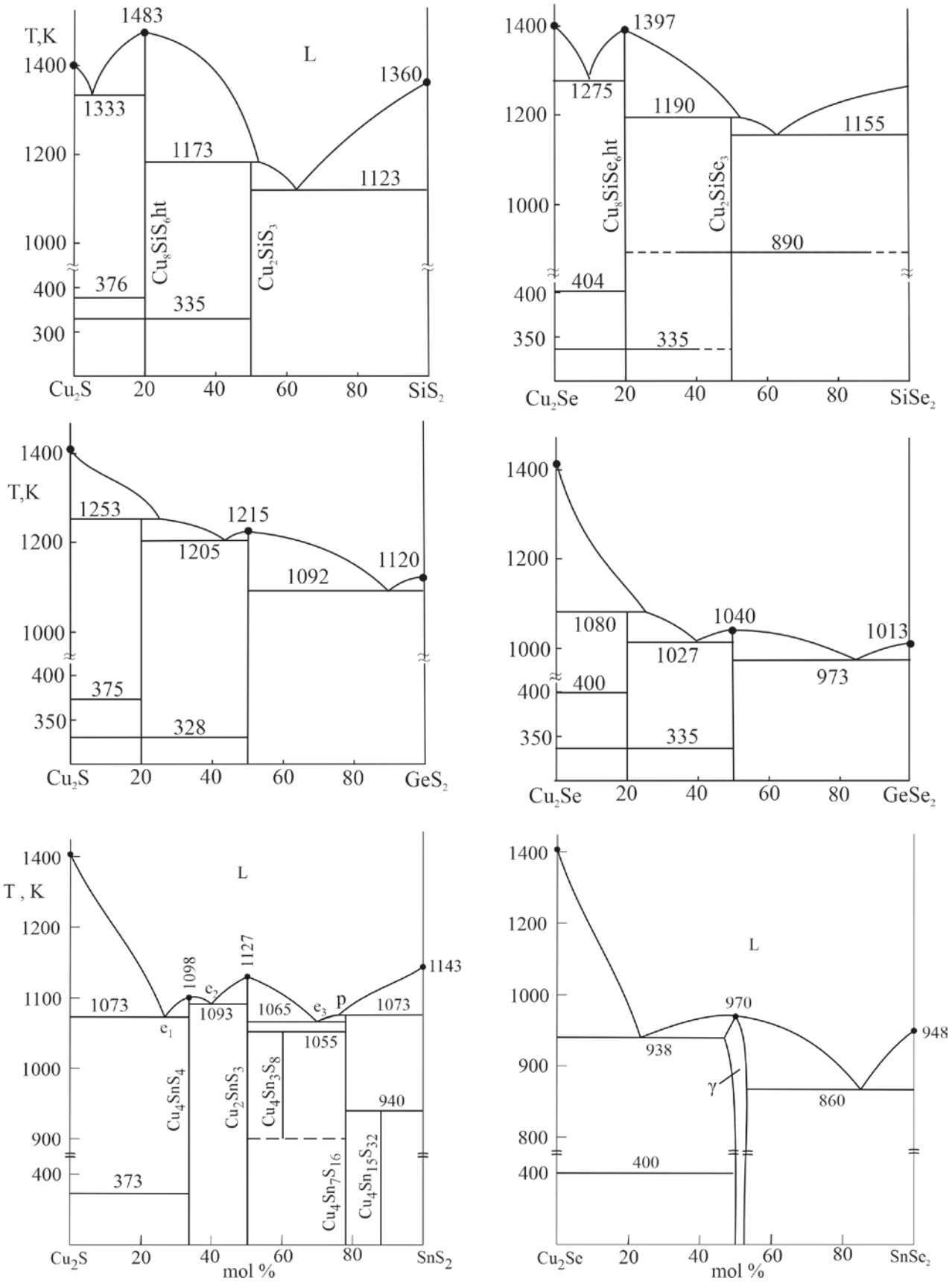

Fig. 3.3. Phase diagrams of quasi-binary systems Cu_2X-$B^{IV}X_2$

The Cu-Si-Se system also was studied only based on the quasi-binary section Cu_2Se-$SiSe_2$. In the study [156] ternary compounds Cu_8SiSe_6 and Cu_2SiSe_3, which melt congruently at 1380 K and incongruently at 1190 K and undergo polymorphic transformations at 335 and 890 K, respectively, were identified. Data [156] for the Cu_2Se-Cu_8SiSe_6 subsystem were confirmed in [157] (Fig. 3.3).

The Cu-Si-Te system. The complete *T-x-y* diagram of this system was constructed by the authors [158]. It has been shown that it is characterized by the formation of one ternary compound Cu_2SiTe_3, melting with decomposition according to a peritectic reaction.

Crystallographic data of copper-silicon chalcogenides [37, 159, 160] are shown in Table 3.1.

3.2. Phase equilibria in Cu-Ge-X systems

The Cu-Ge-S system. Quasi-binary section Cu_2S-GeS_2 of this system has been investigated in several studies [91, 161–164]. According to [161], ternary compounds Cu_8GeS_6 and Cu_2GeS_3 with incongruent melting at 1253 and 1213 K are formed in it. The Cu_8GeS_6 undergoes a polymorphic transformation at 328 K. The author [162] presented a new, more precise version of the *T-x* diagrams of this system (Fig. 3.3), which differs from the data [161] only in that the Cu_2GeS_3 compound melts congruently at 1215 K and forms eutectics with Cu_8GeS_6 and GeS_2.

In the study [164], an isothermal section of the phase diagram of the Cu-Ge-S system at 800 K was constructed, which reflected both of the above-mentioned ternary compounds. In [91] a diagram of solid-phase equilibria at 300 K (Fig. 3.4) and a schematic projection of the liquidus surface were presented. The latter reflects the primary crystallization fields of 11 phases, including ternary compounds Cu_8GeS_6 and Cu_2GeS_3.

The Cu-Ge-Se system. According to [165], the nature of phase equilibria of the Cu_2Se-$GeSe_2$ section is similar to the corresponding sulfide system: ternary compounds Cu_8GeSe_6 and Cu_2GeSe_3 melt incongruently at 1080 K and 1037 K. The phase diagram presented in [166] confirms the existence of the Cu_2GeSe_3 compound with congruent melting at 1033 K, and the Cu_8GeSe_6 compound represented as Cu_6GeSe_5. Later, the system was re-studied in the composition range of 15-60 mol. % $GeSe_2$ [167]. It was shown that the congruent melting temperature of Cu_2GeSe_3 is equal to 1053 K, and Cu_8GeSe_6 melts incongruently at 1083 K. In the review article [168], preference was given to the data of the study [167]. These data were later confirmed in [169] (Fig. 3.4).

The Cu-Ge-Te system was investigated in many studies [91, 170-172]. It was shown that the Cu_2Te-GeTe [170, 171] and Cu_2Te-Cu_3Ge [172] sections are almost quasi-binary. The first one belongs to the eutectic type, and the second one is characterized by the presence of monotectic and degenerate eutectic equilibria. The first version of the complete *T-x-y* diagrams of the Cu-Ge-Te system was constructed in [170]. The Cu_2GeTe_3 compound previously indicated in some studies was not reflected in this diagram [91]. In the second version of the phase diagram presented in [171], this error was corrected. This compound has been shown to form via a peritectic reaction at 773 K. It was also shown that, in contrast to the data [170], there were two immiscibility regions in the system, with one of them arising in the center of the concentration triangle. Finally, the third version of the phase diagram of the system was presented in [91, 172]. It basically confirmed the data of [171] but significantly differed greatly from it by the extent of the fields of primary crystallization of phases and the presence of one wide immiscibility region.

3.3. Phase equilibria in Cu-Sn-X systems

The Cu-Sn-S system. Some polythermal sections of this system were studied in 1974 [174]. It was shown that the Cu_2S-SnS and Cu_2S-SnS_2 sections are quasi-binary. The first one is of the eutectic type, and 4 intermediate phases are formed in the second one: Cu_4SnS_4, Cu_2SnS_3, $Cu_4Sn_3S_6$, and $Cu_2Sn_4S_9$. In a later published study ternary compounds Cu_4SnS_4, Cu_2SnS_3, and $Cu_4Sn_7S_{16}$ have been identified in the Cu_2S-SnS_2 system [175]. The same results were obtained by the authors [176]. Later the Cu_2S-SnS_2 section was re-studied in [177] and a phase diagram reflecting copper-tin sulfides Cu_4SnS_4, Cu_2SnS_3, $Cu_4Sn_3S_6$, and $Cu_2Sn_3S_7$ was presented. Structural studies [175-181] confirmed the existence of Cu_4SnS_4, Cu_2SnS_3, and $Cu_4Sn_7S_{16}$ compounds. We have not found crystallographic data for the other two compounds mentioned above. At the same time, the authors of [182] reported the synthesis of

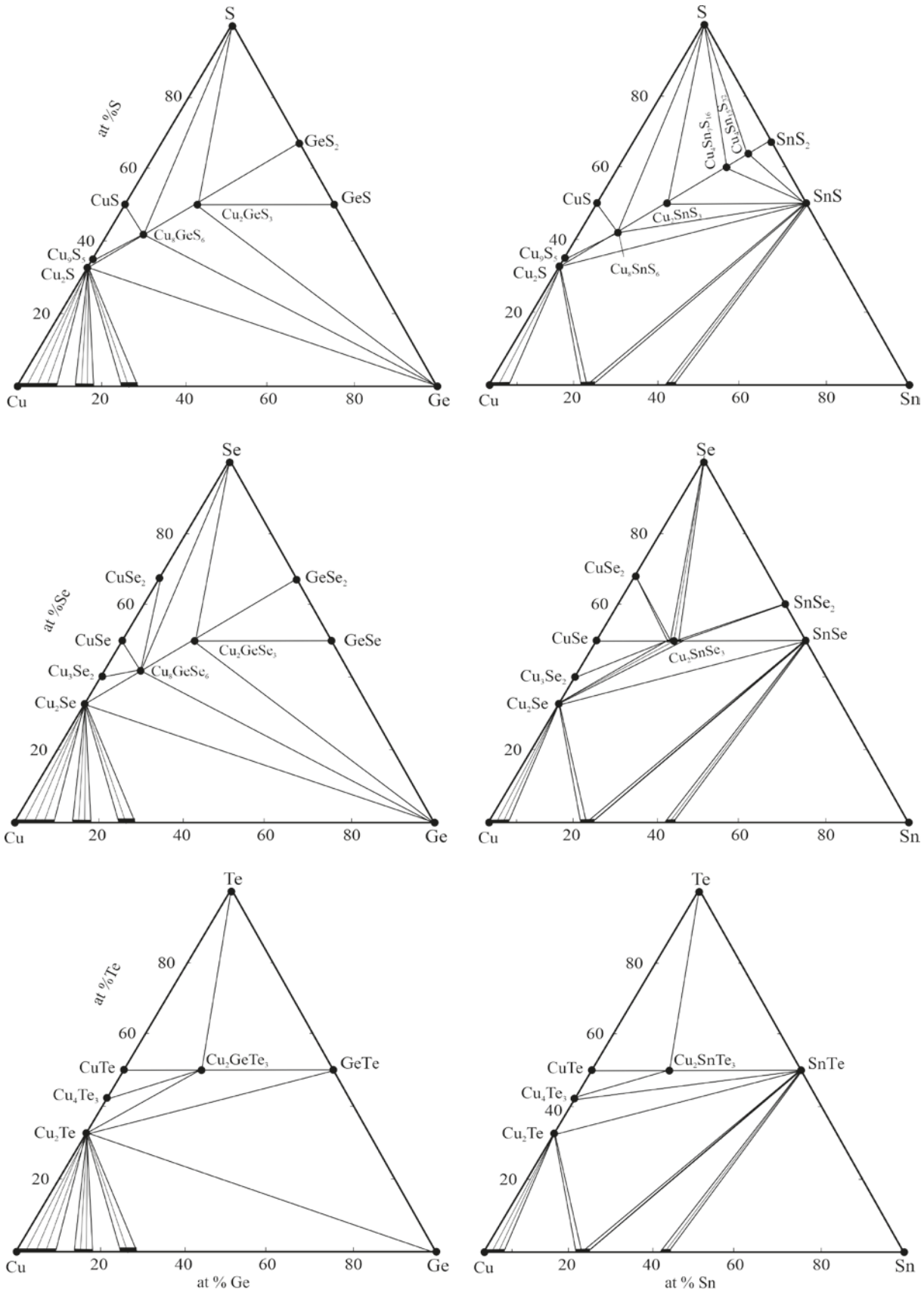

Fig. 3.4. Solid-phase equilibria diagrams of Cu-Ge-X and Cu-Sn-X systems at 300 K

the $Cu_4Sn_{15}S_{32}$ compound with a cubic structure, close in composition to $Cu_2Sn_4S_9$ indicated in [174] and also with a cubic structure. Taking into account the above data, we have constructed a phase diagram of the Cu_2S-SnS_2 system (Fig. 3.3), reflecting five triple compounds. Probably, this system requires further investigation. A diagram of solid-phase equilibria of the Cu-Sn-S system, constructed by us considering the data of these studies, is presented in Fig. 3.4 [175–178].

The Cu-Sn-Se system. The results of the study on this system are summarized in [91, 183]. The only ternary compound of this system is Cu_2SnSe_3, formed on the quasi-binary section of Cu_2Se-$SnSe_2$, it melts congruently at 963 K and crystallizes in a cubic structure [184] (Fig. 3.3). Another quasi-binary Cu_2Se-SnSe section of this system belongs to the eutectic type [184]. A repeated study of the indicated sections [185] led to results similar to those reported in [184]. The results of [185] demonstrated that Cu_2SnSe_3-Se and Cu_2SnSe_3sections, which also belong to the eutectic type are quasi-binary. In [186] a projection of the liquidus surface and some polythermal sections of the Cu-Sn-Se system were presented. The authors [91] pointed out some shortcomings of the study [186] and presented a second version of the projection of the liquidus surface. According to [91], the system has two wide immiscibility regions and associated invariant synthetic and three monotectic equilibria. The solid-phase equilibria diagram of the Cu-Sn-Se system, constructed in [91], is shown in Fig. 3.4. As can be seen, the Cu_2SnSe_3 compound has a noticeable homogeneity region in the stable CuSe-SnSe cross section (g-phase) and forms connodes with all phases in the composition range of Cu_2Se-SnSe-Se.

The Cu-Sn-Te system. The studies [187, 188] present a complete *T-x-y* diagram of this system, characterized by the presence of one ternary compound Cu_2SnTe_3 composition. It has a cubic structure and melts incongruently at 680 K. Later in [91] a version slightly different from the data in [187, 188] of the liquidus surface projection was presented. The isothermal section of the phase diagram at 300 K according to data from [91, 187, 188] is shown in Fig. 3.4. A detailed overview of the system is provided in [189].

3.4. Thermodynamic properties of ternary compounds of Cu-B^{IV}-X systems

The thermodynamic properties of copper-silicon are practically unstudied. There are studies [155, 190] where the thermodynamic functions of phase transitions of the Cu_8SiS_6 and Cu_8SiSe_6 compounds were determined using differential scanning calorimetry (DSC).

The standard thermodynamic functions of copper-germanium chalcogenides were determined by measuring the EMF of concentration cells of type (2.2) [50, 51, 191–194].

The authors planned experiments on the Cu-Ge-S and Cu-Ge-Se systems [191] based on the fact that Cu_8GeS_6 and Cu_8GeSe_6 compounds have polymorphic transitions in the temperature range of EMF measurements. Experiments have shown that the temperature dependences of the EMF for electrode alloys containing Cu_8GeS_6 and Cu_8GeSe_6 compounds are two straight lines with a breakpoint at the temperature of their polymorphic transformation. From the EMF measurement data, partial molar functions of copper were calculated for two modifications of the indicated compounds, which were used to calculate the thermodynamic functions of formation (Table 3.2) and polymorphic transitions (Table 3.3).

The thermodynamic properties of copper-tin chalcogenides have been studied by the EMF method with a solid electrolyte [50, 51, 196], and the Cu_2SnSe_3 compounds were studied also using a classic version of the EMF method with a liquid electrolyte [51] (Table 3.3). As can be seen, the thermodynamic functions of Cu_2SnSe_3, obtained by two modifications of the EDS method, agree well with each other. It was also evident that the numerical values of the thermodynamic functions of copper-tin sulfides according to [196] were significantly lower than the data of [50, 51]. Data for the $Cu_2Sn_4S_9$ and Cu_4SnS_4 compounds [196] were lower than even the sum of the corresponding values for Cu_2S and SnS_2, which is thermodynamically impossible. A similar situation was also observed for the Cu_2GeSe_3 and Cu_8GeSe_6 compounds [193]. In our opinion, this was due to the incorrect formulation of potential-forming reactions by the authors [193, 196]. The results of a new calorimetric study of the Cu_2SnS_3 [197] were also in good agreement with the data obtained by the EDS method [193] (Table 3.2).

Table 3.2. Standard integral thermodynamic functions of ternary compounds of the Cu-B^{IV}-X systems

Phase	$-\Delta_f G^0$	$-\Delta_f H^0$	S^0 J·K^{-1}·mol^{-1}	Ref.
	kJ·mol^{-1}			
Cu_2GeS_3	211.3±2.4	213.7±2,3	190.3±5.5	[194]
RT-Cu_8GeS_6	438.9±2.5	425.9±4.2	536.3±13.1	[191]
HT-Cu_8GeS_6	*445.3±3.1	420.8±5.6	552.1±15.8	[191]
Cu_2GeSe_3	176.8±3.1	173.9±3.1	233.3±5.1	[192]
	80.7±1.5	86.7±6.9	-	[193]
RT- Cu_8GeSe_6	341.1±3.3	327.4±4,5	596.7±11.6	[191]
	105.1±1.9	114.5±9.2	143±2	[193]
HT- Cu_8GeSe_6	*348.1±3.7	315.6±5.0	632.3±12.5	[191]
$Cu_2Sn_4S_9$	659.9±4.3	650.9±29.7	560.3±74.7	[50, 51]
	165.4±1.5	141.6±6.3	639.8±18.3	[196]
Cu_2SnS_3	239.6±1.5	242.6±12.0	196.3±21.9	[50, 51]
	169.3±1.3	150.0±5.5	278.6±15.7	[196]
		263.79 ± 2.28		[197]
Cu_4SnS_4	316.4±2.4	327.7±18.8	266.5±28.2	[50, 51]
	261.3±2.4	220.8±9.4	414.4±20	[196]
Cu_2SnSe_3	189.5±2.6	187.5±4.8	251.6±5.0	[50, 195]
	198.4±0.6	198.5±2.9	237±5	[51]
Cu_2SnTe_3	117.7±1.4	116.2±2.4	264±6	[50, 51]

***Note:** data related to 400 K is marked with an asterisk

Table 3.3. Temperatures and thermodynamic functions of phase transitions of some ternary compounds of the Cu-B^{IV}-X systems

Compound	T_{melt}	$\Delta H_{phase\ trans}$, kJ·mol^{-1}	$\Delta S_{phase\ trans}$, J·mol^{-1}·K^{-1}	Method, Ref.
Cu_8GeS_6	328	5.1±2.4	15.5±7.5	EMF, [191]
	330	15.5±0.6	47.1±1.9	DSC, [155]
Cu_8GeSe_6	335	11.9±2.8	35.5±8.4	EMF, [191]
	330	11.2±0.5	34.0±1.4	DSC, [190]
Cu_8SiS_6	336	14.9±0.6	44.2±1.8	DSC, [155]
Cu_8SiSe_6	325	14.7±0.6	45.3±1.8	DSC, [190]

The values of heat and entropies for polymorphic transitions of $Cu_8B^{IV}X_6$ compounds, obtained by both methods, except for Cu_8GeS_6, are in good agreement as can be seen in Table 3.3. The relatively high errors in the data obtained by the EMF method were because in this method the partial enthalpy and entropy are calculated indirectly from the temperature dependence coefficient of the EMF [51, 110].

3.5. Phase equilibria in quaternary systems consisting of copper chalcogenides and p^2-elements

The concentration planes $2Cu_2X + B^{IV}X' \leftrightarrow 2Cu_2X' + (B^{IV})'X_2$ **(I),** $Cu_2X–B^{IV}X_2–(B^{IV})'X_2$ **(II)** и Cu_2X-Ag_2X-$B^{IV}X_2$ **(III),** (where B^{IV} and $(B^{IV})'$ – Si, Ge, Sn; X and X′ – S, Se, Te) of the corresponding quaternary systems are of greatest interest for the search for solid solutions with different types of substitution based on ternary compounds of Cu-B^{IV}-X systems. In the last decade we have studied some systems of the indicated types (Cu_2Se-$GeSe_2$-$SnSe_2$ [198], Cu_2S-Cu_8SiS_6-Cu_8GeS_6 [155], Cu_2Se-Cu_8SiSe_6-Cu_8GeSe_6 [157], $2Cu_2S+GeSe_2 \leftrightarrow 2Cu_2Se+GeS_2$ [199, 200], Cu_2S-Ag_2S-GeS_2 [37] and Cu_2Se-Ag_2Se-$GeSe_2$ [37]), as well as individual polythermal sections [201–205], composed of ternary compounds-analogues of the $A^I_8B^{IV}X_6$ and $A^I_2B^{IV}X_3$ types. The isothermal sections of the phase diagrams of these systems at room temperature are shown in Fig. 3.5, and the sections based on $Cu_8B^{IV}X_6$ compounds are presented in Fig. 3.6, sections based on $Cu_2B^{IV}X_3$ are shown in Fig. 3.7. These diagrams

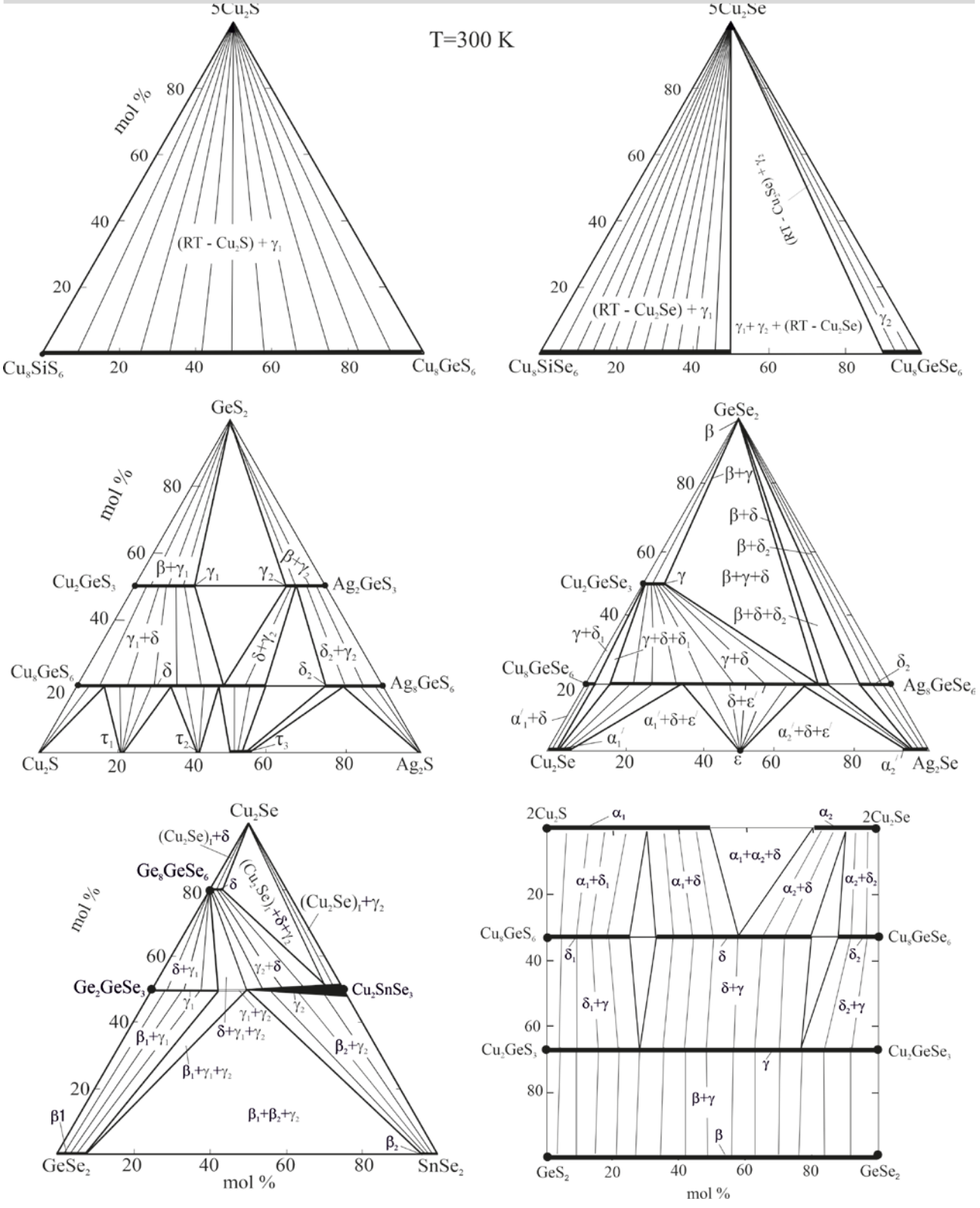

Fig. 3.5. Solid-phase equilibria diagrams at 300 K of some quaternary systems formed by copper chalcogenides and p2-elements

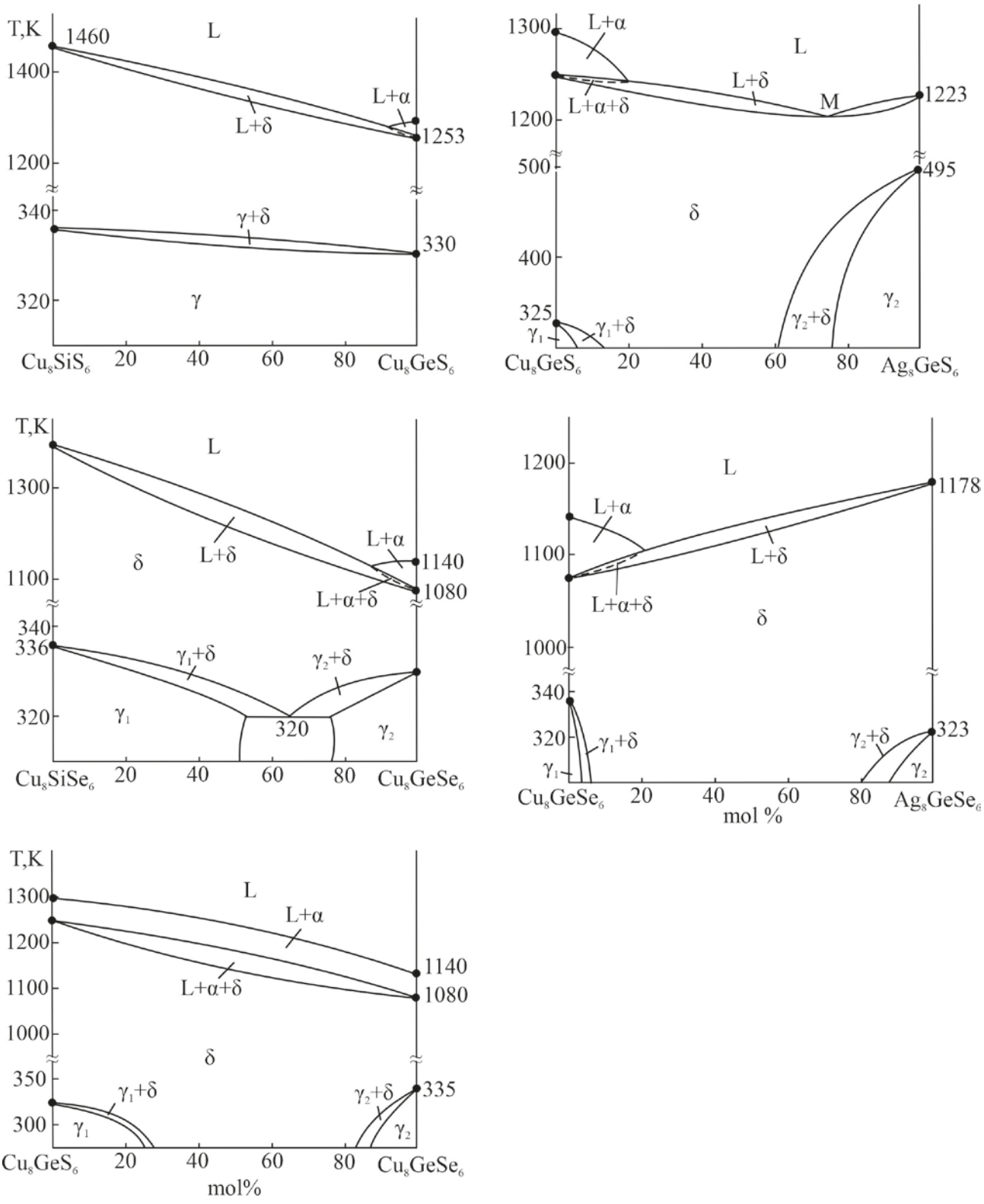

Fig. 3.6. *T-x* diagrams of some systems composed of compounds of the Cu_8GeX_6 type

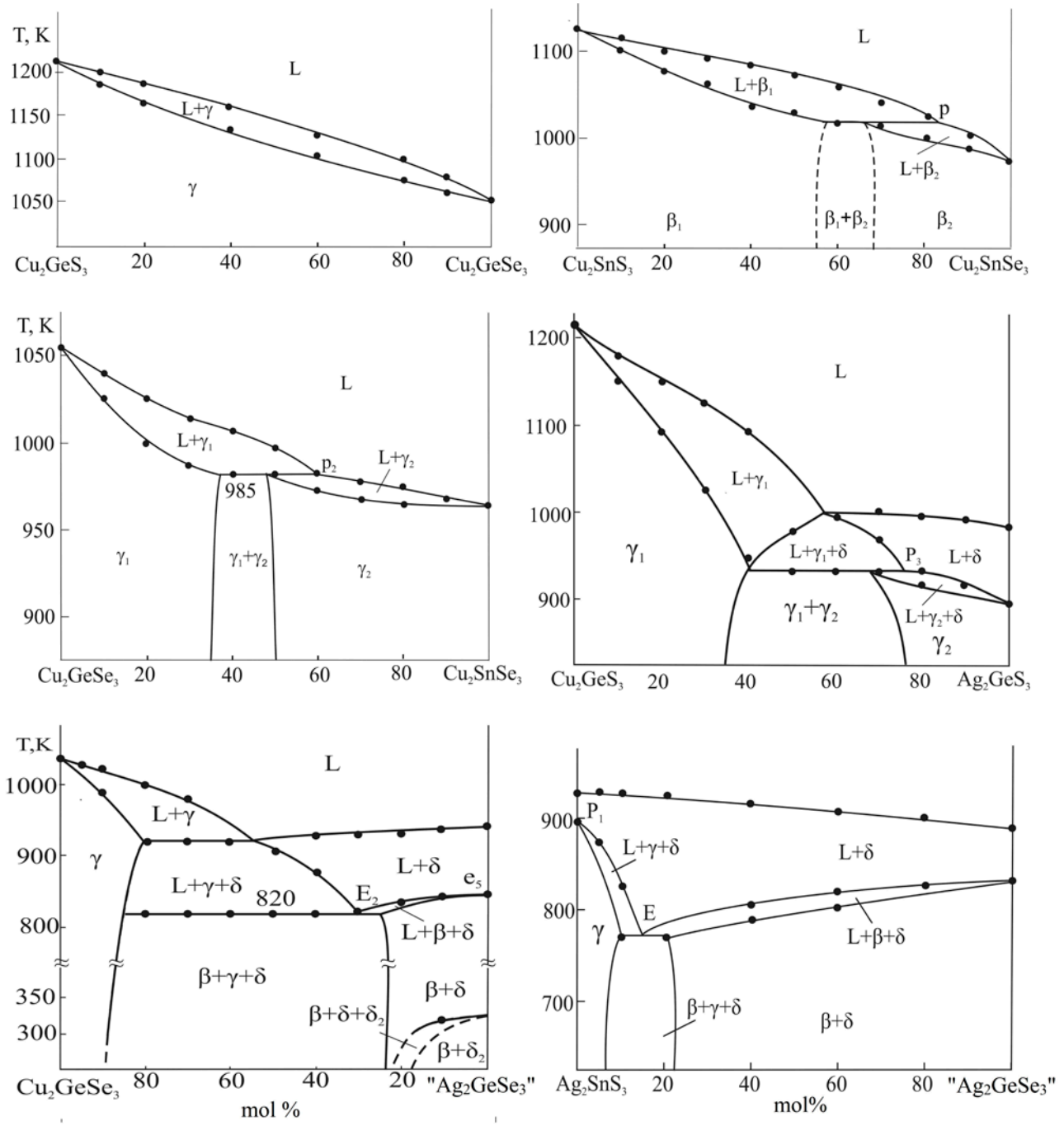

Fig. 3.7. *T-x* diagrams of some systems composed of compounds of the $Cu_2B^{IV}X_3$ type

demonstrate the formation of unlimited or broad solid solutions based on ternary compounds of both types. Several studies [200–205] present the results of a comprehensive study of phase equilibria and thermodynamic properties of the above and some similar systems.

$2Cu_2X + B^{IV}X' \leftrightarrow 2Cu_2X'$ systems. Out of the systems of this type, only the reciprocal system $2Cu_2S+GeSe_2 \leftrightarrow 2Cu_2Se+GeS_2$ has been fully studied [199, 200]). The system is characterized by the formation of continuous or wide regions of chalcogen-substituted solid solutions based on Cu_8GeX_6 and $Cu_2B^{IV}X_3$ compounds (Figs. 3.6–3.8). In the Cu_8GeS_6-Cu_8GeSe_6 system, this is accompanied by a decrease in the temperatures of polymorphic transitions of the original ternary compounds and stabilization of their high-temperature cubic modifications at room temperature and below.

The projection of the liquidus surface of the $2Cu_2S+GeSe_2 \leftrightarrow 2Cu_2Se+GeS_2$ system is shown in Fig. 3.8. It can be used for growing crystals of solid solutions based on ternary compounds by directional crystallization from solution-melts in a wide range of compositions.

$Cu_2X–B^{IV}X_2–(B^{IV})'X_2$ systems. The *T-X* Cu section diagrams of the Cu_8SiS_6-Cu_8GeS_6 [155] and Cu_8SiSe_6-Cu_8GeSe_6 [157] sections are shown in Fig. 3.6. As can be seen, both systems are partially quasi-binary and are characterized by the formation of continuous series of solid solutions between high-temperature cubic modifications of the original ternary compounds. However, they significantly differ by the nature of phase

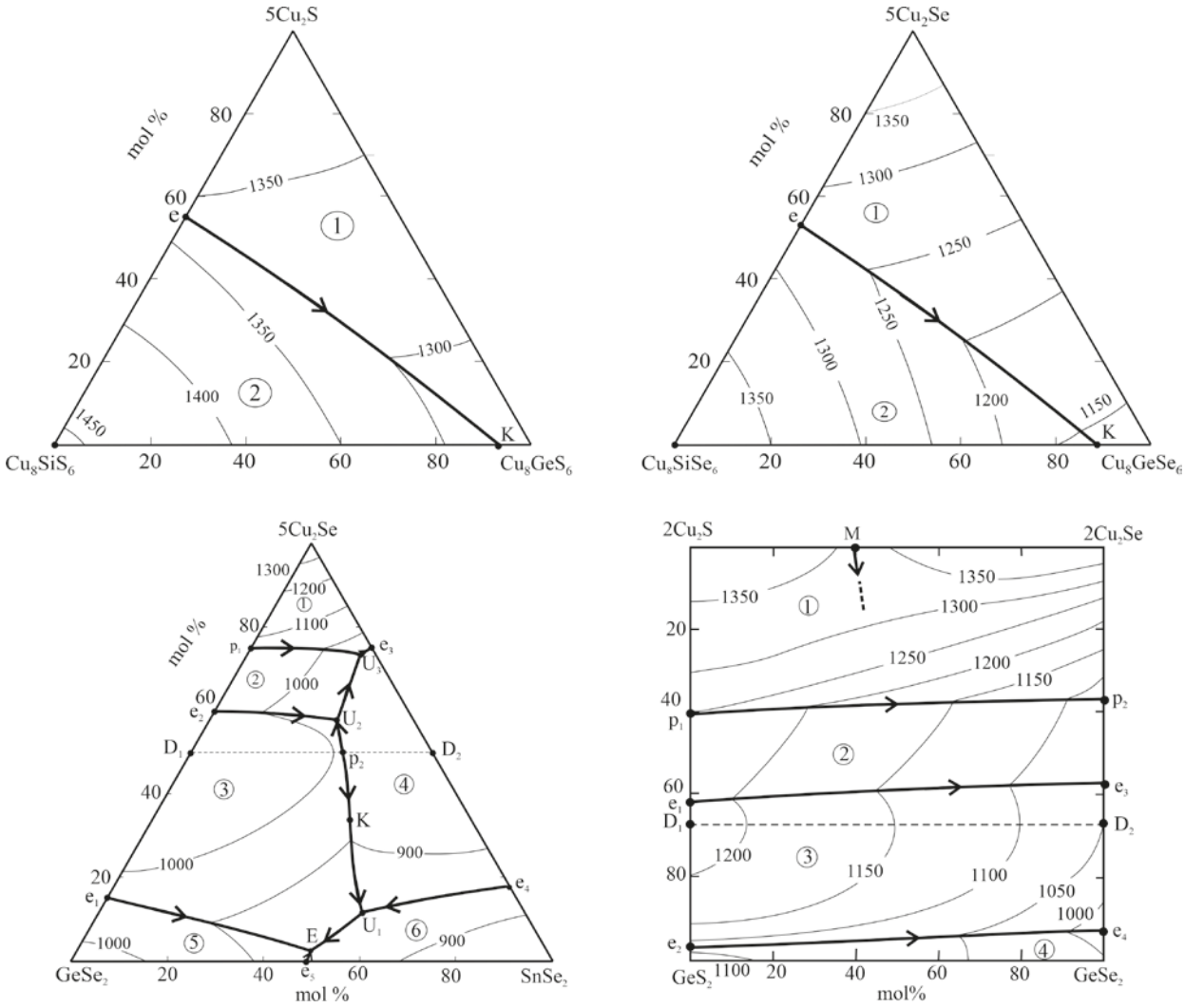

Fig. 3.8. Projections of liquidus surfaces of some quaternary systems composed of copper chalcogenides and p^2-elements

equilibria in the subsolidus region. In the sulfide system, a continuous series of solid solutions are also formed between RT modifications of the initial isostructural compounds, crystallizing in an orthorhombic lattice with sp. gr. $Pna2_1$ or $Pmn2_1$ (Table 3.1). In the Cu_8SiSe_6-Cu_8GeSe_6 system based on RT modifications of the initial compounds, limited regions of solid solutions are formed (g_1- and g_2-phase), and eutectoid equilibrium is established at a temperature of (320 K).

A projection of the liquidus surface was constructed for the Cu_2Se-$GeSe_2$-$SnSe_2$ system [198], and for two systems of this type, their fragments Cu_2S-Cu_8SiS_6-Cu_8GeS_6 [155] and Cu_2Se-Cu_8SiSe_6-Cu_8GeSe_6 [157] were constructed (Fig. 3.8). In the indicated studies, various isothermal and vertical sections of phase diagrams of the considered systems were also constructed.

Cu_2X-Ag_2X-$B^{IV}X_2$ systems. There are data on two vertical sections of phase diagrams: Cu_8GeS_6-Ag_8GeS_6 [204] and Cu_8GeSe_6-Ag_8GeSe_6 [203] (Fig. 3.6). They are characterized by a decrease in phase transition temperatures and a significant expansion of homogeneity regions of d-phases with a cubic structure down to room temperature and below. Both systems are partially quasi-binary, with the HT-$Cu_{2-x}Ag_xS(Se)$ phases primarily crystallizing from melts near incongruently melting copper argyrodites, which based on composition are outside the *T-x* planes of these sections.

Summarizing the above data in this section, it should be noted that the quasi-binary Cu_2X-$B^{IV}X_2$ sections, on which compounds of the $Cu_2B^{IV}X_3$ and $Cu_8B^{IV}X_6$ types were formed have been studied in detail in all Cu-B^{IV}-X systems (Fig. 3.3). Out of then, only the Cu_2S-SnS_2 section is characterized by more complex interactions. At least five triple compounds are formed on it. At the same time, the complete *T-x-y* diagrams are known only for the Cu-Si-Te, Cu-Ge-Te, Cu-Sn-Se, and Cu Sn-Te systems with relatively simple interactions of components. It should also be noted that the thermodynamic properties of most copper-germanium and copper-tin chalcogenides have been studied by the EMF method and mutually consistent sets of standard integral thermodynamic functions have been obtained for them. The studies devoted to the investigation of several quaternary systems composed of copper chalcogenides and p^2-elements are important from the point of view of optimizing the functional properties of $Cu_2B^{IV}X_3$ and $Cu_8B^{IV}X_6$ compounds.

4. Copper chalcogenides with elements of the arsenic subgroup

Ternary Cu-As(Sb, Bi)-chalcogen systems have long been the focus of close attention of researchers for two reasons. Firstly, in these systems, especially in sulfide systems, many crystalline phases with different structural forms are formed [22], which leads to different functional properties and potential applications. According to data from numerous studies [22, 206–236], ternary compounds of these systems are valuable environmentally friendly functional materials with photoelectric, optical, thermoelectric, and other properties. Secondly, many ternary compounds of these systems occur in nature as minerals: enargite and lucionite Cu_3AsS_4; tennantite $Cu_{12}As_4S_{13}$, tetrahedrite $Cu_{12}Sb_4S_{13}$; chalcostibite $CuSbS_2$; synergite $Cu_6As_4S_9$; lautite CuAsS, etc. They are of great interest to mineralogy and geochemistry and provide valuable information about the physical conditions on Earth at the time of their formation [41, 42].

The crystal structures of some of the above minerals are shown in Figure 4.1. The compound $CuSbS_2$ crystallizes in the orthorhombic system (sp. gr. *Pnma*) and has a layered structure consisting of SbS_2 and CuS_3 chains along the axis *b*, formed by the interlocking of square pyramids of Sb and tetrahedral units of CuS_4. These two infinite chains are linked together and create layers that are perpendicular to the axis *c*. The distance between them (2.051 Å) allows intercalation of small atoms, ions or molecules [22]. Tetrahedrite $Cu_{12}Sb_4S_{13}$ has a cubic sphalerite-like structure (sp. gr. $I\bar{4}3m$). Six of the 12 Cu atoms occupy trigonal planar 12e sites, and the rest are distributed among tetrahedral 12d sites. Four of the six tetrahedral positions are occupied by Cu^+, and the other two positions are occupied by Cu ions^{2+} [22]. At the same time, the trigonal planar positions are occupied exclusively by Cu^+ ions. The Sb atoms also occupy a tetrahedral position but are bonded to only three S atoms, resulting in a void in the structure and an unshared pair of electrons, as in Cu_3SbS_3. The combination of factors such as a large number of atoms in the

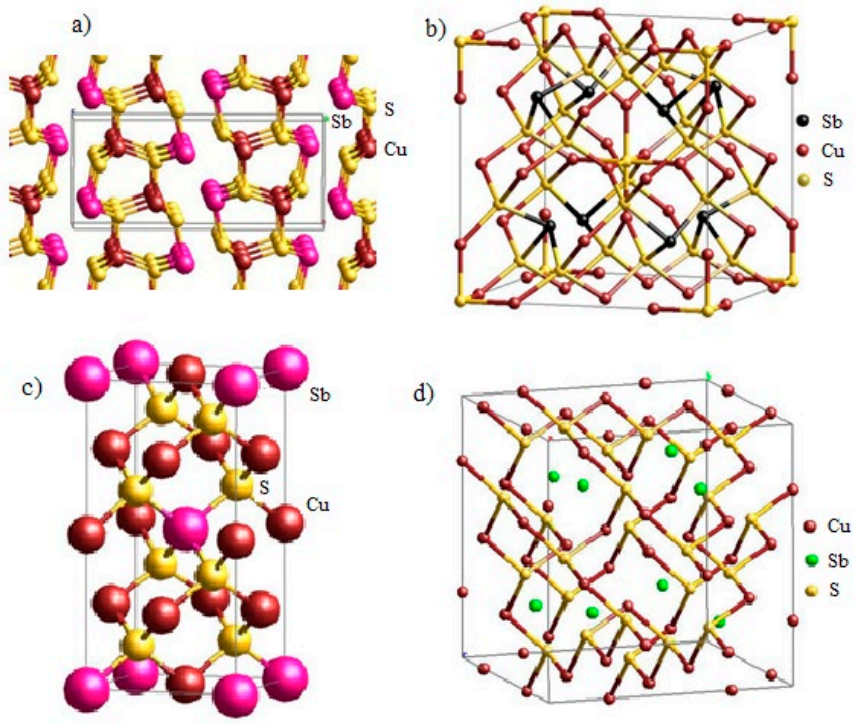

Fig. 4.1. Crystal structures of copper-antimony sulfides: orthorhombic $CuSbS_2$ (a), cubic $Cu_{12}Sb_4S_{13}$ (b), tetragonal Cu_3SbS_4 (c) and orthorhombic Cu_3SbS_3 (d)

unit cell, high anharmonicity and low-energy vibrations of the Cu atom outside the trigonal planar unit [CuS_3] lead to abnormally low thermal conductivity of this material, which is important for thermoelectrics.

Crystallographic data of the most characteristic ternary compounds of the Cu-B^V-X systems are presented in Table 4.1.

Copper-arsenic and copper-antimony sulfides and complex phases based on them [206–212] are considered promising candidates for use as absorbers of *p*-type in solar cells due to the wide availability and environmental safety of raw materials, suitable band gap width and high absorption coefficient. The favorable band gap width of these phases indicates the prospect of their application also as wide-band gap semiconductors in third-generation photovoltaic devices. The largest number of studies [213–221] are devoted to chalcostibite $CuSbS_2$, which is considered a substitute material for $CuInS_2$ due to its similar optical properties and the additional advantage of its higher abundance in the Earth and lower cost of antimony compared to indium.

In a recently published review [222], the Cu_3BiS_3 compound is characterized as a sustainable and cost-effective photovoltaic material.

Synthetic analogues of many chalcogenide minerals of copper with arsenic and antimony [223-228], as well as solutions and composite materials based on them [228-231], possessing low thermal conductivity and an anisotropic crystalline structure, have promising thermoelectric properties. Thus, in the review [228] it was noted that by 2015, for some natural and alloyed tetrahedrite materials, zT values of about ~1.0 at ~723 K had been achieved, which is comparable to conventional thermoelectric *p*-type materials. In recent years, there has been increased interest in copper-bismuth chalcogenides as thermoelectric materials with very low thermal conductivity [232–235].

The authors [236] proposed a new concept for increasing the stability and efficiency of copper thermoelectrics by obtaining composites of the "copper chalcogenide-copper tetrahedrite" type. According to the authors, the proposed solution allows the successful blocking of excessive copper migration and stabilization of the composition and properties of the material during subsequent thermal cycles.

It should also be noted that, according to several studies, copper-bismuth chalcogenides, in particular $CuBiS_2$, exhibit good photothermal

Table 4.1. Crystallographic parameters of the ternary compounds of Cu-B^V-S(Se) systems

Compound	Crystal system, sp. gr. and lattice parameters, nm	Ref.
Cu_3AsS_4	Rhombic, *Pmn*2_1, *a* = 7.399, *b* = 6.428, *c* = 6.145	[238]
$Cu_{12}As_4S_{13}$	Cubic, *I*-43*m, a* = 1.0168	[239]
$Cu_6As_4S_9$	Triclinic, *a* = 9.064, *b* = 9.830, *c* = 9.078, α = 90°, β = 109°30, γ = 107°48	[240]
CuAsS	Rhombic, *Pnma, a* = 11.356, *b* = 3.754, *c* = 5.453	[237]
$Cu_4As_2S_5$	Monoclinic, *C*12/*m*1, *a* = 10.35,*b* = 14.65, *c* = 33.34, β = 96°	[238]
HT-Cu_3AsSe_4	Cubic, *Fm*3*m, a* = 0.5535	[251]
RT-Cu_3AsSe_4	Tetragonal, *I*-42*m, a* = 5.53, *c* = 10.83	[251]
$CuAsSe_2$	Monoclinic, *a* = 5.117, *b* = 12.293, *c* = 9.464, β = 98.546°	[248]
$Cu_4As_2Se_5$	Rhombohedral, *R*3, *a* = 14.0401, *c* = 9.6021	[248]
Cu_3AsSe_3	Cubic, *Pm*-3*m, a* = 5.758	[250]
$Cu_7As_6Se_{13}$	Hexagonal, *R*3, *a* = 14.025, *c* = 9.61, γ = 120	[250]
$CuSbS_2$	Orthorhombic, *Pnma*; *a* = 6.018(1), *b* = 3.7958(6), *c* = 14.495(7)	[264]
RT-Cu_3SbS_3	Monoclinic, *P21/c*; *a* = 7.808(1), *b* = 10.233(2), *c* = 13.268(2), β = 90.31(1)°	[266]
HT-Cu_3SbS_3	Rhombic, *Pnma*; *a*=7.828(3), *b* = 10.276(4), *c* = 6.604(3)	[266]
Cu_3SbS_4	Tetragonal, *I*$\bar{4}$2*m* ; *a* = 5.391(1), *c* = 10.764(1)	[267]
$Cu_{12}Sb_4S_{13}$	Cubic, *I*–43*m, a* = 10.308(1)	[265]
$Cu_{14}Sb_4S_{13}$	Cubic, *I*–43*m*, *a* = 10.448(1)	[261]
HT-Cu_3SbSe_4	Tetragonal, *I*$\bar{4}$2*m, a* = 0.5631, *c*= 1.1230	[272]
RT-Cu_3SbSe_4	Cubic, *Fm*3*m, a* = 0.5637	[100]
HT-Cu_3SbSe_3	Cubic, *F*$\bar{4}$3*m, a* = 0.560	[100]
RT-Cu_3SbSe_3	Orthorhombic, *Pnma, a* = 0.79668, *b* = 1.06587, *c* = 0.68207	[273]
$CuSbSe_2$	Orthorhombic, *Pnma, a* = 0.640, *b* = 0.395, *c* = 1.533	[100]
$CuSb_3Se_5$	Monoclinic, *C2/m*; *a* = 1.36499, *b* = 0.40711, *c* = 1.49215, β = 9 0.31°	[274]
Cu_3BiS_3	Orthorhombic, *P*$2_12_12_1$, *a* = 0.7723, *b* = 1.0395, *c* = 0.6715	[100]
$CuBiS_2$	Orthorhombic, *Pnma, a* = 0.6134(1), *b* = 0. 39111(8), *c* = 1.4548(8),	[264]
$CuBi_3S_5$	Monoclinic, *c*2*m*, *a* = 13.221, *b* =4.023, *c* = 14.077Å	[281]
$CuBi_5S_8$	Monoclinic, *C2/m*; *a* = 1.3214, *b* = 0.4025, *c* = 1.4087, β = 115.6°	[100]
HT-Cu_3BiSe_3	Cubic, *F*$\bar{4}$3*m, a* = 0.5865	[277]
RT-Cu_3BiSe_3	Monoclinic, *a* = 1.366, *b* = 0.417, *c* = 1.486, α = 119.1°	[100]
$CuBiSe_2$	Cubic, *Fm*3*m, a* = 0.569	[100]
$CuBi_3Se_5$	Triclinic, *P*1, *a* = 0.4168, *b* = 0.7182, *c* = 1.3388, α = 85.4°, β = 81.3°, γ = 73°	[278]

properties and anticancer effect [22, 38]. Due to the high X-ray attenuation coefficient, these compounds can visualize computed tomography [39].

4.1. Phase equilibria in Cu-As-X systems

The Cu-As-S system. Numerous studies on phase equilibria and the properties of ternary phases in the Cu–As–S system covering the period up to the beginning of the 90s of the last century are summarized in [91, 237]. It was shown that the available data on the Cu_2S-As_2S_3 section of phase diagrams are contradictory and differ from each other both in the number and composition of ternary compounds, and in the temperatures and nature of their melting. In particular, in [241] it was shown that this system is quasi-binary and is characterized by the formation of Cu_5AsS_4, Cu_3AsS_3, $Cu_{12}As_4S_{13}$, $Cu_4As_2S_5$, and $Cu_6As_4S_9$ ternary compounds. The authors of [237], taking into account data from several studies, presented a slightly different version of

the phase diagram from [238], according to which there are 3 ternary compounds in the system: $Cu_{12}As_4S_{13}$, $Cu_4As_2S_5$, and $Cu_6As_4S_9$. It should be noted that the $Cu_{12}As_4S_{13}$ phase by composition is outside the plane of this section, which could question the data [237] on its quasi-binary nature. In [242], a new review of the literature on the Cu–As–S system was presented and a critical assessment and thermodynamic modelling of the phase diagram were carried out.

The studies [243–246] published by our group presented the results of a comprehensive study of phase equilibria and thermodynamic properties of the Cu-As-S system. The solid-phase equilibrium diagram (Fig. 4.3) reflects Cu_3AsS_4, $Cu_{12}As_4S_{13}$, $Cu_6As_4S_9$ and CuAsS ternary compounds, which are synthetic analogues of known minerals. According to [246], in contrast to previously proposed versions of the phase diagram, the Cu_2S- As_2S_3 section is only partially quasi-binary (Fig. 4.2). This is because below the solidus in the composition range 0-40 mol. % of As_2S_3 this section passes through three-phase Cu_2S+II+IV and II+III+IV fields (Fig. 4.3). In [246] a detailed comparative analysis of the results obtained by authors on this section with literary data was carried out.

The liquidus of this system (Fig. 4.4) consists of 14 primary crystallization fields of phases, two of which (CuS and S) degenerate at the sulfur corner of the concentration triangle. This part of the phase diagram is shown schematically in an enlarged form. The system is characterized by the presence of two wide immiscibility regions formed by the penetration of the corresponding regions of the Cu-S boundary system into the depth of the concentration triangle. Another immiscibility region, originating from the binary system As-S is shown in Fig. 4.4. However, the boundaries of this region are not precisely established and are marked with dotted lines.

The Cu-As-Se system. Phase equilibria in this system are studied using the quasi-binary Cu_2Se-As_2Se_3 section [247–250]. The data from these studies significantly differ from each other. According to [247], a Cu_3AsSe_3 compound is formed in the system by a peritectic reaction at 773, the homogeneity region of which extends from 66.7 to 82 mol. % Cu_2Se. The $CuAsSe_2$ compound stable in the temperature range of 550-720 K is formed as the result of peritectic interaction of Cu_3AsSe_3 with the melt. In [247] the $Cu_6As_4Se_9$ compound, previously indicated in [249] was not confirmed. The second version of the phase diagram of the Cu_2Se-As_2Se_3 system was constructed by the authors [248]. The existence of ternary compounds Cu_3AsSe_3, $Cu_4As_2Se_5$, $CuAsSe_2$ has been demonstrated. The first compound exists in the temperature range of 700–770 K, and the second and third compounds melt with decomposition according to the peritectic reaction at 746 and 683 K. Another variant of the *T-x* diagrams of this system was presented in [250]. Only one ternary compound $CuAsSe_2$, melting incongruently at 725 K is reflected in this diagram.

According to [249], the Cu_2Se-As, Cu_3AsSe_4-As_2Se_3, Cu_2Se-Cu_3As, and Cu_3AsSe_4- Se sections are also practically quasi-binary. The first two belong to the eutectic type, and the subsequent ones are characterized by the presence of monotectic and eutectic equilibria.

In [250] a projection of the liquidus surface of the Cu-As-Se system is presented, on which two ternary compounds Cu_3AsSe_4 and $CuAsSe_2$ are shown. Two immiscibility regions emanating from the Cu-Se binary system were identified. The study also shows the presence of a wide glass formation region in the system, adjacent to the As-Se binary system.

According to [251] the Cu_3AsSe_4 compound melts incongruently at 773 K and undergoes a phase transition at 715 K. The low-temperature modification has a tetragonal structure, and the high-temperature modification has a cubic structure.

The studies [252-254] present the results of the research on phase equilibria and thermodynamic properties of the Cu-As-Se system. It has been established that it is characterized by the presence of five triple compounds: Cu_3AsSe_3, $CuAsSe_2$, $Cu_7As_6Se_9$, Cu_3AsSe_4, and CuAsSe (Fig. 4.3). Out of them, only the first two compounds are located on the quasi-binary Cu_2Se-As_2Se_3 section (Fig. 4.2). The projection of the liquidus surface constructed by us taking into account the data from [252–254] is shown in Fig. 4.4. It reflects primary crystallization fields of all the above copper-arsenic selenides. A complex interaction of components was observed in the Cu_2Se-As_2Se_3-

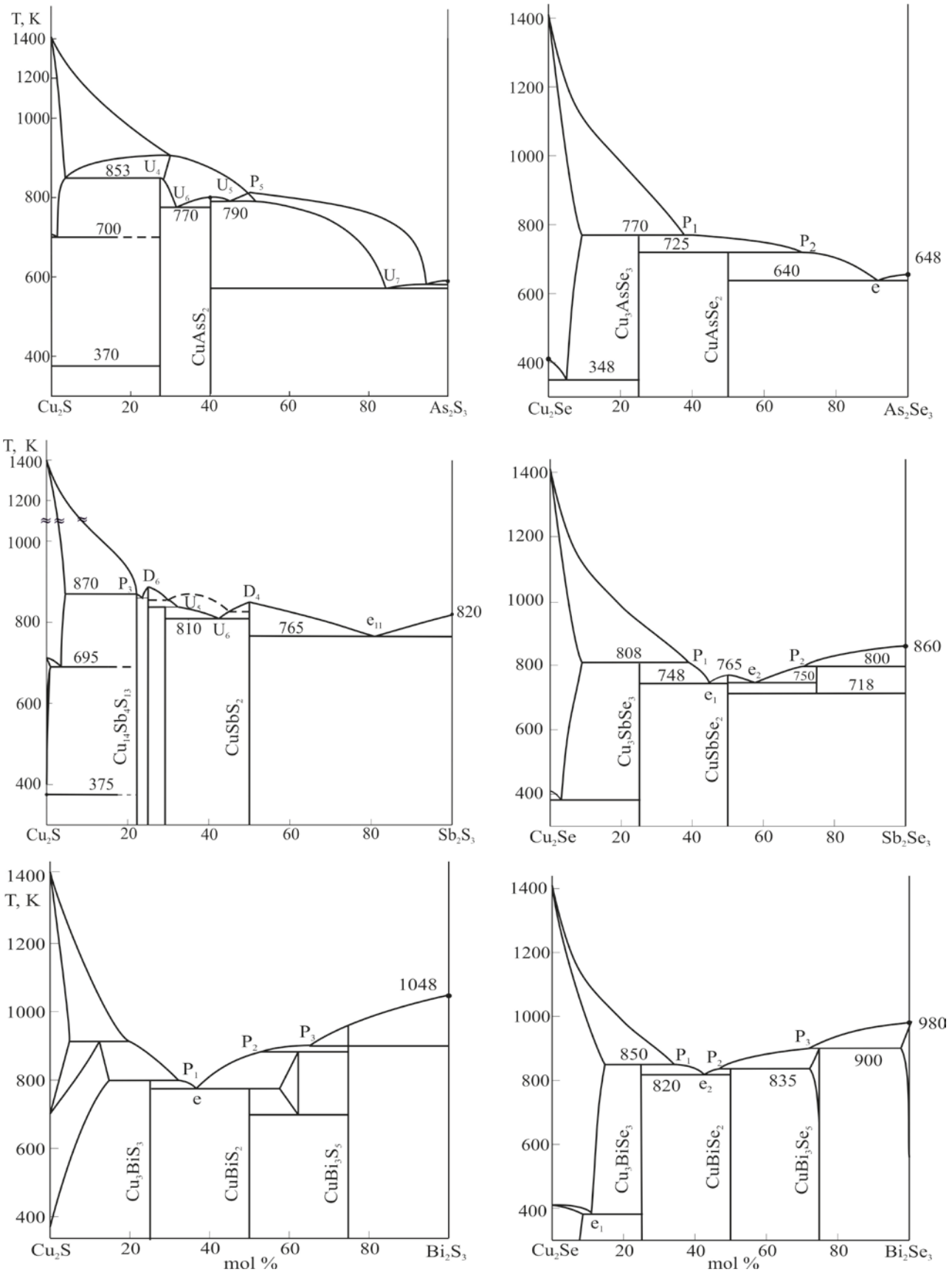

Fig. 4.2. Phase diagrams of the Cu_2X-$B^V_2X_3$ systems

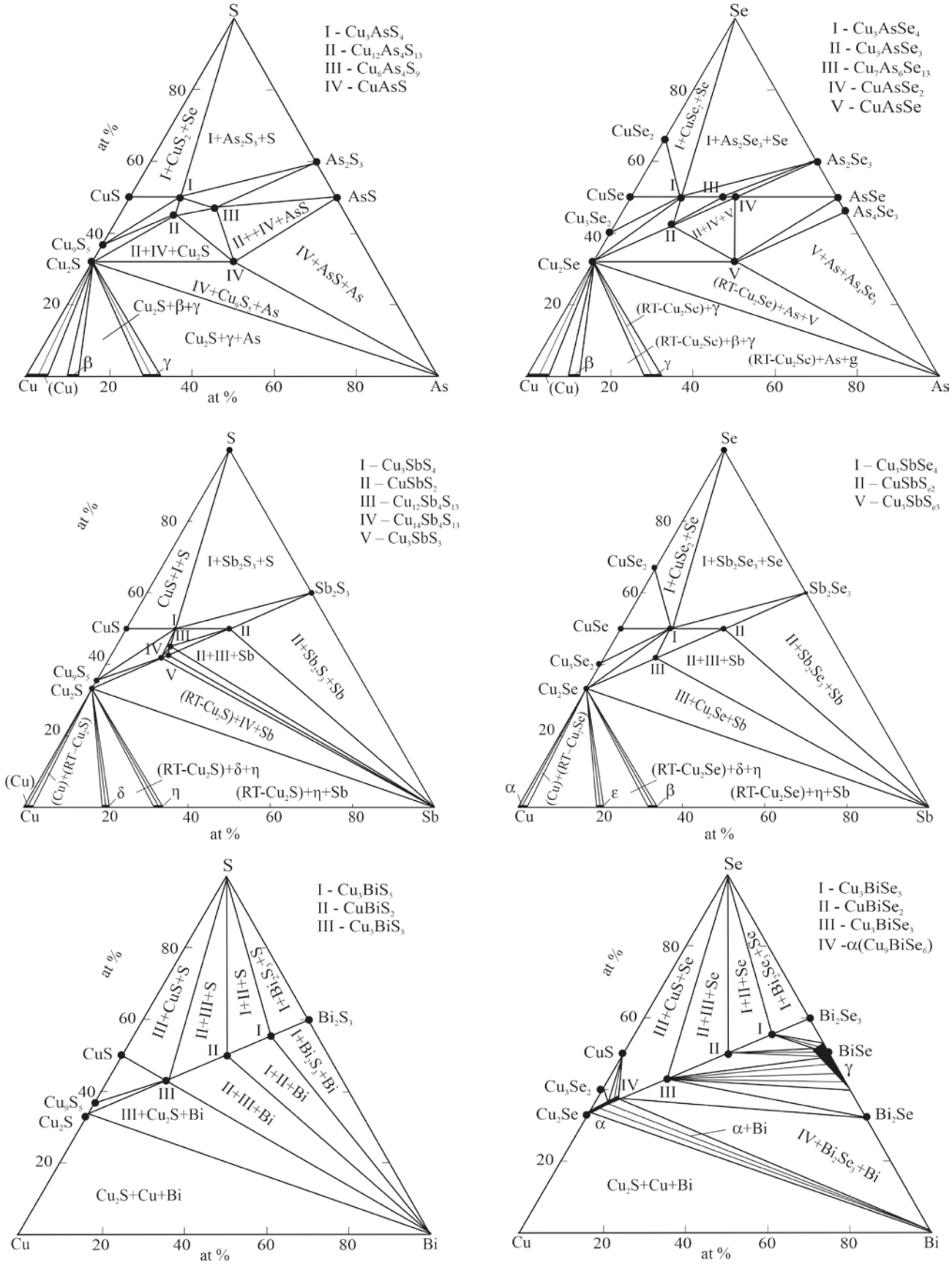

Fig. 4.3. Solid-phase equilibria diagrams of the Cu-B^{V}-X systems at 300 K

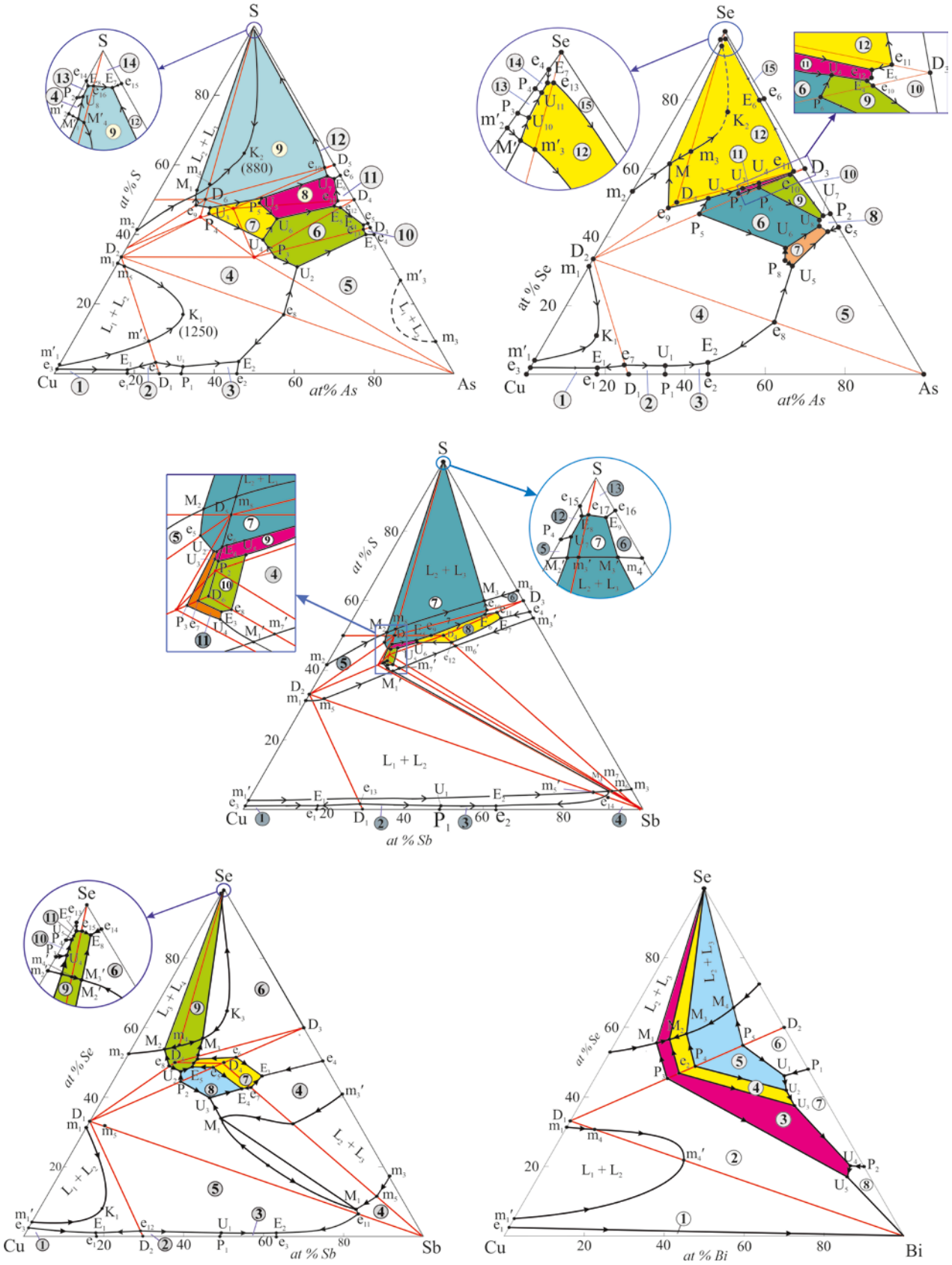

Fig. 4.4. Projections of liquidus surfaces of the Cu-B^{V}-X systems. The colored areas are the fields of primary crystallization of ternary compounds

Cu_3AsSe_4 subsystem, this region of the diagram was described in detail in [254].

The Cu-As-Te system. According to available data [91], ternary compounds are not formed in this system.

4.2. Phase equilibria in Cu-Sb-X systems

The Cu-Sb-S system. The studies of phase equilibria in the Cu-Sb-S system began at the beginning of the last century. The results of numerous studies in different years were summarized in the monograph [91] and studies [256, 257].

We will discuss some studies devoted to the Cu_2S-Sb_2S_3 section. Thus, the authors [258] showed that this section is quasi-binary and forms ternary compounds Cu_3SbS_3 and $CuSbS_2$. According to the data [259] on this section there is only one $CuSbS_2$ compound with congruent melting at 825 K. A detailed re-examination [260] showed that a complex interaction occurs in the vicinity of Cu_3SbS_3, involving the decomposition of this compound below 400 K and the formation of three different phases.

In a recently published study [257], the Cu–S–Sb system was studied using the CALPHAD method and a new version of the *T-x* diagram of the Cu_2S-Sb_2S_3 section, significantly different from previous studies was presented.

The complete *T-x-y* diagram, including various polythermal sections and an isothermal section at 300 K (Fig. 4.3), as well as a projection of the liquidus surface (Fig. 4.4), was shown in studies [261, 262]. According to [261], at room temperature, ternary compounds Cu_3SbS_4, $Cu_{12}Sb_4S_{13}$, $Cu_{14}Sb_4S_{13}$, Cu_3SbS_3, and $CuSbS_2$ exist in the system (Fig. 4.3).

According to [262], the liquidus surface of this system consists of 13 primary crystallization fields of phases. The crystallization fields of CuS and S degenerate at the sulfur corner of the concentration triangle. This part of the phase diagram is shown schematically in an enlarged form. A characteristic feature of the Cu-Sb-S system is two wide immiscibility regions. These regions have the appearance of wide continuous stripes between the immiscibility regions of the boundary binary Cu-S and Sb-S systems and occupy ~ 90% of the total area of the concentration triangle. Some curves of monovariant equilibria intersect the immiscibility regions and are transformed into four-phase monotectic equilibria (M_1 – M_1', M_2 – M_2' and M_3 – M_3' conjugate points in Fig. 4.4).

It should be noted that the complex nature of phase equilibria in a narrow region of compositions, is highlighted by a rectangle and presented in an enlarged form. In [262] data on the coordinates of invariant equilibria on *T-x-y* diagram of the system were presented and a detailed comparative analysis with data from previous studies was carried out. According to this study, the Cu_2S-Sb_2S_3 section (Fig. 4.2) is partially quasi-binary. In the region ⩾50 mol. % Sb_2S_3 the results coincide with the data of studies [258–260], according to which this part of the system is quasi-binary and belongs to the eutectic type. The region ⩽ 25 mol % Sb_2S_3 is also quasi-binary. This part of the phase diagram is characterized by the formation of $Cu_{14}Sb_4S_{13}$ and Cu_3SbS_3 compounds. However, in the intermediate range of compositions (25–50 mol. % Sb_2S_3), the Cu_2S-Sb_2S_3 section is not quasi-binary. The X-ray analysis data presented in [262] convincingly demonstrate the presence of a connode connection between the tetrahedrite $Cu_{12}Sb_4S_{13}$ phase, which according to the composition is located outside this section, with elemental antimony. This leads to the formation of three-phase regions of Cu_3SbS_3+$Cu_{12}Sb_4S_{13}$+Sb and $Cu_{12}Sb_4S_{13}$+$CuSbS_2$+Sb in the specified composition range.

The Cu-Sb-Se system. The quasi-binary Cu_2Se-Sb_2Se_3 section was investigated in studies [91, 259, 268–270]. According to [259], one compound of the $CuSbSe_2$ composition was formed in the system. The phase diagram was refined near this compound in [256]. The $CuSbSe_2$ and Cu_3SbSe_3 ternary compounds are shown on the phase diagram presented in [91]. In a recently published study [270], in addition to these compounds, a compound with the $CuSb_3Se_5$ composition, which exists in a narrow temperature range of 720-800 K, was discovered (Fig. 4.2).

The diagram of solid-phase equilibria at 300 K is shown in Fig. 4.3, and a projection of the liquidus surface, which reflects three ternary compounds $CuSbSe_2$, Cu_3SbSe_3, and Cu_3SbSe_4 is presented in Fig. 4.4. In a recently published study [271], the Cu-Sb-Se system was modelled

using the CALPHAD method and a projection of the liquidus surface was presented.

The Cu-Sb-Te system. According to [91], ternary compounds are not formed in this system. The compound of composition $CuSbTe_2$, indicated in some early studies, was not subsequently confirmed.

4.3. Phase equilibria in Cu-Bi-X systems

The Cu-Bi-S system. Phase equilibria in this system have been studied for more than 100 years. The results of these studies are summarized in [91, 256]. Their results have been shown to differ significantly. The *T-x* diagram constructed by us based on the data [275] is shown in Fig. 4.2. According to this diagram, Cu_3BiS_3, $CuBiS_2$, and $CuBi_3S_5$ sulfides are formed in the system. All of them melt with decomposition according to the peritectic reaction. The Cu_2S-Bi section is also quasi-binary, characterized by the presence of monotectic and degenerate eutectic equilibria [276]. According to the solid-state equilibrium diagram [91], three copper-bismuth sulfides exist at room temperature: $CuBi_3S_5$, $CuBiS_2$, and Cu_3BiS_3 (Fig. 4.3).

The Cu-Bi-Se system. According to [276] the Cu_2Se-Bi section is quasi-binary and forms a phase diagram with monotectic and degenerate eutectic equilibria for Bi.

The first version of the *T-x* diagram of the Cu_2Se-Bi_2Se_3 quasi-binary section is presented in [277]. It is shown that it belongs to the eutectic type with limited mutual solubility of the components. The ordering occurs in the region of Cu_2Se-based solid solutions at 25 mol. % Bi_2Se_3 (Cu_3BiSe_3). According to [277] the Cu_3BiSe_3 phase crystallizes in the cubic syngony (superstructure close to the CaF_2 type). According to the data [100], the Cu_3BiSe_3 compound has a monoclinic structure.

The literature also contains information on the synthesis and crystal structure of ternary compounds $CuBiSe_2$ and $CuBi_3Se_5$ (Table 4.1). The first compound crystallizes in a cubic lattice, while the second has a triclinic structure.

The study [279] summarizes all available results on phase equilibria in the Cu-Bi-Se system and presents a complete picture of phase equilibria, including a series of polythermal sections, an isothermal section at room temperature (Fig. 4.3) and a projection of the liquidus surface (Fig. 4.4). In this system, as in the sulfur-containing one, three ternary compounds $CuBi_3Se_5$, $CuBiSe_2$, and Cu_3BiSe_3 melting incongruently (Fig. 4.2) are formed. The study also presents a new version of the phase diagram of the quasi-binary Cu_2Se-Bi_2Se_3 section. The formation of the three above-mentioned ternary compounds melting by the peritectic reaction at 900 K ($CuBi_3Se_5$), 835 K ($CuBiSe_2$), and 850 K (Cu_3BiSe_3) was confirmed. It has also been established that the Cu_3BiSe_3 compound is outside the homogeneity region of Cu_2Se, which has a maximum length of ~17 mol. % Bi_2Se_3 at 850 K.

The Cu-Bi-Te system. According to available data [91], ternary compounds are not formed in this system.

4.4. Thermodynamic properties of copper chalcogenides with p^3-elements

The standard integral thermodynamic functions of copper-arsenic sulfides and selenides are determined by measuring the EMF of concentration cells of type (2.2) with a solid electrolyte [245, 246] (Table 4.2). These data sets for Cu_3AsS_4, $Cu_6As_4S_9$, and CuAsS compounds were significantly (up to 20%) lower than those shown in [280] and were closer to the data of [283, 284]. Unfortunately, the thermodynamic data [280-284] were presented without errors, which complicates the assessment of their reliability. We believe that the data in [280] were significantly overestimated.

Data on the standard integral thermodynamic functions of copper-antimony and copper-bismuth chalcogenides are shown in Table 4.2. For almost all of these compounds, complete mutually consistent sets of thermodynamic quantities were obtained using the EMF method with Cu^+ conductive electrolyte. Thermodynamic functions of $CuSbS_2$, Cu_3SbS_3, and $CuSbS_2$ determined by the EMF method [261, 285] except D_fG^0(298 K) for the latter compound are in good agreement with calorimetric data [263, 286].

Thus, mutually consistent sets of data on phase equilibria and thermodynamic properties are available for ternary Cu-B^V-S(Se) systems, and for five systems complete *T-x-y* diagrams were constructed and the primary crystallization fields of ternary phases were determined.

Table 4.2. Standard thermodynamic functions of formation and standard entropies of ternary phases of the Cu-BV-S(Se) systems

Compound	$-\Delta_f G^0$ (298 K)	$-\Delta_f H^0$ (298 K)	S^0_{298} J·K^{-1}·mol^{-1}	Ref.
	kJ·mol^{-1}			
Cu_3AsS_4	179.2±0.6	172.2±2.6	278±8	[245, 246]
	211.6	215.7	276.6	[283]
	230.4	224.0	285.0	[281]
		179.0	256.4	[282]
			277.2	[284]
$Cu_6As_4S_9$	445.3±1.6	434.6±7.5	668±22	[245, 246]
	517.8	505.1	673.0	[280]
$Cu_{12}As_4S_{13}$	701.8±2.5	673.7±10.7	1050±13	[245, 246]
CuAsS	69.5±0.3	64.1±1.7	109±5	[245, 246]
	76.2	76.5	100.0	[280]
Cu_3AsSe_4	147.3±0.5	146.3±1.5	307±13	[253]
$Cu_7As_6Se_9$	441.8±2.3	446.1±11.7	970±27	[284]
$CuAsSe_2$	66.6±0.4	67.3±2.0	150.9±6.2	[255]
	99.5±4.8	97.9±5.1	158±5	[285]
Cu_3AsSe_3	141.8±0.5	140.0±2.0	258.5±5.6	[285]
CuAsSe	55.1±0.3	55.6±2.0	109.5±4.7	[285]
Cu_3SbS_4	254.7 ± 2.3	247.8 ± 2.3	295.6 ± 7.0	[261]
$CuSbS_2$	128.5 ± 2.2	126.9 ± 2.4	147.5 ± 3.8	[261]
	*132.7±4.2	130.8±4.4	-	[263]
	130.6±6.0	131.7±5.2	-	[286]
$Cu_{12}Sb_4S_{13}$	958.7 ± 9.6	929.7 ± 11.2	1092.0 ± 29.0	[261]
Cu_3SbS_3	226.4 ± 2.3	219.0 ± 2.6	265.5 ± 7.2	[261]
	*221.6±6.0	215.0±6.2	-	[286]
$Cu_{14}Sb_4S_{13}$	971.7 ± 9.8	984.8 ± 11.9	1018.0 ± 33.0	[261]
Cu_3SbSe_4	191.6±2.5	178.6±5.4	358.18	[285]
$CuSbSe_2$	101.4±1.8	98.5±2.2	173±8	[285]
	77.3±1.3	104.8±1.7	-	[286]
Cu_3SbSe_3	175.6±2.5	164.0±5.3	311±15	[286]
$CuBiS_2$	138.6±4.0	138.2±2.9	156±12	[50]
Cu_3BiS_3	213.0±4.4	209.9±5.2	264±21	[50]
$CuBi_3S_5$	248.7±1.9	248.6±5.8	421.9±7.8	[50]
$CuBiSe_2$	107.6±0.8	105.9±2.51	189.8±2.4	[279]
Cu_3BiSe_3	162.5±1.2	155.9±5.7	315.0±8.5	[279]
Cu_9BiSe_6	324.8±3.5	313.1±18.6	659±28	[279]

Note: - our calculation from calorimetric data [286]

5. Conclusions

Thus, the above-presented results of numerous studies demonstrate significant successes in the development of environmentally friendly and affordable functional materials based on copper chalcogenides with p^1-p^3-elements. The analysis shows that the improvement and optimization of the functional properties of these materials is largely associated with targeted research on the variation of their composition and structure.

This review summarizes the studies of phase equilibria in ternary systems Cu-Tl(B^{IV}, B^V)-X (B^{IV} – Si, Ge, Sn; B^V – As, Sb, Bi; X – S, Se, Te) and some concentration planes and sections of quaternary systems that form various types of substitutional solid solutions based on ternary

compounds of the described systems. Even though the studied phase diagrams cover only a small part of such systems, they contain valuable information that offers great opportunities for scientifically based manipulation of composition and structure, including the concept of entropy engineering. Here we also present data on the fundamental thermodynamic properties of ternary compounds of the considered systems. Most of these data were obtained using the EMF method, which allowed to ensure not only the consistency of $\Delta_f G^0$, $\Delta_f H^0$, and S^0 functions, but also the mutual consistency of these values with phase diagrams.

At the same time, it should be noted that in studies of the physical properties of complex copper chalcogenides, phase diagrams and thermodynamic data were not used fully when selecting sample compositions and synthesis conditions. We believe that addressing this gap and further development of research on phase equilibria and thermodynamic properties of similar and more complex systems are important. This would allow us to obtain complex copper-based chalcogenides, thermodynamically stable over wide ranges of compositions and temperatures, including high-entropy phases with good applied characteristics.

Author contributions

Babanly M. B. – idea, text writing, scientific editing of the text; Mashadieva L. F., Imamalieva S. Z. and Babanly D. M – search and analysis of literary data, text writing, preparation of figures and tables; Tagiev D. B and Yusibov Yu. A. – processing of literature data and editing of the text.

Conflict of interests

The authors declare that they have no known competing financial interests or personal relationships that could have influenced the work reported in this paper.

References

1. *Physical-chemical properties of semiconductor substances**. Reference-book. A. V. Novoselova, V. B. Lazarev (eds.). Moscow: Nauka Publ., 1976. 339 p. (In Russ.)

2. Abrikosov N. Kh., Bankina V. F., Poretskaya L. V., Skudnova E. V., Chizhevskaya S. N. *Semiconductor chalcogenides and their base alloys**. Moscow: Nauka Publ., 1974. 220 p. (In Russ.)

3. Aven M., Prener J. S. *Physics and chemistry of II-VI compounds*. North-Holland Publishing Co; First Edition. 1967. 844 p.

4. Lazarev V. B., Berul S. I., Salov A. V. *Ternary semiconductor compounds in A^I-B^V-C^{VI} systems**. Moscow: Nauka Publ.; 1982. 150 p. (In Russ.)

5. Ahluwalia G. K. (ed.). *Applications of chalcogenides: S, Se, and Te*. Springer, 2016. 461p.

6. Woodrow P. *Chalcogenides: advances in research and applications*. New York: Nova Science Publishers, 2018. 111 p.

7. Scheer R., Schock H. W. *Chalcogenide photovoltaics: physics, technologies, and thin film devices*. Weinheim: Wiley-VCH, 2011. 384 p.

8. Alonso-Vante N. *Chalcogenide materials for energy conversion: pathways to oxygen and hydrogen reactions*. New York: Springer; 2018. 234 p. https://doi.org/10.1007/978-3-319-89612-0

9. Khan M. M. *Chalcogenide-based nanomaterials as photocatalysts*. Amsterdam: Elsevier, 2021. 376 p.

10. Hasan M. Z., Kane C. L. *Colloquium: topological insulators*. *Reviews of Modern Physics*. 2010;82: 3045–3067. https://doi.org/10.1103/RevModPhys.82.3045

11. Hagmann A. J. Chalcogenide topological insulators. In: *Chalcogenide from 3D to 2D and beyond*. Woodhead Publishing Series in Electronic and Optical Materials, 2020. p. 305–337. https://doi.org/10.1016/b978-0-08-102687-8.00015-4

12. Flammini R., Colonna S., Hogan C., ... Ronci F. Evidence of β-antimonene at the Sb/Bi_2Se_3 interface. *Nanotechnology*. 2018;29(6): 065704. https://doi.org/10.1088/1361-6528/aaa2c4

13. Tian W.,Yu W.,Shi J., Wang Y. The property, preparation and application of topological insulators: a review. *Material*. 2017;10(7): 814. https://doi.org/10.3390/ma10070814

14. Babanly M. B., Chulkov E. V., Aliev Z. S., Shevel'kov A. V., Amiraslanov I. R. Phase diagrams in materials science of topological insulators based on metal chalkogenides, *Russian Journal of Inorganic Chemistry*. 2017;62(13): 1703–1729. https://doi.org/10.1134/S0036023617130034

15. Pacile D., Eremeev S. V., Caputo M., ... Papagno M. Deep insight into the electronic structure of ternary topological insulators: A comparative study of $PbBi_4Te_7$ and $PbBi_6Te_{10}$. *Physica Status Solidi (RRL)*. 2018;12(12): 1800341-8. https://doi.org/10.1002/pssr.201800341

16. Nurmamat M., Okamoto K., Zhu S., ... Kimura A. Topologically non-trivial phase-change compound $GeSb_2Te_4$. *ACS Nano*. 2020;14(7): 9059–9065. https://doi.org/10.1021/acsnano.0c04145

17. Shvets I. A., Klimovskikh I. I., Aliev Z. S., ... Chulkov E. V. Impact of stoichiometry and disorder on the electronic structure of the $PbBi_2Te_{4-x}Se_x$ topological insulator. *Physical Review B*. 2017;96: 235124–235127. https://doi.org/10.1103/PhysRevB.96.235124

18. Otrokov M. M., Klimovskikh I. I., Bentmann H. ... Chulkov E. V. Prediction and observation of an antiferromagnetic topological insulator. *Nature*. 2019;576: 416–422. https://doi.org/10.1038/s41586-019-1840-9

19. Jahangirli Z. A., Alizade E. H., Aliev Z. S., ... Chulkov E. V. Electronic structure and dielectric function of Mn-Bi-Te layered compounds. *Journal of Vacuum Science and*

Technology B. 2019;37: 062910. https://doi.org/10.1116/1.5122702

20. Eremeev S. V., Rusinov I. P., Koroteev Yu. M., ... Chulkov E. V. Topological magnetic materials of the $(MnSb_2Te_4)\cdot(Sb_2Te_3)_n$ van der Waals compounds family. *The Journal of Physical Chemistry Letters*. 2021;12(17): 4268–4277. https://doi.org/10.1021/acs.jpclett.1c00875

21. Garnica M., Otrokov M. M., Casado Aguilar P., ... Miranda R. Native point defects and their implications for the Dirac point gap at $MnBi_2Te_4$(0001). *npj Quantum Materials*. 2022;7: 7. https://doi.org/10.1038/s41535-021-00414-6

22. Coughlan C., Ibanez M., Dobrozhan O., Singh A., Cabot A., Ryan K. M. Compound copper chalcogenide nanocrystals. *Chemical Reviews*. 2017;117(9): 5865–6109. https://doi.org/10.1021/acs.chemrev.6b00376

23. Xing C., Lei Y., Liu M., Wu S., He W. Environment-friendly Cu-based thin film solar cells: materials, devices and charge carrier dynamics. *Physical Chemistry Chemical Physics*. 2021;23: 16469–16487. https://doi.org/10.1039/D1CP02067F

24. Fu H. Environmentally friendly and earth-abundant colloidal chalcogenide nanocrystals for photovoltaic applications. *Journal of Materials Chemistry C*. 2018;6: 414–445. https://doi.org/10.1039/C7TC04952H

25. Kumar M., Meena B., Subramanyam P., Suryakala D., Subrahmanyam C. Emerging copper-based semiconducting materials for photocathodic applications in solar driven water splitting. *Catalysts*. 2022;12(10): 1198. https://doi.org/10.3390/catal12101198

26. Akhil S., Balakrishna R. G. $CuBiSe_2$ quantum dots as ecofriendly photosensitizers for solar cells. *ACS Sustainable Chemistry and Engineering Journal*. 2022;10(39): 13176–13184. https://doi.org/10.1021/acssuschemeng.2c04333

27. Deng T., Wei T. R., Song Q., ... Chen L. Thermoelectric properties of *n*-type $Cu_4Sn_7S_{16}$-based compounds. *RSC Advances*. 2019;9: 7826. https://doi.org/10.1039/c9ra00077a

28. Choudhury A., Mohapatra S., Asl H. Y., ... Petricek V. New insights into the structure, chemistry, and properties of Cu_4SnS_4. *Journal of Solid State Chemistry*. 2017;253: 192–201. http://dx.doi.org/10.1016/j.jssc.2017.05.033

29. Ivanchenko M., Jing H. Smart design of noble metal–copper chalcogenide dual plasmonic heteronanoarchitectures for emerging applications: progress and prospects. *Chemistry of Materials*. 2023;35(12): 4598–4620. https://doi.org/10.1021/acs.chemmater.3c00346

30. Zhou N., Zhao H., Li X., ...Tong X. Activating earth-abundant element-based colloidal copper chalcogenide quantum dots for photodetector and optoelectronic synapse applications. *ACS Materials Letters*. 2023;*5*(4): 1209–1218. https://doi.org/10.1021/acsmaterialslett.3c00035

31. Polevik A. O., Sobolev A. V., Glazkova I. S., ... Shevelkov A. V. Interplay between Fe(II) and Fe(III) and its impact on thermoelectric pProperties of iron-substituted colusites $Cu_{26-x}Fe_xV_2Sn_6S_{32}$. *Compounds*. 2023;3: 348–364. https://doi.org/10.3390/compounds3020027

32. Polevik A. O., Efimova A. S., Sobolev A. V., ... Shevelkov A. V. Atomic distribution, electron transfer, and charge compensation in artificial iron-bearing colusites $Cu_{26-x}Fe_xTa_{2-\gamma}Sn_6S_{32}$. *Journal of Alloys and Compounds*. 2024;976: 173280. https://doi.org/10.1016/j.jallcom.2023.173280

33. Nasonova D. I., Sobolev A. V., Presniakov I. A., Presniakov I. A., Andreeva K. D., Shevelkov A. V. Position and oxidation state of tin in Sn-bearing tetrahedrites $Cu_{12-x}Sn_xSb_4S_{13}$. *Journal of Alloys and Compounds*. 2019;778: 774–778. https://doi.org/10.1016/j.jallcom.2018.11.168

34. Reddy V. R. M., Pallavolu M. R., Guddeti P. R., ... Park C. Review on Cu_2SnS_3, Cu_3SnS_4, and Cu_4SnS_4 thin films and their photovoltaic performance. *Journal of Industrial and Engineering Chemistry*. 2019;76: 39–74. https://doi.org/10.1016/j.jiec.2019.03.035

35. Lin S., Li W., Pei Y. Thermally insulative thermoelectric argyrodites. *Materials Today*. 2021;48: 198–213. https://doi.org/10.1016/j.mattod.2021.01.007

36. Nilges T., Pfitzner A. A structural differentiation of quaternary copper argyrodites: structure – property relations of high temperature ion conductors, *Zeitschrift für Kristallographie - Crystalline Materials*. 2005; 220(2-3): 281–294. https://doi.org/10.1524/zkri.220.2.281.59142

37. Babanly M. B., Yusibov Y. A., Imamaliyeva S. Z., Babanly D. M., Alverdiyev I. J. Phase diagrams in the development of the argyrodite family compounds and solid solutions based on them. *Journal of Phase Equilibria and Diffusion*. 2024;45: 228–255. https://doi.org/10.1007/s11669-024-01088-w

38. Wu X., Liu K., Wang R., Yang G., Lin J., Liu X. Multifunctional $CuBiS_2$ nanoparticles for computed tomography guided photothermal therapy in preventing arterial restenosis after endovascular treatment. *Frontiers in Bioengineering and Biotechnology*. 2020; 8: 585631. https://doi.org/10.3389/fbioe.2020.585631

39. Askari N., Askari M. B. Apoptosis-inducing and image-guided photothermal properties of smart nano $CuBiS_2$. *Materials Research Express*. 2019;6: 065404. https://doi.org/10.1088/2053-1591/ab0c3e

40. Zhou M., Tian M., Li C. Copper-based nanomaterials for cancer imaging and therapy. *Bioconjugate Chemistry*. 2016;27(5): 1188-99. https://doi.org/10.1021/acs.bioconjchem.6b00156

41. Mindat.org: *Open database of minerals, rocks, meteorites and the localities they come from*. Available at: http://www.mindat.org

42. Filippou D., Germain P., Grammatikopoulos T. Recovery of metal values from copper—arsenic minerals and other related resources. *Mineral Processing and Extractive Metallurgy Review*. 2007;28: 247–298. https://doi.org/10.1080/08827500601013009

43. Afinogenov Yu. P., Goncharov E. G., Semenova G. V., Zlomanov V. P. *Physicochemical analysis of multicomponent systems*[*]. Moscow: MFTIB Publ.; 2006. 332 p. (In Russ.)

44. Lazarev V. B., Shevchenko V. I., Marenkin S. F. Some problems of physics, chemistry and materials science of new semiconductors. In: *Physical methods for studying inorganic materials*. Moscow: Nauka Publ.; 1981. p.19–34. (In Russ.)

45. West D. R. F. *Ternary phase diagrams in materials science*. Boca Raton: CRC Press; 2013. 3rd edition. p. 240. https://doi.org/10.1201/9781003077213

46. Saka H. *Introduction to phase diagrams in materials science and engineering*. London: World Scientific Publishing Company; 2020. pp.188. https://doi.org/10.1142/11368

47. Babanly M. B., Mashadiyeva L. F., Babanly D. M., Imamaliyeva S. Z., Taghiyev D.B., Yusibov Y.A. Some issues of complex investigation of the phase equilibria and

thermodynamic properties of the ternary chalcogenide systems by the EMF method. *Russian Journal of Inorganic Chemistry*. 2019;64(13): 1649–1671. https://doi.org/10.1134/S0036023619130035

48. Imamaliyeva S. Z. Phase diagrams in the development of thallium-ree tellurides with Tl_5Te_3 structure and multicomponent phases based on them overview. *Condensed Matter and Interphases*. 2018;20(3): 332–347. https://doi.org/10.17308/kcmf.2018.20/570

49. Babanly M. B., Mashadiyeva L. F., Imamaliyeva S. Z., Tagiev D. B., Babanly D. M., Yusibov Yu. A. Thermodynamic properties of complex copper chalcogenides. Review. *Chemical Problems*. 2024;3: 243–280. https://doi.org/10.32737/2221-8688-2024-3-243-280

50. Babanly M. B., Yusibov Yu. A., Babanly N. B. The EMF method with solid-state electrolyte in the thermodynamic investigation of ternary copper and silver chalcogenides. In: *Electromotive force and measurement in several systems*. S. Kara (ed.). Intechweb.Org. 2011. p. 57–78. https://doi.org/10.5772/28934

51. Babanly M. B., Yusibov Yu. A. *Electrochemical methods in thermodynamics of inorganic systems*. Baku: ELM Publ.; 2011. 306 p. (In Russ.)

52. Babanly M. B, Akhmadyar A., Kuliev A. Thermodynamic properties of intermediate phases in Tl-Sb(Bi)-Te systems. *Russian Journal of Physical Chemistry*. 1985;59(3): 335–336.

53. Yusibov Y. A., Babanly M. B., Gasanov R. F. Thermodynamic properties and solid phase equilibrium of Tl-Ga-Te system*. *Inorganic Materials*. 1991;27(7): 1402–1406. (In Russ.)

54. Babanly M. B., Kuliev A. A. Phase equilibria and thermodynamic properties in the system Ag-Tl-Te*. *Russian Journal of Inorganic Chemistry*. 1982;27(6); 1538–1546. (In Russ.)

55. Babanly M. B., Muradova G. V., Ilyasly T. M., Babanly D. M. Solid-phase equilibria and thermodynamic properties of the Tl_2Se-As_2Se_3-Se system. *Russian Journal of Inorganic Chemistry*. 2012;57: 270–273. https://doi.org/10.1134/S0036023612020039

56. Aliev Z. S., Babanly M.B. Solid-state equilibria and thermodynamic properties of compounds in the Bi-Te-I system. *Inorganic Materials*. 2008;44(10): 1076–1080. https://doi.org/10.1134/S0020168508100099

57. Jafarov Y. I., Ismaylova S. A., Aliev Z. S., Imamaliyeva S. Z., Yusibov Y. A., Babanly M. B. Experimental study of the phase diagram and thermodynamic properties of the Tl-Sb-S system. *CALPHAD*. 2016;55: 231–237. https://doi.org/10.1016/j.calphad.2016.09.007

58. Babanly D.M., Aliev Z.S., Jafarli F.Y., Babanly M.B. Phase equilibria in the Tl-TlCl-Te system and thermodynamic properties of the compound Tl_5Te_2Cl. *Russian Journal of Inorganic Chemistry*. 2011;56: 442–449. https://doi.org/10.1134/S0036023611030065

59. Seidzade A. E., Orujlu E. N., Babanly D. M., Imamaliyeva S. Z., Babanly M. B. Solid-phase equilibria in the SnTe–Sb_2Te_3–Te system and the thermodynamic properties of the tin–antimony tellurides. *Russian Journal of Inorganic Chemistry*. 2022;67(5): 683–690. https://doi.org/10.1134/S003602362205014X

60. Aliev Z. S., Zúñiga F. J., Koroteev Y. M., ... Chulkov E. V. Insight on a novel layered semiconductors: CuTlS and CuTlSe. *Journal of Solid State Chemistry*. 2016;242: 1–7. https://doi.org/10.1016/j.jssc.2016.05.036

61. Vijayan K., Thirumalaisamy L., Vijayachamundeeswari S. P., Sivaperuman K., Ahsan N., Okada Y. A novel approach for designing a sub-bandgap in $CuGa(S,Te)_2$ thin films assisted with numerical simulation of solar cell devices for photovoltaic application. *ACS Omega*. 2023;8(25): 22414–22427. https://doi.org/10.1021/acsomega.2c08196

62. Vijayan K., Vijayachamundeeswari S. P. Scrutinizing the effect of substrate temperature and enhancing the multifunctional attributes of spray deposited copper gallium sulfide ($CuGaS_2$) thin films. *Phase Transitions*. 2023;96(8): 607–619. https://doi.org/10.1080/01411594.2023.2238110

63. Maeda T., Nakanishi R., Yanagita M., Wada T. Control of electronic structure in $Cu(In, Ga)(S, Se)_2$ for high-efficiency solar cells. *Japanese Journal of Applied Physics*. 2020;59: SGGF12. https://doi.org/10.35848/1347-4065/ab69e0

64. Shukla S., Sood M., Adeleye D., ... Siebentritt S. Over 15% efficient wide-band-gap $Cu(In,Ga)S_2$ solar cell: suppressing bulk and interface recombination through composition engineering. *Joule*. 2021;5(7): 1816–1831. https://doi.org/10.1016/j.joule.2021.05.004

65. Yang Y., Xiong X., Han J. Modification of surface and interface of copper indium gallium selenide thin films with sulfurization. *Emerging Materials Research*. 2022;11(3): 325–330. https://doi.org/10.1680/jemmr.21.00171

66. Stanbery B. J., Abou-Ras D., Yamada A., Mansfield L. CIGS photovoltaics: reviewing an evolving paradigm. *Journal of Physics D: Applied Physics*. 2021;55(17): 173001. https://doi.org/10.1088/1361-6463/ac4363

67. Li W., Song Q., Zhao C., ... Yang C. Toward high-efficiency $Cu(In,Ga)(S,Se)_2$ solar cells by a simultaneous selenization and sulfurization rapid thermal process. *ACS Applied Energy Materials Journal*. 2021;4(12): 14546–14553. https://doi.org/10.1021/acsaem.1c03198

68. Khavari F., Keller J., Larsen J. K., Sopiha K. V., Törndahl T., Edoff M. Comparison of sulfur incorporation into $CuInSe_2$ and $CuGaSe_2$ thin-film solar absorbers. *Physica Status Solidi A*. 2020;217(22). https://doi.org/10.1002/pssa.202000415

69. Wang Y., Yang Y., Wang L., ... Guo Z. Design, photoelectric properties and electron transition mechanism of Cr doped p-$CuGaS_2$ compound based on intermediate band effect. *Materials Today Physics*. 2021;21: 100545. https://doi.org/10.1016/j.mtphys.2021.100545

70. Fan F.J., Liang Wu L., Yu S.-H. Energetic I-III-VI_2 and I_2-II-IV-VI4 nanocrystals: synthesis, photovoltaic and thermoelectric applications. *Energy Environmental Science*. 2014;7: 190-208. https://doi.org/10.1039/C3EE41437J

71. Torimoto T., Kameyama T., Uematsu T., Kuwabata S. Controlling optical properties and electronic energy structure of I–III–VI semiconductor quantum dots for improving their photofunctions. *Journal of Photochemistry and Photobiology C: Photochemistry Reviews*. 2023;54: 100569. https://doi.org/10.1016/j.jphotochemrev.2022.100569

72. Gullu H. H., Isik M., Gasanly N. M. Structural and optical properties of thermally evaporated Cu-Ga-S (CGS) thin films. *Physica B: Condensed Matter*. 2018;547: 92–96. https://doi.org/10.1016/j.physb.2018.08.015

73. Soni A., Gupta V., Arora C. M., Dashora A., Ahuja B. L. Electronic structure and optical properties of $CuGaS_2$ and

$CuInS_2$ solar cell materials. *Solar Energy*. 2010;84(8): 1481–1489. https://doi.org/10.1016/j.solener.2010.05.010

74. Candeias M. B., Fernandes T. V., Falcão B. P., ... Leitão J. P. Cu(In,Ga)Se_2-based solar cells for space applications: proton irradiation and annealing recovery. *Journal of Materials Science*. 2023;58: 16385–16401. https://doi.org/10.1007/s10853-023-09033-x

75. Plata J. J., Posligua V., Márquez A. M., Sanz J. F., Grau-Crespo R. Charting the lattice thermal conductivities of I–III–VI_2 chalcopyrite semiconductors. *Chemistry of Materials Journal*. 2022;34(6): 2833–2841. https://doi.org/10.1021/acs.chemmater.2c00336

76. Djelid K., Seddik T., Merabiha O., ... Bin Omran S. Effects of alloying chalcopyrite $CuTlSe_2$ with Na on the electronic structure and thermoelectric coefficients: DFT investigation. *The European Physical Journal Plus*. 2022;137: 1347. https://doi.org/10.1140/epjp/s13360-022-03577-8

77. Gudelli V. K., Kanchana V., Vaitheeswaran G., Svane A., Christensen N. E. Thermoelectric properties of chalcopyrite type $CuGaTe_2$ and chalcostibite $CuSbS_2$. *Journal of Applied Physics*. 2013;114: 1223707-8. https://doi.org/10.1063/1.4842095

78. Plirdpring T., Kurosaki K., Kosuga A., ... Yamanaka S. Chalcopyrite $CuGaTe_2$: a high-efficiency bulk thermoelectric material. *Advanced Materials*. 2012;24(127): 3622–3626. https://doi.org/10.1002/adma.201200732

79. Kurosaki K., Goto K., Kosuga A., Yamanaka S. Thermoelectric and thermophysical characteristics of Cu_2Te-Tl_2Te pseudo binary system. *Materials Transactions*. 2006;47(6): 1432-1435. https://doi.org/10.2320/matertrans.47.1432

80. Matsumoto H., Kurosaki K., Muta H., Yamanaka S. Thermoelectric properties of $TlCu_3Te_2$ and $TlCu_2Te_2$. *Journal of Electronic Materials*. 2009;38: 1350–1353. https://doi.org/10.1007/s11664-009-0664-z

81. Jiang C., Tozawa M., Akiyoshi K.,... Torimoto T. Development of Cu–In–Ga–S quantum dots with a narrow emission peak for red electroluminescence. *The Journal of Chemical Physics*. 2023;158: 164708. https://doi.org/10.1063/5.0144271

82. Kim Y.-K., Ahn S.-H., Chung K., Cho Y.-S., Choi C.-J. The photoluminescence of $CuInS_2$ nanocrystals: Effect of non-stoichiometry and surface modification. *Journal of Materials Chemistry*. 2012;22: 1516–1520. https://doi.org/10.1039/c1jm13170b

83. Isik M., Gasanly N.M., Gasanova L. G., Mahammadov A. Z. Thermoluminescence study in $Cu_3Ga_5S_9$ single crystals: application of heating rate and T_m-T_{stop} methods. *Journal of Luminescence*. 2018;199: 334–338. https://doi.org/10.1016/j.jlumin.2018.03.076

84. Kim J.-H., Han H., Kim M. K., ... Lim J. A. Solution-processed near-infrared Cu(In,Ga)$(S,Se)_2$ photodetectors with enhanced chalcopyrite crystallization and bandgap grading structure via potassium incorporation. *Science Reports*. 2021;11: 7820. https://doi.org/10.1038/s41598-021-87359-9

85. Nakamura M., Yamaguchi K., Kimoto Y., Yasaki Y., Kato T., Sugimoto H. Cd-free Cu(In,Ga)$(Se,S)_2$ thin-film solar cell with record efficiency of 23.35%. *IEEE Journal of Photovoltaics*. 2019;9(6): 1863–1867. https://doi.org/10.1109/JPHOTOV.2019.2937218

86. Clarke D., Breguel R. Analysis of thermodynamic properties of Cu(In,Ga)Se_2 thin-film solar cells for viable space application. *PAM Review: Energy Science and Technology*. 2018;5: 131–149. https://doi.org/10.5130/pamr.v5i0.1501

87. Shevelkov A. V. Chemical aspects of the design of thermoelectric materials, *Russian Chemical Reviews*. 2008;77: 1–19. https://doi.org/10.1070/rc2008v077n01abeh003746

88. Berger R., Eriksson L. Crystal structure, refinement of monoclinic $TlCu_3Se_2$. *Journal of Less-Common Metals*. 1990;61: 101–108. https://doi.org/10.1016/0022-5088(90)90318-e

89. Klepp K. O., Yvon K. Thallium dithiotricuprate (I). *Acta Crystallographica Section B Structural Crystallography and Crystal Chemistry*. 1980;36: 2389–2391. https://doi.org/10.1107/s0567740880008795

90. Norén L., Larsson K., Delaplane R. G., Berger R. Size or polarisability effects? A comparative study of $TlCu_7S_4$ and $TlCu_7Se_4$. *Journal of Alloys and Compounds*. 2001;314: 114–123. https://doi.org/10.1016/S0925-8388(00)01202-0

91. Babanly M. B., Yusibov Y. A., Abishev V. T. *Ternary chalcogenides based on copper and silve*[*] Baku: BSU Publ.; 1993. 342 p. (In Russ.)

92. Abishev V. T., Babanly M. B., Kuliyev A. A. Phase equilibria in the $T_{l2}S$–$C_{u2}S$ system. *ChemChemTech [Izv. Vyssh. Uchebn. Zaved. Khim. Khim. Tekhnol.]*. 1978;21(5): 630–632.

93. Mammadov M. I., Alizade M. Z., Zamanov S. K., Aliyev O. M. Study of the phase diagram of the Tl_2S-Cu_2S system[*]. *Russian Journal of Inorganic Chemistry*. 1978;14(8): 1527–1529. (In Russ.)

94. Gardes B., Brun G., Raymond A., Tedenac J. C. Trois phases ternaire Cu-Tl-S. *Materials Research Bulletin*. 1979;14(7): 943–946. https://doi.org/10.1016/0025-5408(79)90161-2

95. Sobbott E. Das system Tl_2S-Cu_2S. *Monatshefte Chemie*. 1994;115(12): 1397–1400. https://doi.org/10.1007/BF00816337

96. Babanly M. B., Un L. T., Kuliev A. A. System Tl_2S–CuTlS–S[*]. *Russian Journal of Inorganic Chemistry*. 1985;30(4): 1047–1050. (In Russ.)

97. Babanly M.B., Un L.T., Kuliev A.A. System Tl–Tl_2S–CuTlS–Cu[*]. *Russian Journal of Inorganic Chemistry*.1985;30(4): 1043–1046. (In Russ.)

98. Babanly M. B., Un L. T., Kuliev A. A. System Cu-Tl-S[*]. *Russian Journal of Inorganic Chemistry*. 1986;32(7): 1837–1844. (In Russ.)

99. Abishov V. T., Babanly M. B., Kuliev A. A. Phase equilibria in the Cu_2Se-Tl_2Se system[*]. *Inorganic Materials*. 1979;15(11): 1926. (In Russ.)

100. Voroshilov Yu. V., Evstigneeva T. L., Nekrasov I. Ya. *Crystal chemical tables of ternary chalcogenides*[*]. Moscow: Nauka Publ.; 1989. 224 p. (In Russ.)

101. Babanly N. B. Thermodynamic properties of some ternary phases of the Cu-Tl-Se system. *Inorganic Materials*. 2011;47: 1306–1310. https://doi.org/10.1134/S0020168511120016

102. Babanly N. B. Phase diagram of the Tl-Tl_2Se-Cu_2Se-Cu system. *Journal of Qafqaz University-Chemistry*. 2015;5(1): 43–50.

103. Kovaleva I. S., Kranchevich K. S., Nikolskaya G. F. Section of Cu_2Te–Tl_2Te_3 in the Cu–Tl–Te system.[*] *Inorganic Materials*. 1971;7(5): 865–867. (In Russ.)

104. Babanly N. B., Salimov Z. E., Akhmedov M. M., Babanly M. B. Thermodynamic study of the Cu–Tl–Te system by the EMF method with solid electrolyte $Cu_4RbCl_3I_2$. *Russian Journal of Electrochemistry*. 2012;48: 68–73. https://doi.org/10.1134/S1023193512010041

105. Kleep K. O. Darstellung und Kristallostructur von $TlCu_3Te_2$: ein Tellurocuprat mit aufgefuelltem $CuAl_2$-typ. *Journal of the Less-Common Metals*. 1987;127: 79–89. https://doi.org/10.1016/0022-5088(87)90194-9

106. Bradtmöller S., Böttcher P. Crystal structure of copper tetrathallium trutelluride $CuTl_4Te_3$. *Zeitschrift für Kristallographie*. 1994;209: 97. https://doi.org/10.1524/zkri.1994.209.1.97

107. Babanly M. B., Salimov Z. E., Babanly N. B., Imamaliyeva S. Z.Thermodynamic properties of copper thallium tellurides. *Inorganic Materials*. 2011;47: 361–364. https://doi.org/10.1134/S0020168511040030

108. Babanly N. B., Aliev Z. S., Yusibov Yu. A., Babanly M. B. A thermodynamic study of Cu—Tl-S system by EMF method with $Cu_4RbCl_3I_2$ solid electrolyte. *Russian Journal of Electrochemistry*. 2010;46: 354–358. https://doi.org/10.1134/S1023193510030146

109. Babanly M. B., Yusibov Y. A., Abishov V. T. *Method of electromotive forces in the thermodynamics of complex semiconductor substances*[*]. Baku: BSU Publ.; 1992. 327 p. (In Russ.)

110. Morachevsky A. G., Voronin G. F., Heiderich V. A., Kutsenok I. B. *Electrochemical methods of research in the thermodynamics of metallic systems*[*]. Moscow: ICC "Akademkniga" Publ.; 2003. 334 p. (In Russ.)

111. Aliev Z. S., Musayeva S. S. Imamaliyeva S. Z., Babanlı M. B. Thermodynamic study of antimony chalcoiodides by EMF method with an ionic liquid. *Journal of Thermal Analysis and Calorimetry*. 2018;133(2): 1115–1120. https://doi.org/10.1007/s10973-017-6812-4

112. Osadchii E. G., Korepanov Y. I., Zhdanov N. N. A multichannel electrochemical cell with glycerin-based liquid electrolyte. *Instruments and Experimental Techniques*. 2016;59: 302–304. https://doi.org/10.1134/S0020441216010255

113. Voronin M. V., Osadchii E. G. Determination of thermodynamic properties of silver selenide by the galvanic cell method with solid and liquid electrolytes. *Russian Journal of Electrochemistry*. 2011;47: 420–426. https://doi.org/10.1134/S1023193511040203

114. Orujlu E. N., Babanly D. M., Alakbarova T. M., Orujov N. I., Babanly M. B. Study of the solid-phase equilibria in the GeTe-Bi_2Te_3-Te system and thermodynamic properties of GeTe-rich germanium bismuth tellurides. *The Journal of Chemical Thermodynamics*. 2024;196: 107323. https://doi.org/10.1016/j.jct.2024.107323

115. Aliyev F. R., Orujlu E. N., Mashadiyeva L. F., Dashdiyeva G. B., Babanly D. M. Solid – phase equilibria and thermodynamic properties of the Sb-Te-S system. *Physics and Chemistry of Solid State*. 2024;25(1): 26–34. https://doi.org/10.15330/pcss.25.1.26-34

116. Moroz M., Tesfaye F., Demchenko P., ... Hupa L. Phase equilibria and thermodynamic properties of selected compounds in the Ag-Ga-Te-AgBr system. *Journal of Phase Equilibria and Diffusion*. 2024;45: 447–458. https://doi.org/10.1007/s11669-024-01095-x

117. Moroz M., Tesfaye F., Demchenko P., ... Gladyshevskii R. Synthesis, thermodynamic properties, and structural characteristics of multicomponent compounds in the Ag–Ni–Sn–S System. *JOM*. 2023;75: 2016–2025. https://doi.org/10.1007/s11837-023-05784-9

118. Moroz M. V., Demchenko P. Y., Tesfaye F... Reshetnyak O. V. Thermodynamic properties of selected compounds of the Ag–In–Se system determined by the electromotive force method. *Physics and Chemistry of Solid State*. 2022;23(3): 575–581. https://doi.org/10.15330/pcss.23.3.575-581

119. Babanly N. B., Orujlu E. N., Imamaliyeva S. Z., Yusibov Y. A., Babanly M. B. Thermodynamic investigation of silver-thallium tellurides by EMF method with solid electrolyte Ag_4RbI_5. *The Journal of Chemical Thermodynamics*. 2019;128: 78–86. https://doi.org/10.1016/j.jct.2018.08.012

120. Amiraslanova A. J., Mammadova A. T., Imamaliyeva S. Z., Alverdiyev I. J., Yusibov Yu. A., Babanly M. B. Thermodynamic investigation of Ag_8GeTe_6 and $Ag_8GeTe_{6-x}Se_x$ solid solutions by the emf method with a solid Ag^+ conducting electrolyte. *Russian Journal of Electrochemistry*. 2023;12: 834–842. https://doi.org/10.31857/s0424857023120034

121. Babanly M. B., Abishov V. T., Kuliev A. A. Crystal lattice of Cu(Ag)TlX compounds and phase equilibria in Cu(Ag)TlS-Cu(Ag)TlSe systems. *ChemChemTech [Izv. Vyssh. Uchebn. Zaved. Khim. Khim. Tekhnol.]*. 1981;24(8): 931–934.

122. Babanly M. B., Lee Tai Un, Kuliev A. A. Phase equilibria in CuTlS(Se)-AgTlS(Se) systems[*]. *Inorganic Materials*. 1985;21(10): 1649–1652. (In Russ.)

123. Lee Tai Un, Babanly M. B., Kuliev A. A. System AgTlS+CuTlSe«AgTlSe+CuTlS[*]. *Russian Journal of Inorganic Chemistry*. 1985;30(9): 2353–2355. (In Russ.)

124. Babanly M. B., Lee Tai Un, Kuliev A. A. Study of phase equilibria in the CuTlS-CuTlSe-AgTlTe system. *ChemChemTech [Izv. Vyssh. Uchebn. Zaved. Khim. Khim. Tekhnol.]*. 1986;29(2): 112–113.

125. Chalbaud L. M., Delgado G. D., Delgado J. M., Mora A. E., Sagredo V. Synthesis and single-crystal structural study of Cu_2GeS_3. *Materials Research Bulletin*. 1997;32(10): 1371–1376. https://doi.org/10.1016/S0025-5408(97)00115-3

126. Li Y., Cao T., Liu G., ... Zhou M. Enhanced thermoelectric properties of Cu_2SnSe_3 by (Ag, In)-Co-doping. *Advanced Functional Materials*. 2016;26: 6025–6032. https://doi.org/10.1002/adfm.201601486

127. Ma R. L., Liu G., Li Y., ... Li L. Thermoelectric properties of S and Te-doped Cu_2SnSe_3 prepared by combustion synthesis. *Journal of Asian Ceramic Societies*. 2018;1: 13–19. https://doi.org/10.1080/21870764.2018.1439609

128. Prasad S., Rao A., Gahtori B., ... Kuo Y.-K. The low and high temperature thermoelectric properties of Sb doped Cu_2SnSe_3. *Materials Research Bulletin*. 2016;83: 160–166. https://doi.org/10.1016/j.materresbull.2016.06.002

129. Ding M., Bai C., Lang Y., ...Almutairi Z. Enhanced thermoelectric performance of Cu_2SnSe_3 by synergic effects via cobalt-doping. *Journal of Alloys and Compounds*. 2024;988: 174272. https://doi.org/10.1016/j.jallcom.2024.174272

130. Ma R. L., Liu G., Li J., ... Li L. Effect of secondary phases on thermoelectric properties of Cu_2SnSe_3. *Ceramics International*. 2017;43(9): 7002–7010. https://doi.org/10.1016/j.ceramint.2017.02.126

131. Siyar M., Siyar M., Cho J. Y., ... Parker C. Thermoelectric properties of Cu_2SnSe_3-SnS. *Journal of Composite Materials*. 2019;12(13): 2040–2043. https://doi.org/10.3390/ma12132040

132. Zhao D., Wang X., Wu D. Enhanced thermoelectric properties of graphene, Cu_2SnSe_3 composites. *Crystals*. 2017;7: 71. https://doi.org/10.3390/cryst7030071

133. Yang J., Lu B., Song R., ...Qiao G.. Realizing enhanced thermoelectric properties in Cu_2GeSe_3 via a synergistic effect of In and Ag dual-doping. *Journal of the European Ceramic Society*. 2022;42(1): 169–174. https://doi.org/10.1016/j.jeurceramsoc.2021.10.009

134. Yang J., Song R., Zhao L., ...Qiao G. Magnetic Ni doping induced high power factor of Cu_2GeSe_3-based bulk materials. *Journal of the European Ceramic Society*. 2021;41(6): 3473–3479. https://doi.org/10.1016/j.jeurceramsoc.2020.12.037

135. Wang R., Li A., Huang T., ... Wang G. Enhanced thermoelectric performance in Cu_2GeSe_3 via (Ag, Ga)-co-doping on cation sites. *Journal of Alloys and Compounds*. 2018;769: 218–225. https://doi.org/10.1016/j.jallcom.2018.07.318

136. Jacob S., Delatouche B., Péré D., Jacob A., Chmielowski R. Insights into the thermoelectric properties of the Cu_2Ge $(S_{1-x}Se_x)_3$ solid solutions. *Materials Today*. 2017;4: 12349–12359. https://doi.org/10.1016/j.matpr.2017.10.003

137. Pejjai B., Reddy V. R. M., Gedi S., Park C. Review on earth-abundant and environmentally benign Cu–Sn–X(X = S, Se) nanoparticles by chemical synthesis for sustainable solar energy conversion. *Journal of Industrial and Engineering Chemistry*. 2018;60: 19–52. https://doi.org/10.1016/j.jiec.2017.09.033

138. Lokhande A. C., Chalapathy R. B. V., He M., Joo E. Development of Cu_2SnS_3 (CTS) thin film solar cells by physical techniques: A status review. *Solar Energy Materials and Solar Cells*. 2016;153: 4–107. https://doi.org/10.1016/j.solmat.2016.04.003

139. Chantana J., Chantana J., Uegaki H., Minemoto T. Influence of Na in Cu_2SnS_3 film on its physical properties and photovoltaic performances. *Thin Solid Films*. 2017;636: 431-437. https://doi.org/10.1016/j.tsf.2017.06.044

140. Chaudhari J. J., Joshi U. S. Fabrication of high quality Cu_2SnS_3 thin film solar cell with 1.12% power conversion efficiency obtain by low cost environment friendly sol-gel technique. *Materials Research Express*. 2018;5: 036203. https://doi.org/10.1088/2053-1591/aab20e

141. De Wild J., Babbe F., Robert E. V. C. Silver-doped Cu_2SnS_3 absorber layers for solar cells application. *IEEE Journal of Photovoltaics*. 2018;8: 299–304. https://doi.org/10.1109/JPHOTOV.2017.2764496

142. Oliva F., Arqués L., Acebo L. Characterization of Cu_2SnS_3 polymorphism and its impact on optoelectronic properties. *Journal of Materials Chemistry A*. 2017;5: 23863–23871. https://doi.org/10.1039/C7TA08705E

143. Zaki M. Y., Sava F., Simandan I. D., ... Galca A. C. Cu_2SnSe_3 phase formation from different metallic and binary chalcogenides stacks using magnetron sputtering. *Materials Science in Semiconductor Processing*. 2023;153: 107195. https://doi.org/10.1016/j.mssp.2022.107195

144. Pallavolu M. R., Banerjee A. N., Minnam Reddy V. R., Joo S. W., Barai H. R., Park C. Status review on the Cu_2SnSe_3 (CTSe) thin films for photovoltaic applications. *Solar Energy*. 2020;208: 1001–1030. https://doi.org/10.1016/j.solener.2020.07.095

145. Yang C., Luo Y., Xia Y., ... Cui J. Improved thermoelectric performance of *p*-type argyrodite Cu_8GeSe_6 via the simultaneous engineering of the electronic and phonon transports. *ACS Applied Materials and Interfaces Journal*. 2022;14: 16330–16337. https://doi.org/10.1021/acsami.2c02625

146. Zong P., Li Y., Negishi R., Li Z., Zhang C., Wan C. Thermoelectric performance of Cu_8SiS_6 with high electronic band degeneracy. *ACS Applied Electronic Materials Journal*. 2023;6(5): 2832–2838. https://doi.org/10.1021/acsaelm.3c00423

147. Schwarzmüller S., Souchay D., Günther D., ... Oeckler O. Argyrodite-type $Cu_8GeSe_{6-x}Te_x$ ($0 \leqslant x \leqslant 2$): temperature-dependent crystal structure and thermoelectric properties. *Zeitschrift für anorganische und allgemeine Chemie*. 2018;664: 1915–1922. https://doi.org/10.1002/zaac.201800453

148. Fan Y., Wang G., Wang R., ... Zhou X.-Y. Enhanced thermoelectric properties of *p*-type argyrodites Cu_8GeS_6 through Cu vacancy. *Journal of Alloys and Compounds*. 2020;822: 153665. https://doi.org/10.1016/j.jallcom.2020.153665

149. Jiang B., Qiu P., Eikeland E., ... Chen L. Cu_8GeSe_6-based thermoelectric materials with an argyrodite structure. *Journal of Materials Chemistry C*. 2017;5: 943–952. https://doi.org/10.1039/C6TC05068A

150. Brammertz G., Vermang B., ElAnzeery H., Sahayaraj S., Ranjbar S., Meuris M., Poortmans J. Fabrication and characterization of ternary Cu_8SiS_6 and Cu_8SiSe_6 thin film layers for optoelectronic applications. *Thin Solid Films*. 2016;616: 649–654. https://doi.org/10.1016/j.tsf.2016.09.049

151. Gao L., Lee M.-H., Zhang J. Metal-cation substitutions induced the enhancement of second harmonic generation in A8BS6 (A = Cu, and Ag; B = Si, Ge, and Sn). *New Journal of Chemistry*. 2019;43: 3719–3724. https://doi.org/10.1039/C8NJ06270F

152. Cambi L., Monselise G. G. *Gazzetta Chimica Italiana*. 1936;66: 696-700. Quoted from [153]

153. Venkatraman M., Blachnik R., Schlieper A. The phase diagrams of M_2X-SiX_2 (M is Cu, Ag; X is S, Se). *Thermochimica Acta*. 1995;249: 13–20. https://doi.org/10.1016/0040-6031(95)90666-5

154. Olekseyuk I. D., Piskach L. V., Zhbankov O. Y., Parasyuk O. V., Kogut Y. M., Phase diagrams of the quasi-binary systems Cu_2S–SiS_2 and Cu_2SiS_3–PbS and the crystal structure of the new quaternary compound Cu_2PbSiS_4. *Journal of Alloys and Compounds*. 2005;399(1-2): 149–154. https://doi.org/10.1016/j.jallcom.2005.03.086

155. Bayramova U. R., Babanly K. N., Ahmadov E. I., Mashadiyeva L. F., Babanly M. B. Phase equilibria in the Cu_2S-Cu_8SiS_6-Cu_8GeS_6 system and thermodynamic functions of phase transitions of the $Cu_8Si_{(1-x)}Ge_xS_6$ argyrodite phases. *Journal of Phase Equilibria and Diffusion*. 2023;44: 509–519. https://doi.org/10.1007/s11669-023-01054-y

156. Shpak O., Kogut Y., Fedorchuk A., Piskach L., Parasyuk O. The Cu_2Se–PbSe–$SiSe_2$ system and the crystal structure of $CuPb_{1.5}SiSe_4$. *Lesia Ukrainka Eastern European National University Scientific Bulletin. Series: Chemical Sciences*. 2014;21(298): 39–47.

157. Bayramova U. R., Babanly K. N., Mashadiyeva M. F., Yusibov Yu. A., Babanly M. B. Phase equilibria in the Cu_2Se-Cu_8SiSe_6-Cu_8GeSe_6 system. *Russian Journal of Inorganic Chemistry*. 2023;68(11): 16714–1625. https://doi.org/10.1134/s0036023623602027

158. Dogguy M., Rivet J., Flahaut J. Description du systeme ternaire Cu-Si-Te. *Journal of the Less Common Metals*. 1979;63(2): 129–145. https://doi.org/10.1016/0022-5088(79)90238-8

159. Chen X. A., Vada H., Sato A., Nozaki H. Synthesis, structure and electronic properties of Cu_2SiQ_3 (Q = S, Se). *Journal of Alloys and Compounds*. 1999;290(1-2): 91–96. https://doi.org/10.1016/s0925-8388(99)00208-x

160. Rivet J., Flahaut J., Laurelle P. Sur un groupe de composes ternaires a structure teraedrique. *Comptes Rendus Hebdomadaires des Seances de l Academie des Sciences*. 1963;257: 161–164.

161. Khanafer M., Rivet J., Flahaut J. Etude du système Cu_2S-GeS_2, Surstructure du composé Cu_2GeS_3. Transition de phase de Cu_8GeS_6. *Bulletin de la Société Chimique de France*. 1973;3: 859–862. (In French.)

162. Alverdiyev I. J. Refinement of the phase diagram of the Cu_2S-GeS_2 system. *Chemical Problems*. 2019;3(17): 423–428. https://doi.org/10.32737/2221-8688-2019-3-423-428

163. Chang Y. A., Neumann J. P., Choudary U. V. *Phase diagrams and thermodynamic properties of ternary copper-sulfur-metal systems*. Washington: International Copper Research Association; 1979. 191 p.

164. Lychmanyuk O. S., Gulay L. D., Olekseyuk I. D., Stępień-Damm J., Daszkiewicz M., Pietraszko A. Investigation of the Ho_2X_3-Cu_2X-ZX_2 (X = S, Se; Z = Si, Ge) systems. *Polish Journal of Chemistry*. 2008;81(3): 353–367.

165. Carcaly C., Chezeau N., Rivet J., Flahaut J. Description of the systeme $GeSe_2$-Cu_2Se. *Bulletin de la Société Chimique de France*. 1973;1(4): 1191–1195. (In French)

166. Rogacheva E. I., Melikhova N., Panasenko N. M. A Study of the system Cu_2Se-$GeSe_2$. *Inorganic Materials**. 1975;11(5): 719–722. (In Russ.)

167. Piskach L. V., Parasyuk O. V., Romanyuk Ya. E. The phase equilibria in the quasi-binary Cu_2GeS_3/Se_3–CdS/Se/ systems. *Journal of Alloys and Compounds*. 2000;299(1-2): 227–231 https://doi.org/10.1016/S0925-8388(99)00797-5

168. Tomashik V. N. *Cu-Ge-Se (Copper–Germanium–Selenium)*. G. Effenberg, S. Ilyenko (eds.). Springer Materials – the Landolt-Börnstein database. 2006;11(1). p. 288–299.

169. Alverdiyev I. J. Refinement of the phase diagram of the Cu_2Se-GeSe system. *Chemical Problems*. 2019;17(3): 423–428. https://doi.org/10.32737/2221-8688-2019-3-423-42

170. Abrikosov N. Kh., Bankina V. F., Sokolova I. F. Cu-Ge-Te system*. *Inorganic Materials*. 1973;9(1): 129–131. (In Russ.)

171. Dogguy M., Carcaly C., J. Rivet, Flahaut J. Description du systeme ternaire Cu-Ge-Te. *Journal of the Less Common Metals*. 1977;51(2): 181–199. https://doi.org/10.1016/0022-5088(77)90081-9

172. Yusibov Yu. A., Abyshov V. T., Nabiyev B. A., Babanly M. B. Cu-Cu_2Te-Cu_3Ge system*. *Inorganic Materials*. 1991;27(11): 2282–2284. (In Russ.)

173. Olekseyuk I. D., Piskach L. V., Susa L. V. The Cu_2GeTe_3-CdTe system and the structure of compound $Cu_2CdGeTe_4$. *Russian Journal of Inorganic Chemistry*. 1996;41: 1356–1358.

174. Khanafer W., Rivet J., Flahaut J. Etude du ternaire Cu–Sn–S. Diagrammes d'equilibre des systémes Cu_2S–SnS, Cu_2S–Sn_2S_3 et Cu_2S–SnS_2. Etude cristallographique des composés Cu_4SnS_4, Cu_2SnS_3, $Cu_2Sn_4S_9$, et $Cu_4Sn_3S_8$. *Bulletin de la Société Chimique de France*. 1974;12: 267–276. (In French)

175. Moh G. H. Tin-containing mineral systems. Part II: Phase relations and mineral assemblage in the Cu–Fe–Zn–S system. *Chemie Der Erde*. 1975;34: 1–61.

176. Chang Y. A., Neuman J. P., Choudary U. V. Phase diagrams and thermodynamic properties of ternary copper-sulfur- metal systems: Cu-S-Sn. In: *Phase diagrams. Thermodynamic properties ternary copper- sulfur- metal systems*. 1979;7: 159–170.

177. Fiechter S., Martinez M., Schmidt G., Henrion W., Tomm Y. Phase relations and optical properties of semiconducting ternary sulfides in the system Cu–Sn–S. *Journal of Physics and Chemistry of Solids*. 2003;64(9-10): 1859–1862. https://doi.org/10.1016/S0022-3697(03)00172-0

178. Jaulmes S., Rivet J., Laruelle P. Cuivre–etain–soufre Cu_4SnS_4. *Acta Crystallographica Section B Structural Crystallography and Crystal Chemistry*. 1977;33: 540–542. https://doi.org/10.1107/s0567740877004002

179. Onoda M., Chen X., Sato A., Wada H. Crystal structure and twinning of monoclinic Cu_2SnS_3. *Materials Research Bulletin*. 2000;35: 1563–1570. https://doi.org/10.1016/S0025-5408(00)00347-0

180. Chen X., Wada H., Sato A., Mieno M. Synthesis, electrical conductivity, and crystal structure of $Cu_4Sn_7S_{16}$ and structure refinement of Cu_2SnS_3. *Journal of Solid State Chemistry*. 1998;139: 144–151. https://doi.org/10.1006/JSSC.1998.7822

181. Jemetio J. P. F., Zhou P., Kleinke H. Crystal structure, electronic structure and thermoelectric properties of $Cu_4Sn_7S_{16}$. *Journal of Alloys and Compounds*. 2006;417: 55–59. https://doi.org/10.1016/j.jallcom.2005.09.030

182. Jaulmes S., Julien Pouzol M, Rivet J., Jumas J. C., Maurin M. Structure cristalline du sulfure de cuivre et detain $CuSn_{3.75}S_8$. *Acta Crystallographica Section B Structural Crystallography and Crystal Chemistry*. 1982; B38(1): 51–54. https://doi.org/10.1107/s0567740882002027

183. Tomashik V., Lebrun N., Perrot P. *Copper-selenium-tin*. In: *Landolt–Börnstein New Series. Group IV: physical chemistry, vol. 11, ternary alloy systems. Subvolum C. Non-ferrous metal systems. Pt. 1. Selected semiconductor systems*. Verlag, Berlin, Heidelberg: Springer; 2006. p. 361–373. https://doi.org/10.1007/10915981_26

184. Rivet J., Laruelle P., Flahaut J. Phase diagrams of the SnSe-Cu_2Se and $SnSe_2$-Cu_2Se systems. Order-disorder phenomena and thermoconductivity of Cu_2SnSe_3 compound. *Bulletin de la Société Chimique de France*. 1970;(5): 1667–1670.

185. Berger L. I., Kotina E. K. Phase diagrams of the Cu_2Se-$SnSe_2$, Cu_2SnSe_3-SnSe and Cu_2Se-SnSe systems. *Inorganic Materials*. 1973;9(3): 330–322.

186. Berger L. I., Kotina E. G., Oboznenko Yu. V., Obodovskaya A. E. Cross sections of the system Cu-Sn-Se. *Inorganic Materials*. 1973;9(2): 203–207.

187. Carcaly C., Rivet J., Flahaut J. Description du système ternaire Cu-Sn-Te. *Journal of the Less Common*

Metals. 1975;41(1): 1–18. https://doi.org/10.1016/0022-5088(75)90089-2

188. Carcaly C., Rivet J., Flahaut J. Commentaires sur le système Cu-Sn-Te. *Journal of the Less Common Metals*. 1977;51(1): 165–171. https://doi.org/10.1016/0022-5088(77)90184-9

189. Tomashik V., Lebrun N. Copper-tin-tellurium. In: *Landolt–Börnstein New Series. Group IV: physical chemistry, vol. 11, ternary alloy aystems. Subvolum C. Non-ferrous metal systems. Pt. 1. Selected semiconductor systems*. Verlag, Berlin, Heidelberg: Springer; 2006. pp. 374–386. https://doi.org/10.1007/10915981_27

190. Bayramova U. R., Ahmadov E. I., Babanly D. M., Mashadiyeva L. F., Babanly M. B. Calorimetric study of phase transition of Cu_8GeSe_6 and comparison with other argyrodite family compounds. *Chemical Problems*. 2023;4(21): 396–403. https://doi.org/10.32737/2221-8688-2023-4-396-403

191. Alverdiyev I. J., Imamaliyeva S. Z., Akhmedov E. I., Yusibov Yu. A., Babanly M. B. Thermodynamic properties of some ternary compounds of the argyrodite family. *Azerbaijan Chemical Journal*. 2023;4: 21–30. https://doi.org/10.32737/0005-2531-2023-4-21-30

192. Yusibov Yu. A., Aliyeva Z. M., Babanly M. B. Thermodynamic properties of the Cu_2GeSe_3 compound. *Azerbaijan Chemical Journal*. 2023;1: 108–114. https://doi.org/10.32737/0005-2531-2023-1-108-114

193. Abbasov A. S., Aliyeva N. A., Aliyev I. Ya., Asadov Y. G., Askerova A. A. Thermodynamic properties of the Cu_2GeSe_3 and Cu_8GeSe_6. *Report of the Academy of Sciences of the Azerbaijan SSR*. 1987;42(12): 27–28.

194. Alverdiev I. J., Abbasova V. A., Yusibov Yu. A., Tagiev D. B., Babanly M. B. Thermodynamic study of Cu_2GeS_3 and $Cu_{2-x}Ag_xGeS_3$ solid solutions by the EMF method with a $Cu_4RbCl_3I_2$ solid electrolyte. *Russian Journal of Electrochemistry*. 2018;54(2): 153–158. https://doi.org/10.1134/s1023193518020027

195. Alverdiyev I. J. Thermodynamic study of Cu_2SnSe_3 by EMF method with solid electrolyte Cu_4RbCl_3I. *Azerbaijan Journal of Physics*. 2019; XXV(3): 29-33.

196. Mustafayev F. M., Abbasov A. S., Aliyev I. Ya. Thermodynamic investigation of the Cu_2S-SnS_2. *Report of the Academy of Sciences of the Azerbaijan SSR*. 1987;43(1): 51–54. (In Russ.)

197. Stolyarova T. A., Brichkina E. A., Osadchii E. G. Standard enthalpy of Cu_2SnS_3 (mohite) formation from sulfides. *Russian Journal of Inorganic Chemistry*. 2020;65: 636–639. https://doi.org/10.1134/S003602362005023X

198. Mashadieva L. F., Alieva Z. M., Mirzoeva R. Dzh., Yusibov Yu. A., Shevel'kov A. V., Babanly M. B. Phase equilibria in the Cu_2Se–$GeSe_2$–$SnSe_2$ system. *Russian Journal of Inorganic Chemistry*. 2022;67(5): 670–682. https://doi.org/10.1134/S0036023622050126

199. Bagheri S. M., Alverdiyev I. J., Aliev Z. S., Yusibov Y. A., Babanly M. B. Phase relationships in the $1.5GeS_2$+Cu_2GeSe_3«$1.5GeSe_2$ +Cu_2GeS_3 reciprocal system. *Journal of Alloys and Compounds*. 2015;625: 131–137. https://doi.org/10.1016/j.jallcom.2014.11.118

200. Alverdiyev I. J., Aliev Z. S., Bagheri S. M., Mashadiyeva L. F., Yusibov Y. A., Babanly M. B. Study of the $2Cu_2S+GeSe_2 \leftrightarrow Cu_2Se+GeS_2$ reciprocal system and thermodynamic properties of the $Cu_8GeS_{6-x}Se_x$ solid solutions. *Journal of Alloys and Compounds*. 2017;691: 255–262. https://doi.org/10.1016/j.jallcom.2016.08.251

201. Amiraslanova A. J., Mammadova A. T., Alverdiyev I. J., Yusibov Yu. A., Babanly M. B. $Ag_8GeS_6(Se_6)$ – Ag_8GeTe_6 systems: phase relations, synthesis, and characterization of solid solutions. *Azerbaijan Chemical Journal*. 2023;1: 22–29. https://doi.org/10.32737/0005-2531-2023-1-22-29

202. Alverdiev I. J., Bagheri S. M., Aliyeva Z. M., Yusibov Yu. A., Babanly M. B. Phase equilibria in the Ag_2Se–$GeSe_2$–$SnSe_2$ system and thermodynamic properties of $Ag_8Ge_{1-x}Sn_xSe_6$ solid solutions. *Inorganic Materials*. 2017;53(8): 786–796. https://doi.org/10.1134/S0020168517080027

203. Abbasova V. A., Alverdiyev I. J., Mashadiyeva L. F., Yusibov Y. A., Babanly M. B. Phase relations in the Cu_8GeSe_6-Ag_8GeSe_6 system and some properties of solid solutions. *Azerbaijan Chemical Journal*. 2017;1: 30–33.

204. Abbasova V. A., Alverdiyev I. J., Rahimoglu E., Mirzoyeva R. J., Babanly M. B. Phase relations in the Cu_8GeS_6-Ag_8GeS_6 system and some properties of solid solutions. *Azerbaijan Chemical Journal*. 2017;2: 25–29.

205. Alverdiev I. J., Abbasova V. A., Yusibov Yu. A., Babanly M. B. Thermodynamic properties of the Cu_8GeS_6-Ag_8GeS_6 solid solutions. *Condensed Matter and Interphases*. 2017;19(1): 22–26. (In Russ., abstract in Eng.). https://doi.org/10.17308/kcmf.2017.19/172

206. Centeno P., Alexandre M., Neves F., ... Mendes M. J. Copper-arsenic-sulfide thin-films from local raw materials deposited via RF co-sputtering for photovoltaics. *Nanomaterials*. 2022;12(19): 3268. https://doi.org/10.3390/nano12193268

207. McClary S. A., Taheri M. M., Blach D. D., ... Agrawal R. Nanosecond carrier lifetimes in solution-processed enargite (Cu_3AsS_4) thin films. *Applied Physics Letters*. 2020;117(16): 162102. https://doi.org/10.1063/5.0023246

208. Studenyak I. P, Molnar Z. R., Makauz I. I. Deposition and optical absorption studies of Cu–As–S thin films. *Semiconductor Physics, Quantum Electronics and Optoelectronics*. 2018;21(2): 167–172. https://doi.org/10.15407/spqeo21.02.167

209. Wallace S. K., Svane K. L., Huhn W. P., ... Walsh A. Candidate photoferroic absorber materials for thin-film solar cells from naturally occurring minerals: enargite, stephanite, and bournonite. *Sustainable Energy and Fuels*. 2017;1(6): 1339–1350. https://doi.org/10.1039/C7SE00277G

210. Wallace S. K., Butler K. T., Hinuma Y., Walsh A. Finding a junction partner for candidate solar cell absorbers enargite and bournonite from electronic band and lattice matching. *Journal of Applied Physics*. 2019;125(5): 055703. https://doi.org/10.1063/1.5079485

211. Ballow R. B., Miskin K. K., Abu-Omar M. M. Synthesis and characterization of $Cu_3(Sb_{1-x}As_x)S_4$ semiconducting nanocrystal alloys with tunable properties for optoelectronic device applications. *Chemistry of Materials Journal*. 2017;29(2): 573–578. https://doi.org/10.1021/acs.chemmater.6b03850

212. Alqahtani T., Khan M. D., Lewis D. J., Zhong X. L., O'Brien P. Scalable synthesis of Cu–Sb–S phases from reactive melts of metal xanthates and effect of cationic manipulation on structural and optical properties. *Scientific*

Reports. 2021;11(1): 1–17. https://doi.org/10.1038/s41598-020-80951-5

213. Ornelas-Acosta R. E., Shaji S., Avellaneda D., Castillo G. A., Das Roy T. K., Krishnan B. Thin films of copper antimony sulfide: A photovoltaic absorber material. *Materials Research Bulletin*. 2015;61: 215–225. https://doi.org/10.1016/j.materresbull.2014.10.027

214. Vinayakumar V., Shaji S., Avellaneda D., Aguilar-Martínez J. A., Krishnan B. Copper antimony sulfide thin films for visible to near infrared photodetector applications. *RSC Advances***.** 2018;8: 31055–31065. https://doi.org/10.1039/C8RA05662E

215. Van Embden J., Mendes J. O., Jasieniak J. J., Chesman A. S. R., Della Gaspera E. Solution-processed $CuSbS_2$ thin films and superstrate solar cells with CdS/In_2S_3 buffer layers. *ACS Applied Energy Materials Journal*. 2020;3(8): 7885–7895. https://doi.org/10.1021/acsaem.0c01296

216. Chalapathi U., Bhaskar P. U., Sangaraju S., Al-Asbahi B. A., Park S.-H. $CuSbS_2$ thin films and solar cells produced from Cu/Sb/Cu stacks via sulfurization. *Heliyon*. 2024;10(6): e27504. https://doi.org/10.1016/j.heliyon.2024.e27504

217. Zhang M., Wang C., Chen C., Tang J. Recent progress in the research on using $CuSbS_2$ and its derivative $CuPbSbS_3$ as absorbers in case of photovoltaic devices. *Front. Optoelectron*. 2021;14(4): 450–458. https://doi.org/10.1007/s12200-020-1024-0

218. Riha S. C., Koegel A. A., Emery J. D., Pellin M. J., Martinson A. B. F. Low-temperature atomic layer deposition of $CuSbS_2$ for thin-film photovoltaics. *ACS Applied Materials and Interfaces Journal*. 2017;9(5): 4667–4673. https://doi.org/10.1021/acsami.6b13033

219. Chalapathi U., Poornaprakash B., Ahn C. H., Park S.-H. Two-stage processed $CuSbS_2$ thin films for photovoltaics: effect of Cu/Sb ratio. *Ceramics International*. 2018;44(12): 14844–14849. https://doi.org/10.1016/j.ceramint.2018.05.117

220. Banu S., Ahn S. J., Ahn S. K., Yoon K., Cho A. Fabrication and characterization of cost-efficient $CuSbS_2$ thin film solar cells using hybrid inks. *Solar Energy Materials and Solar Cells*. 2016;151: 14–23. https://doi.org/10.1016/j.solmat.2016.02.013

221. Raju N. P., Lahiri S., Thangavel R. Electronic and optical properties of $CuSbS_2$ monolayer as a direct band gap semiconductor for optoelectronics. *AIP Conference Proceedings*. 2021;2352(1): 020001. https://doi.org/10.1063/5.0052990

222. Libório M. S., Queiroz J. C. A, Sivasankar S. M., Costa T. H. C., Cunha A. F., Amorim C. O. A review of Cu_3BiS_3 thin films: a sustainable and cost-effective photovoltaic material. *Crystals*. 2024;14(6): 524. https://doi.org/10.3390/cryst14060524

223. Nasonova D. I., Verchenko V. Yu., Tsirlin A. A., Shevelkov A. V. Low-temperature structure and thermoelectric properties of pristine synthetic tetrahedrite $Cu_{12}Sb_4S_{13}$. *Chemistry of Materials*. 2016;28(18): 6621–6627. https://doi.org/10.1021/acs.chemmater.6b02720

224. Hathwar V. R., Nakamura A., Kasai H., … Nishibori E. Low-temperature structural phase transitions in thermoelectric tetrahedrite, $Cu_{12}Sb_4S_{13}$, and Tennantite, $Cu_{12}As_4S_{13}$. *Crystal Growth and Design Journal*. 2019;19(7): 3979–3988. https://doi.org/10.1021/acs.cgd.9b00385

225. Yaroslavzev A. A., Kuznetsov A. N., Dudka A. P., Mironov A. V., Buga S. G., Denisov V. V. Laves polyhedra in synthetic tennantite, $Cu_{12}As_4S_{13}$, and its lattice dynamics. *Journal of Solid State Chemistry*. 2021;297: 122061. https://doi.org/10.1016/j.jssc.2021.122061

226. Tanishita T., Suekuni K., Nishiate H., Lee C.-H., Ohtaki M. A strategy for boosting thermoelectric performance of famatinite Cu_3SbS_4. *Physical Chemistry Chemical Physics*. 2020;22(4): 2081–2086. https://doi.org/10.1039/c9cp06233e

227. Du B., Zhang R., Chen K., Mahajan A., Reece M. J. The impact of lone-pair electrons on the lattice thermal conductivity of the thermoelectric compound $CuSbS_2$. *Journal of Materials Chemistry A*. 2017;5(7): 3249–3259. https://doi.org/10.1039/C6TA10420G

228. Chetty R., Bali A., Mallik R. C. Tetrahedrites as thermoelectric materials: an overview. *Journal of Materials Chemistry C*. 2015;3(48): 12364–12378. https://doi.org/10.1039/c5tc02537k

229. Suekuni K., Takabatake T. Research update: Cu–S based synthetic minerals as efficient thermoelectric materials at medium temperatures. *ACS Applied Materials and Interfaces Journal*. 2016;4(10): 104503–104513. https://doi.org/10.1063/1.4955398

230. Levinsky P., Candolfi C., Dauscher A., Tobola J., Hejtmánek J., Lenoir B. Thermoelectric properties of the tetrahedrite–tennantite solid solutions $Cu_{12}Sb_{4-x}As_xS_{13}$ and $Cu_{10}Co_2Sb_{4-y}As_yS_{13}$ ($0 \leqslant x, y \leqslant 4$). *Physical Chemistry Chemical Physics*. 2019;21(8): 4547–4555. https://doi.org/10.1039/C9CP00213H

231. Powell A. V. Recent developments in Earth-abundant copper-sulfide thermoelectric materials. *Journal of Applied Physics*. 2019;126(10): 100901. https://doi.org/10.1063/1.5119345

232. Hobbis D., Wang H., Martin J., Nolas G. S. Thermal properties of the very low thermal conductivity ternary chalcogenide $Cu_4Bi_4M_9$ (M = S, Se). *Physica Status Solidi (RRL) – Rapid Research Letters*. 2020;14(8). https://doi.org/10.1002/pssr.202000166

233. Ye Z., Peng W., Wang F., … Wang J. Quasi-layered crystal structure coupled with point defects leading to ultralow lattice thermal conductivity in *n*-type $Cu_{2.83}Bi_{10}Se_{16}$. *ACS Applied Energy Materials*. 2021;4(10): 11325–11335. https://doi.org/10.1021/acsaem.1c02154

234. Bhui A., Dutta M., Mukherjee M., … Biswas K. Ultralow thermal conductivity in Earth-abundant $Cu_{1.6}Bi_{4.8}S_8$: anharmonic rattling of interstitial Cu. *Chemistry of Materials*. 2021;33(8): 2993–3001. https://doi.org/10.1021/acs.chemmater.1c00659

235. Aishwarya K., Maruthasalamoorthy S., Thenmozhi R., … Navamathavan R. Enhanced seebeck coefficient of Cu-Bi-S heterogeneous composite synthesized via solvothermal method. *ECS Journal of Solid State Science and Technology*. 2023;12(12): 123005. https://doi.org/10.1149/2162-8777/ad13b1

236. Mikuła A., Mars K., Nieroda P., Rutkowski P. Copper chalcogenide–copper tetrahedrite composites—a new concept for stable thermoelectric materials based on the chalcogenide system. *Materials*. 2021;14(10): 2635. https://doi.org/10.3390/ma14102635

237. Rikel M., Harmelin M., Prince A. Arsenic-copper-sulfur system. In: *Ternary alloys*. Petzow G., Effenberg G., Aldinger F. (eds.). Weinheim: VGH; 1994;11: 109–127.

238. Pfitzner A., Bernert T. The system Cu_3AsS_4-Cu_3SbS_4 and investigations on normal tetrahedral structures. *Zeitschrift für Kristallographie - Crystalline Materials*. 2004;219(1): 20–26. https://doi.org/10.1524/zkri.219.1.20.25398

239. Maske S., Skinner B. J. Studies of the sulfosalts of copper: I. phases and phase relations in the system Cu-As-S. *Economic Geology*. 1971;66: 901–918. https://doi.org/10.2113/gsecongeo.66.6.901

240. Makovicky E., Skinner B. J. Studies of the sulfosalts of copper: IV. Structure and twinning of sinnerite, $Cu_6As_4S_9$. *American Mineralogist*. 1975;60: 998–1012.

241. Kurz G., Blachnik R. New aspects of the system Cu-As-S. *Journal of the Less Common Metals.* 1989;155: 1–8. https://doi.org/10.1016/0022-5088(89)90441-4

242. Prostakova V., Shishin D., Jak E. Thermodynamic optimization of the Cu–As–S system. *Calphad*. 2021;72: 102247. https://doi.org/10.1016/j.calphad.2020.102247

243. Gasanova Z. T., Mashadieva L. F., Yusibov Y. A., Babanly M. B. Phase equilibria in the Cu_2S–Cu_3AsS_4–S system. *Russian Journal of Inorganic Chemistry.* 2017;62(5): 591–597. https://doi.org/10.1134/S0036023617050126

244. Gasanova Z. T., Aliev Z. S., Yusibov Y. A., Babanly M. B. Phase equilibria in the Cu-Cu_2S-As system. *Russian Journal of Inorganic Chemistry.* 2012;57(8): 1158–1162. https://doi.org/10.1134/s0036023612050075

245. Babanly M. B., Gasanova Z. T., Mashadieva L. F., Zlomanov V. P., Yusibov Y. A. Thermodynamic study of the Cu-As-S system by EMF measurements with $Cu_4RbCl_3I_2$ as a solid electrolyte. *Inorganic Materials*. 2012;48(3): 225–228. https://doi.org/10.1134/s0020168512020021

246. Mashadiyeva L. F., Babanly D. M., Hasanova Z. T., Yusibov Yu. A., Babanly M. B. Phase relations in the Cu-As-S system and thermodynamic properties of copper-arsenic sulfides. *Journal of Phase Equilibria and Diffusion.* 2024. (In press.)

247. Khvorostenko A. S., Kirilenko V. V., Popov B. I. Phase diagram of the As_2Se_3–Cu_2Se system*. *Inorganic Materials*. 1972;8(1): 73–79. (In Russ.)

248. Blachnik R., Kurz G. Compounds in the system Cu_2Se-As_2Se_3. *Journal of Solid State Chemistry.* 1984;55(2): 218–224. https://doi.org/10.1016/0022-4596(84)90267-6

249. Gambi L, Elli M. La chimica et I'industria. 1968;50: 94–98.

250. Cohen K., Rivet J., Dugue J. J. Description of the Cu – As – Se ternary system. *Journal of Alloys and Compounds*. 1995;224(2): 316–329. https://doi.org/10.1016/0925-8388(95)01534-5

251. Blachnik R., Gather B. Enthalpies of melting of some ternary ABX_2-compounds. *Zeitschrift fuer Naturforschung*. 1972;327: 1417–1413. https://doi.org/10.1515/znb-1972-1129

252. Mashadieva L. F., Gasanova Z. T., Yusibov Yu. A., Babanly M. B. Phase equilibria in the Cu–Cu_2Se–As system. *Russian Journal of Inorganic Chemistry.* 2017;62(5): 598–603. https://doi.org/10.1134/S0036023617050151

253. Mashadieva L. F., Gasanova Z. T., Yusibov Yu. A., Babanly M. B. Phase Equilibria in the Cu_2Se–Cu_3AsSe_4–Se system and thermodynamic properties of Cu_3AsSe_4. *Inorganic Materials*. 2018;54(1): 8–16. https://doi.org/10.1134/S0020168518010090

254. Mashadiyeva L. F., Hasanova Z. T., Yusibov Yu. A., Babanly M. B. Phase equilibria in the Cu_2Se–Cu_3AsSe_4–As_2Se_3 system. *Azerbaijan Chemical Journal.* 2024;3: 83–93. https://doi.org/10.32737/0005-2531-2024-3-83-93

255. Hasanova Z. T. Thermodynamic study of the $CuAsSe_2$ compound by EMF method with solid electrolyte. *New Materials, Compounds and Applications*. 2021;5(3): 205–211. Available at: http://jomardpublishing.com/UploadFiles/Files/journals/NMCA/V5N3/Hasanova.pdf

256. Peccerillo E., Durose K. Copper–antimony and copper–bismuth chalcogenides —Research opportunities and review for solar photovoltaics. *MRS Energy and Sustainability*. 2018;5: 1–56. https://doi.org/10.1557/mre.2018.10

257. Cui J., Zhang Y., Hao X., Liu X., Shen Y. Thermodynamic calculation of S–Sb system and Cu–S–Sb system. *Calphad.* 2021;75: 102362. https://doi.org/10.1016/j.calphad.2021.102362

258. Cambi L., Elli M. Processi idrotermali, sintesi di solfosali da ossidi di metalli e metalloidi, nota II— Cuprosolfoantimoniti. *La Chimica el'Industria,* 1965;47: 136–147.

259. Kuliev R. A., Krestovnikov A. N., Glazov V. M. Synthesis and thermodynamic properties of alloys of the Cu_2S-Sb_2S_3 system. *Russian Journal of Physical Chemistry*. 1969;43(12): 3063–3066.

260. Ilyasheva N. A. Study of the Cu_2S-Sb_2S_3 system at 320–400 °C*. *Inorganic Materials*. 1963;9(10): 1677–1679. (In Russ.)

261. Mashadiyeva L. F., Mammadli P. R., Babanly D. M., Ashirov G. M., Shevelkov A. V., Yusibov Y. A. Solid-phase equilibrium in the Cu-Sb-S ternary system and thermodynamic properties of ternary phases. *JOM*. 2021;73(5): 1522-1530. https://doi.org/10.1007/s11837-021-04624-y

262. Mashadiyeva L. F., Babanly D. M., Poladova A. N., Yusibov Y. A., Babanly M. B. Liquidus surface and phase relations in the Cu-Sb-S system. In: *Properties and Uses of Antimony*. David J. Jenkins (ed.). *Nova Science Publishers*. 2022: 45-72. https://doi.org/10.52305/OJKB5395

263. Bryndzia L. T., Kleppa O. J. High-temperature reaction calorimetry of solid and liquid phases in part of the quasi-binary system Cu_2S-Sb_2S_3. *American Mineralogist*. 1988;73(7-8): 707–713.

264. Kyono A., Kimata M. Crystal structures of chalcostibite ($CuSbS_2$) and emplectite ($CuBiS_2$): Structural relationship of stereochemical activity between chalcostibite and emplectite. *American Mineralogist.* 2005;90(1): 162–165 https://doi.org/10.2138/am.2005.1585

265. Lemoine P., Bourgès C., Barbier T., Nassif V., Cordier S., Guilmeau E. High temperature neutron powder diffraction study of the $Cu_{12}Sb_4S_{13}$ and $Cu_4Sn_7S_{16}$ phases. *Journal of Solid State Chemistry*. 2017;247: 83–89. https://doi.org/10.1016/j.jssc.2017.01.003

266. Pfitzner A. Cu_3SbS_3: Zur Kristallstruktur und Polymorphie. *Zeitschrift für anorganische und allgemeine Chemie.*, 1994;620: 1992–1997. https://doi.org/10.1002/zaac.19946201126

267. Pfitzner A., Reiser S. Refinement of the crystal structures of Cu_3PS_4 and Cu_3SbS_4 and a comment on normal tetrahedral structures. *Zeitschrift für Kristallographie*. 2002;217(2): 51–54. https://doi.org/10.1524/zkri.217.2.51.20632

268. Golovey M. I., Tkachenko V. I., Rigan M. Yu., Stasyuk N. P. State diagram of the Cu_2Se-Sb_2Se_3 system in the region of existence of the $CuSbSe_2$ compound*. *Inorganic Materials*. 1990;26(5): 933–934. (In Russ)

269. Scott W, Conch J. R. Phase diagram and properties of Cu_3SbSe_4 and other $A_3^IB^VC_4^{VI}$ compounds. *Materials Research Bulletin*. 1973;8(10): 1257–1267. https://doi.org/10.1016/0025-5408(73)90164-5

270. Shtykova M. A., Molokeev M. S., Zakharov B. A., … Andreev O. V. Structure and properties of phases in the $Cu_{2-x}Se$-Sb_2Se_3 system. The $Cu_{2-X}Se$-Sb_2Se_3 phase diagram. *Journal of Alloys and Compounds*. 2022;906: 164384. https://doi.org/10.1016/j.jallcom.2022.164384

271. Liu R., Wang J., Cui D. Thermodynamic modeling of the Cu-Sb-Se system. *Journal of Phase Equilibria and Diffusion*. 2023;44: 687–703. https://doi.org/10.1007/s11669-023-01074-8

272. Pfitzner A. Crystal structure of tricopper tetraselenoantimonate (V), Cu_3SbSe_4 *Zeitschrift für Kristallographie – Crystalline Materials*. 1994;209: 685. https://doi.org/10.1524/zkri.1994.209.8.685

273. Chorba O., Filep M., Pogodin A., Malakhovska T., Sabov M. Crystals growth and refinement of the Cu_3SbSe_3 crystal structure. *Ukrainian Chemistry Journal*. 2022; 88(9): 25–33. https://doi.org/10.33609/2708-129X.88.09.2022.25-33

274. Schwarzmüller S., Amsler M., Goedecker S., Huppertz H. 4p-pavonite-type $Cu_{1.8}Sb_{5.4}Se_9$: a one-dimensional copper ion conductor. *SSRN*. 2024. https://doi.org/10.2139/ssrn.4852905

275. Buhlman B. Untersuchungen im System Bi_2S_3-Cu_2S und geologische Schlussfolgerungen. *Neues Jahrbuch für Mineralogie, Monatshefte*. 1971: 137–141.

276. Gather B., Blachnik R. Temperature-composition diagrams in the Cu_2(VIb)-(Vb) sections of the ternary Cu-(Vb)-(VIb) systems (Vb = As, Sb, Bi, VIb = S, Se, Te). *Journal of the Less Common Metals*. 1976;48(2): 205–212. https://doi.org/10.1016/0022-5088(76)90003-5

277. Golovey M. I., Voroshilov Yu. V., Potoriy M. V. Study of Cu (Ag, Tl)-B^V-Se systems. *ChemChemTech [Izv. Vyssh. Uchebn. Zaved. Khim. Khim. Tekhnol.]*. 1985;28(1): 7–11.

278. Liautard B., Garcia J. C., Brun G., Tedenac J. C., Maurin M. Crystal structure of $Cu_{(1+3x)}Bi_{(5-x)}X_8$ (X = S,Se) alloys. *European Journal of Solid State and Inorganic Chemistry*. 1990;27: 819–830. https://doi.org/10.1002/chin.199108005

279. Babanly N. B., Yusibov Yu. A., Aliyev Z. S., Babanly M. B. Phase equilibria in the system Cu-Bi-Se and thermodynamic properties of selenobismuthides of copper. *Russian Journal of Inorganic Chemistry*. 2010;55(9): 1471–1481. https://doi.org/10.1134/S0036023610090238

280. Prostakova V., Shishin D., Jak E. Thermodynamic optimization of the Cu–As–S system. *Calphad*. 2021;72: 102247. https://doi.org/10.1016/j.calphad.2020.102247

281. Sugaki A., Kitakaze A., Hayashi K. Synthesis of minerals in the Cu-Fe-Bi-S system under hydrothermal condition and their phase relations. *Bulletin de Minéralogie*. 1981;104: 484-495. https://doi.org/10.3406/bulmi.1981.7499

282. Filippou D., Germain P., Grammatikopoulos T. Recovery of metal values from copper—arsenic minerals and other related resources. *Mineral Processing and Extractive Metallurgy Review*. 2007;28: 247–298. https://doi.org/10.1080/08827500601013009

283. Zikanova T. A., Muldagalieva R. A., Kuzgibekova Kh., Isabaev S. M. Heat capacity and thermodynamic functions of copper orthoarsenate. *High Temperatu*. 2000;38(3): 492–493. https://doi.org/10.1007/bf02756014

284. Skinner B. J., Luce F. D., Makovicky E. Studies of the sulfosalts of copper: III Phases and phase relations in the system Cu-Sb-S. *Economic Geology*. 1972;67: 924–938. https://doi.org/10.2113/GSECONGEO.67.7.924

285. Babanly N. B., Yusibov Y. A., Mirzoyeva R. J., Shykhiyev Yu. M., Babanly M. B. $Cu_4RbCl_3I_2$ solid superionic conductor in thermodynamic study of three-component copper chalcogenides. *Russian Journal of Electrochemistry*. 2009;45(4): 405–410. https://doi.org/10.1134/s1023193509040089

286. Tkachenko V. I., Regan M. Yu., Voroshilov Yu. V., Golovey M. I. In: *Abstracts of reports. IV All-Union. Council on chemistry and technology of chalcogens and chalcogenides**. Karaganda; 1980. p. 200. (In Russ.)

**Translated by author of the article*

Information about the authors

Mahammad B. Babanly, DSc in Chemistry, Professor, Associate Member of the Azerbaijan National Academy of Sciences, Deputy-director of the Institute of Catalysis and Inorganic Chemistry (Baku, Azerbaijan).
https://orcid.org/0000-0001-5962-3710
babanlymb@gmail.com

Leyla F. Mashadieva, PhD in Chemistry, Senior Scientific Fellow of Institute of Catalysis and Inorganic Chemistry (Baku, Azerbaijan).
https://orcid.org/0000-0003-2357-6195
leylafm76@gmail.com

Samira Z. Imamaliyeva, DSc in Chemistry, Assistance Professor, Institute of Catalysis and Inorganic Chemistry (Baku, Azerbaijan).
https://orcid.org/0000-0001-8193-2122
samira9597a@gmail.com

Dunya M. Babanly, DSc in Chemistry, Assistance Professor, French-Azerbaijani University (Baku, Azerbaijan).
https://orcid.org/0000-0002-8330-7854
dunya.babanly@ufaz.az

Dilgam B. Taghiyev, Academician of the Azerbaijan National Academy of Sciences, Director of the Institute of Catalysis and Inorganic Chemistry (Baku, Azerbaijan).
https://orcid.org/0000-0002-8312-2980
dtagiyev@rambler.ru

Yusif A. Yusibov, DSc in Chemistry, Professor, Rector of the Ganja State University (Ganja, Azerbaijan).
https://orcid.org/0000-0003-4081-6170
yusifyusibov1951@gmail.com

Received 03.06.2024; approved after reviewing 21.06.2024; accepted for publication 16.09.2024; published online 25.12.2024.

Translated by Valentina Mittova